



**POLITEHNICA UNIVERSITY OF TIMISOARA
CIVIL ENGINEERING FACULTY**

HABILITATION THESIS

**Contributions to the behavior of composite elements
for buildings placed in seismic areas
and high quality construction works through monitoring**

Assoc. Prof. Daniel DAN, PhD

- JUNE 2013 -

TABLE OF CONTENTS

(a) Abstract		3
(b) Achievements and development plans		5
(b-i) Scientific, professional and academic achievements		5
1. Introduction		5
1.1 Articles constituting the habilitation thesis		8
2. Experimental and theoretical studies concerning the load bearing capacity of steel and composite joints for buildings placed in seismic areas		10
2.1 Introduction		10
2.2 Steel – Concrete Composite Structure For Multi-Storey Buildings		11
2.2.1 Structural detailing		11
2.2.2 Structural system		14
2.2.3 Structural stiffening		14
2.2.4 Seismic analysis		16
2.3 Theoretical study on steel – concrete composite joint		18
2.3.1 Structural steel joint analysis		19
2.3.2 Composite steel-concrete joint analysis		22
2.4 Experimental study on steel – concrete composite joint		25
2.4.1 Calibration of the experimental join. Numerical analysis		26
2.4.2. Experimental tests on steel and steel composite joints under symmetrical and asymmetrical loads		27
2.5 Comparative study concerning the behaviour of the structural steel and steel-concrete composite joint under symmetrical and asymmetrical loads		28
2.6 Conclusions		32
3. Theoretical and Experimental Study on Composite Steel-Concrete Shear Walls with Vertical Steel Encased Profiles		34
3.1 Introduction		34
3.1.1 International literature review in the field of composite shear walls		35
3.2 Theoretical study and design of the specimens		39
3.2.1 Design of the experimental specimens		39
3.2.2 Specimen fabrication		42
3.2.3 Numerical analysis and calibration of experimental specimens		42
3.2.4 Material properties		44
3.3 Experimental investigation		45
3.3.1 Testing methodology and test set-up		45
3.3.2 Experimental observations		47
3.3.3 General behavior of the specimens		48
3.4 Test results and discussions		53
3.4.1 Dissipated energy		54
3.4.2 Capacity degeneration		55
3.4.3 Strain analysis		55
3.4.4 Ductility coefficient		58
3.5 Conclusions		59
3.6 Retrofitting solutions for damaged composite steel concrete walls		60
3.6.1 Introduction		60
3.6.2 Experimental tests on seismically damaged CSRCW retrofitted with CFRP		60
3.6.2.1 Behavior and results of reference elements		61

3.6.2.2 Repair and strengthening of the specimens	62
3.6.2.3 Testing methodology and test set-up	64
3.6.3 Experimental results and comparative study	66
3.6.3.1 General behavior and failure modes of FRP strengthened specimens	66
3.6.3.2 Load displacement response diagrams	67
3.6.3.3 Stiffness analysis	69
3.6.3.4 Strain analysis	69
3.6.3.5 Dissipated energy	71
3.6.3.6 Ductility considerations	72
3.6.4 Conclusions	72
4. Monitoring the constructional structural works and structural health of buildings	74
4.1 Quality Control of the Constructional Works at the Commercial Center Iulius Mall –Timisoara	74
4.1.1 Introduction	74
4.1.2 Constructive systems and technological solutions used	74
4.1.3 Conclusions	79
4.2 Structural health monitoring of reinforced concrete chimneys	80
4.2.1 Introduction	80
4.2.2 General description of the structure	80
4.2.3 Structural issues of the chimneys after 30 years of service	80
4.2.4 Investigation methods	81
4.2.5 Solutions for rehabilitation	81
4.2.6 Health monitoring of chimneys	82
4.2.7 Evaluation of the service period left for the chimneys	84
4.2.8 Structural analysis	84
4.2.8.1 Numerical models	85
4.2.8.2 Materials	85
4.2.8.3 Supports, loads and finite element mesh	86
4.2.8.4 Results and discussions	87
4.2.9 Conclusions	88
(b-ii) Scientific, professional and academic future development plans	89
(b-iii) References	99

HABILITATION THESIS

(a) ABSTRACT

The present thesis summarises the research of my activity, after the PhD thesis was defended at the Politehnica University of Timișoara and confirmed by the Ministry of Education and Research, on the basis of Order no. 3896 / 24. 04. 2003.

The habilitation thesis presents two main research activities that I performed and omits a series of activities considered secondary and complementary to the main ones.

My first research area consists in theoretical and experimental studies regarding the behaviour of steel composite elements for buildings placed in seismic areas.

This PhD research domain was further studied and supplemented with the discovery and the use of innovative composite solutions.

It is worth mentioning that my activity in the field of steel composite elements, continues a research domain from the *Civil Engineering Department*, initiated by: Prof. PhD. Eng. Constantin Avram, corresponding Member of Academy, Prof. Ph. D. Eng. Valentin Bota, Associate Prof. Ph. D. Agneta Tudor and the researcher Ph. D. Liana Bob; the last two persons mentioned being also the authors of the Romanian Code for the Design of Steel Concrete Composite Elements.

The second research area is focused on monitoring the structural health of special constructions or highly important buildings, on monitoring certain constructions in order to validate certain calculus principles. Within this research I have studied various applicative construction issues, i.e.: the subjects approached are closely connected to the execution activity and to the monitoring of the buildings behaviour in time. Therefore, I have applied new concepts for the energetic efficient buildings, as regards their construction and monitoring in order to validate the energetic performances.

Consequently, during the post PhD thesis period, my research activity and the results of the activities developed led to the discovery of certain innovative elements in the field of construction.

I am going to present some of my main contributions and professional achievements for each research field:

- Developing a theoretical and experimental study on composite joints for buildings under asymmetrical loads, real scale 1:1;
- Proposing new innovative solutions for shear walls with steel encased profiles, as alternative solution for high rise buildings placed in seismic areas;
- Performing theoretical and experimental studies regarding the behaviour of the steel concrete composite walls with steel encased profiles. Presenting the results by comparing the new proposed solution with the classical one;
- Retrofitting of damaged composite steel concrete walls using CFRP, testing and validating the proposed solutions for the structural rehabilitation of shear walls affected by earthquake;
- Monitoring the constructional structural works of “Commercial Centre Iulius Mall Timișoara”;
- Structural health monitoring of two chimneys from the Rovinari power plant;
- Promoting the concepts of Passive House and Nearly Zero Energy Buildings as possible solution for sustainable buildings in temperate climate and proposing a monitoring system to validate the above mentioned concept.

I intend to continue the research on the above mentioned fields as follows.

In the field of *the behaviour of steel concrete composite shear walls with high strength concrete* I aim to:

- Identify innovative solutions for composite steel-concrete shear walls with partially encased profiles, for solid composite walls and with various configurations of openings;
- Find new technologies to make shear walls using fibre reinforced concrete;
- Strengthen composite shear walls using Fiber Reinforced Polymers as possible strengthening solutions for structural elements damaged under seismic events.

In the field of *monitoring the structural health of special constructions or highly important buildings and monitoring certain constructions in order to validate certain calculus principles* I plan to:

- Find efficient solutions for sustainable buildings in Romania
- Finish the research programme of monitoring the passive house and nearly energy building;
- Provide a practice guide based on recorded data.

After finishing PhD Thesis, in the mentioned fields, I was an active participant in the research programme FP6 PROHITECH “Earthquake Protection of Historical buildings by reversible mixed Technologies” and COST C25 action: “Sustainability of Constructions-Integrated Approach to Life-time Structural Engineering”; these are research themes complementary to my main fields of interests.

It is worth mentioning that the results obtained within the frame of the first research area, i.e.: the field of steel concrete composite elements, were obtained during the project PN II IDEI 1004/2008, contract 621/2009, financed by CNCSIS –UEFISCDI (2009-2012) which I coordinated. I acknowledge the financial support received for the research.

The studies and research activities in the field of energy efficiency of the buildings are under implementation in the project PN-II-PT-PCCA-2011-3.2-1214 contract no: 74/2012, entitled “Nearly Zero Energy Building and Passive House - sustainable solutions for residential buildings” financed by UEFISCDI. I have to mention that I am the coordinator of this research program, too.

(b) Achievements and development plans

(b-i) Scientific, professional and academic achievements

1. Introduction

The main research field where I was involved consists in theoretical and experimental studies regarding the behaviour of steel composite elements for buildings placed in seismic areas.

Continuing the subject of my PhD thesis entitled “Contribution to the design of the steel concrete composite elements” further studies were made on steel concrete composite joints under asymmetrical loads. They were made within the frame of the project “Optimisation of new composite solutions used for structural elements for buildings (Optimizarea soluțiilor moderne compuse/compozite otel-beton utilizate la realizarea structurilor pentru construcții)”, CT 33550 AT2-190 / 2003-2004.

New research works were performed in the field of composite elements during the research grant “Retrofitting of shear walls and precast walls using CFRP with openings” (Consolidarea cu compozite polimerice armate cu fibre a pereților și a planșelor din beton armat cu goluri create ulterior)”, CT 98/2006-2008, where I was member.

After that, new innovative composite solutions for shear walls with steel encased profiles were tested and analyzed in a large research program entitled “Innovative structural systems using steel-concrete and composite materials, (Sisteme structurale inovative din materiale compuse otel beton și compozite polimerice)”, PN II IDEI 1004 / 2008-2011.

It is worth mentioning that my activity in the field of steel composite elements, continues a research domain from the *Civil Engineering Department*, initiated by: Prof. Ph. D. Eng. Constantin Avram, corresponding Member of Academy, Prof. PhD. Eng. Valentin Bota, Associate Prof. Ph. D. Agneta Tudor and the researcher Ph. D. Liana Bob; the last two persons mentioned being also the authors of the Romanian Code for the Design of Steel Concrete Composite Elements. The researches were completed with new studies on retrofitting of traditional and historical buildings, using new materials as Carbon Reinforced Polymers.

As a leader or as a research team member, involved in national and international grants, I can mention the followings contributions related to the mentioned domain:

- presenting a state-of-the-art programme on the composite steel concrete shear walls evolution and test programs with emphasis on cyclic loading tests;
- conceiving an experimental program to investigate the seismic performance of composite steel concrete shear walls;
- coordinating 6 quasi-static cyclic tests on composite steel-concrete shear walls with different steel shapes encased in concrete;
- assessing and processing of the recorded data and of the observed behavior;
- presenting a general report including cyclic and monotonic load-drift envelopes, aspects related to the strengthening, strain, stiffness, energy dissipation, ductility properties of the tested elements;
- co-coordinating the Ph. D. thesis in the field of composite walls presented by Eng. Fabian Alexandru, from Politehnica University of Timisoara. One of the scientific referents of the thesis was an international well recognized expert in the field of composite steel-concrete structures, i.e.: Prof. Ph. D. Eng. Andre Plumier University of Liege. The fact that this international expert accepted to be one of the scientific referents and the fact that he truly appreciated the performed work underline the importance and the quality of the research and they serve as a significant acknowledgement (confirmation) of both the thesis itself and of the researchers.

The theoretical and experimental program, included in the above mentioned thesis, was supported by the CNCSIS – UEFISCSU project, number PNII - IDEI ID_1004/2008, Contract

621/2009, entitled “Innovative Structural Systems Using Steel-Concrete Composite Materials and Fiber Reinforced Polymer Composites”.

As results of the research performed in the composite constructional field, three main contributions were formulated and listed below:

-Regarding the prescription of EC4 - § 6.7.3.1(3) – where it is stated that: “The longitudinal reinforcement that may be used in calculation should not exceed 6% of the concrete area ($\rho < 6\%$)”, it was demonstrated, after theoretical and experimental studies, that it is possible to use reinforcement ratios at the edge of the element, between 5.5 and 8.7 %, without compromising the ductile behavior mode of the elements. Using higher reinforcement ratios at the edges can lead to obtaining elements with higher strength and ductility performances than those obtained by reinforced concrete elements.

-Although the prescription of EC8 - § 5.4.3.4.2(12) – mentions that: “The transverse reinforcement of the boundary elements may be determined in accordance with EN 1992-1-1:2004 alone, if one of the following conditions is fulfilled: a) The value of the normalized design axial force v_d is not greater than 0.15; or, b) the value of v_d is not greater than 0.20 and the q -factor used in the analysis is reduced by 15%”, however, in the experimental program, the values of the normalized axial force v_d for the tested elements were between 0.015 and 0.021; during the experimental research, the necessity of the cross-ties for the vertical reinforcements placed at the edges in order to assure the confinement of compressed zone, was observed.

-The experimental values, obtained for the multiplication factor α_u / α_1 , for the tested elements, were between 1.30 and 1.51, with greater values than those mentioned in EC8 – § 7.3.2 where the multiplication factor for composite walls was $\alpha_u / \alpha_1 = 1.1$.

As author or coauthor, I published more than 25 research papers between 2009 and 2012 in the field of composite elements: 2 ISI Journal Papers; 3 ISI Proceeding Conference Papers; 7 papers indexed in International Data Base and 13 papers published in the proceedings of international conferences organized under the aegis of highly important professional institutions (ECCS, *fib*, IABSE).

The most important papers were published in international recognized journals, such as: Journal of Constructional Steel Research and Engineering Structures. Taking into account the actuality of the research theme and the results produced, the followings papers cited my results published, in the last period:

[1] Carrasco E., Rodriguez E., Ribeiro G., Queiroz G., Paula F. – „Ultimate compressive strength of enveloped laminar concrete panels, *Construction and building materials*, vol. 27, 2012

[2] Farzad H., Ali G., Alireza R. – Investigating the properties of steel shear walls reinforced with carbon fiber, *Journal of Constructional Steel Research*, Vol. 70, 2012

[3] Sassu M., Andreini M., Anna De Falco, Gesi C. & Potenza A. - “Consolidamento sismico di un edificio in c.a. a pilotis anni”60 con setti in c.a. e colonne di presidio in acciaio”, XIV Convegno ANIDIS, *L'Ingegneria Sismica in Italia*, BARI, 2011.

[4] Ricci I., Palermo M., Gasparini G., Silvestri S., Trombetti T. - Results of pseudo-static tests with cyclic horizontal load on cast in situ sandwich squat concrete walls, *Engineering Structures* Volume 54 (2013) p131–149, DOI 10.1016/j.engstruct.2013.03.046

[5] Mosoarca M. - Seismic Behaviour of Reinforced Concrete Shear Walls with Regular and Staggered Openings After the Strong Earthquakes Between 2009 and 2011, *Engineering Failure Analysis* DOI: 10.1016/j.engfailanal.2013.05.014, 2013

As international recognition, it must be mentioned that other contributions related to an innovative anchorage system used for CFRP elements presented in the paper: Nagy-Gyorgy T., Mosoarca M., Stoian V., Gergely J. & Dan D. - “Retrofit of reinforced concrete shear walls with CFRP composites”, *fib Symposium Keep Concrete Attractive*, Budapest, 2005, 897-902, was cited in well-known international journals by:

[6] Ceroni, F., Evaluation of Bond Strength in Concrete Elements Externally Reinforced

with CFRP Sheets and Anchoring Devices, *Journal of Composites for Construction*, 14, 2010, pp. 1090-0268.

[7] Ceroni, F Debonding strength and anchorage devices for reinforced concrete elements strengthened with FRP sheets, *Composites Part B-Engineering*, 39, 2008, 1359-8368.

In terms of applicability of the previous research conducted, it is important to mention that the completion of the studies on composite steel-concrete welded joints enabled extensive investigation and performance evaluation of a multistory building constructed in Timisoara during 1990-1994. The structure of the building enclosed joints identical to those studied experimentally and theoretically. The research was evaluated by its dissemination at 20 International Conferences and Journals, 7 of them being indexed in ISI Web of Knowledge Data Base and 3 in International Data Base circuit.

It has to be mentioned that for eight years I was member in the management team of the Testing Laboratory that is organized at the CCI Department, within Faculty of Civil Engineering at Politehnica University of Timisoara. During this period the laboratory was accredited by the National Authority, being the first university laboratory in civil engineering ever to obtain this certification.

In the same interval, a National Research Center was also established, functioning as an organism connected to the Testing Laboratory. While holding this administrative position, I was a key person in the constant development of the laboratory, encouraging its expansion through important research contracts both with the industrial and the academic environment. The results of my management activity were quantifiable by constant development of laboratory facilities (equipment, data acquisition systems, testing stands, etc.), i.e.: acquisition of equipment in an amount of over 60,000 euro. In view of all of the above mentioned, it is considered that all the requirements for a proper research activity have been met by the existing infrastructure, with minor adjustments in the future.

In the second research area focused on structural health monitoring of special buildings, I have been participating since 2002 at the processes of monitoring and expertising two of the chimneys from the Rovinari power plant. I elaborated the research report regarding the strengthening of the mentioned chimneys and I performed personally all the tests regarding the quality of the materials extracted from the structural elements.

As a structural designer, I elaborated more than 200 projects that were already built in the nearest area of Timisoara city, Romania.

As member of the design team I participated in the design processes of more than 1310 projects, out of which 670 are traditional residential buildings.

I received the professional recognition by the most important professional association IABSE – International Association for Bridge and Structural Engineering, FIB – Federation for Structural Concrete and AICPS – Romanian Association of Structural Design Engineers.

During 2004 – 2013 I obtained the professional certifications mentioned in the followings:

- Laboratory Chief for research and testing activities - attested by State Inspectorate for Constructions (2004)
- Quality Design Checker of Romanian Ministry for Public Works and Buildings (2005)
- Energy Auditor of Romanian Ministry for Public Works and Buildings (2005)
- Research Expert for Research Projects of Romanian Ministry of Research and Education (06)
- Structural Health Monitor of Buildings (2006).

The scientific activity in the mentioned period increased constantly attending the following level:

- ISI journals – 3
- ISI proceedings – 22
- BDI journals - 12
- BDI proceedings - 10
- Papers for International conferences – 44
- Citations in the international literature - 64
- Books – 2 as author, 2 as editor
- Research Grants – 12
- Participation at international conferences with communications – 26.
- Number of projects checked and verified – 415
- Number of energetic certificate elaborated – 208

It has to be mentioned that during 2002 - 2013, I elaborated in total 107 papers (33 as corresponding author) written in English and 27 in Romanian.

1.1 Articles constituting the habilitation thesis

This is a survey of the results constituting my habilitation thesis. It is based on the following articles.

1. **Dan D.** - Experimental tests on seismically damaged composite steel concrete walls retrofitted with CFRP composites, *Engineering Structures*, 2012; 45, 338 – 348 (**ISI Journal**)
2. **Dan D.**, Fabian A., Stoian V. - Theoretical and experimental study on composite steel - concrete shear walls with vertical steel encased profiles, *Journal of Constructional Steel Research*, 2011; 67, 800 – 813 (**ISI Journal**)
3. **Dan D.**, Fabian A. & Stoian V. - Nonlinear behavior of composite shear walls with vertical steel encased profiles, *Engineering Structures*, 2011; 33, 2794 – 2804 (**ISI Journal**)
4. **Dan D.**, Stoian V., Nagy Gyorgy T., Codrut F., Pruna L. - Structural analysis, rehabilitation and further development of health monitoring program concerning two reinforced concrete chimneys, IABSE'2010 - Large Structures and Infrastructures for Environmentally Constrained and Urbanised Areas , Venice Italy, p656-657/6e, (**INGENTA, Google Scholar**)
5. Fabian A., **Dan D.**, Stoian V. - Numerical Analysis on Composite Steel Concrete Structural Shear Walls with Steel Encased Profiles, *Steel Structures in Seismic Areas STESSA'09*, Philadelphia USA, 2009, p345-350, (**ISI Proceedings**)
6. **Dan D.**, STOIAN V., Nagy-György T., Demeter I. - Experimental Studies on Steel and Steel Concrete Composite Joints Under Symmetrical and Asymmetrical Loads, *Steel Structures in Seismic Areas STESSA'09*, Philadelphia USA, 2009, p187-192 (**ISI Proceedings**)
7. **Dan D.**, Stoian V., Nagy-György T., Dăescu C. - Composite joint for buildings placed in seismic areas theoretical and experimental studies, 9-th International Conference on Steel, Space and Composite Structures, Yantai Beijing, China, 2007, p647-654 (**ISI Proceedings**)
8. Nagy-György T., Moșoarcă M., Stoian V., Gergely J. & **Dan D.** - Retrofit of reinforced concrete shear walls with CFRP composites, *fib Symposium Keep Concrete Attractive*, Budapest, 2005, 897-902, (**INGENTA**)

9. **Dan D.**, Stoian V. - Quality control of the construction works at the Commercial Center Iulius Mall Timisoara, Buletinul Științific Al Universității "Politehnica" din Timișoara, Tom 51 (65)/2005

10. **Dan D.**, Stoian V., Nagy-György T., Dăescu C. - Energy efficiency of old and new buildings, Sustainable construction. Materials and Practice, Challenge of the Industry for New Millenium SB'07, Lisabona Portugalia, 2007, p48-55, (**ISI Proceedings**)

2. Experimental and Theoretical Studies Concerning the Load Bearing Capacity of Steel and Composite Joints for Buildings Placed In Seismic Areas

Summary: In the last period the interest for multi-storey buildings has increased due to the development of the cities around the world. In fact the price of the land has increased so much as that investors want to build tall buildings in a small areas. The general behaviour of the tall buildings is analyzed using dedicated software, but many times the particular elements must be studied in experimental laboratories.

At the “Politehnica” University of Timisoara, it was developed a theoretical and an experimental program for a specific steel and composite (steel-concrete) joint, used for a multi-storey building. The testing specimens were designed both for the structural steel and the composite joint. The calibration of the experimental elements was performed in the elastic and post-elastic range using numerical analysis. The main objective of the studies was to observe and evaluate the behaviour and the failure mode for steel and composite joint. Two load hypotheses on the joint were considered: symmetrical and asymmetrical.

Keywords: composite steel-concrete joint, structural analysis, nonlinear analysis, post elastic behaviour, experimental tests.

2.1 Introduction

The design of the building structures placed in a seismic area deals with some special provisions in order to satisfy the design concept for earthquake loads. In the case of steel and steel-concrete composite structures, the designer must conceive special details according to these specific codes: Eurocode 3 [2.1] or Eurocode 4 [2.2].

The energy dissipation approach, for the design of buildings in seismic zones, imposes specific provisions in order to dissipate the seismic energy through suitable mechanisms, which concentrate inelastic deformations in predefined zones.

Thus, some inelastic deformations must be concentrated in predefined zones for seismic energy dissipation. Therefore, it is important to evaluate correctly the load bearing capacity of each basic structural element, such as beams, columns and joints too.

Next, one example of structural design of steel-concrete structures is presented underlining the above mentioned philosophy design. The joints are calculated as rigid joints realised by welding technology.

For the designed structure some numerical analysis were performed in order to confirm the joint behaviour. One of the first composite and one the most representative construction built in Timișoara is an administrative building assembly. The Timișoara city is located in a seismic zone with $a_g=0.16g$. The assembly consists of three main buildings each of them having a different number of storeys; the functional requirements to have wide spaces at each level, led to a skeletal frame system for each building. All these buildings are provided with an underground level, but different numbers of upper levels.

The highest (Figure 2.1) has 12 levels. For each building, the underground level consists of a stiff reinforced concrete box, composed of an assembly of structural walls and columns together with floor and footings. The upper levels are space frame structure and consisted of plane frames arranged in two orthogonal directions, connected through reinforced concrete floor slabs. The beams are steel welded members and the columns are steel-concrete composite elements.



Figure 2.1 Main façade of the administrative building



Figure 2.2 Structural skeleton of the administrative building

The structural solution is justified by the span width with unexaggerated cross sectional dimensions for the columns, adequate lateral stiffness and cost effective fire protection, due to the presence of the concrete. Complete prefabrication in the workshop, followed by the transportation of the structural elements and their erection in the final position assure a high construction rhythm (Figure 2.2). The composite system has the desired characteristics of the conventional systems, such as strength, stiffness and ductility. Also it represents a performing system, as a seismic resistant system for buildings.

2.2 Steel – Concrete Composite Structure For Multi-Storey Buildings

2.2.1 Structural detailing

The columns were realised as composite elements. The structural steel of the columns was realised as double symmetric section composed by welded steel plates. It is particularly suitable for transmitting bending moments in both axes. The reinforcement is realised from longitudinal steel rolled bars tied with transverse steel reinforcement - square and octagon ties.

The composite beams are I sections, obtained from welded steel bands connected at the upper flange with reinforced concrete slab by shear connectors (Figure 2.3).

The steel section of the central part of the beams has hexagonal holes in the web to access technological ducts as can be seen in Figure 2.4.

Because the Romanian seismic code provisions (P100-1992) imposes rigid connections between beam and column frames, the steel beams were designed as follows: two cantilevers welded at the columns adjacent to beam span by the complete penetration technology and a central part which will be welded at the constructional site.

The connection between the cantilever part and the central part of the transverse beam is represented in Figure 2.3. The connection consists of a flange front welding and web continuity by two steel welded plates.

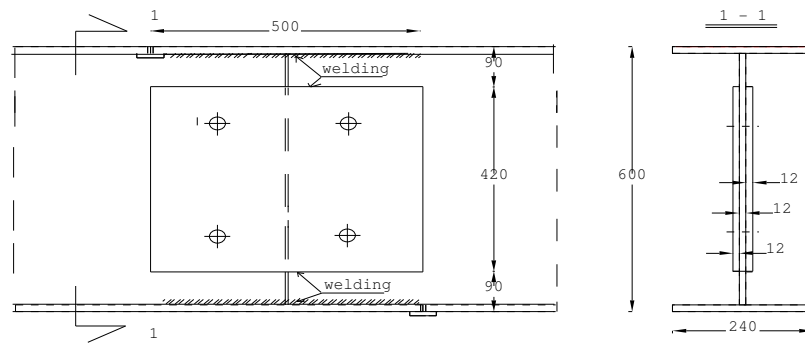


Figure 2.3 The typical beam connection

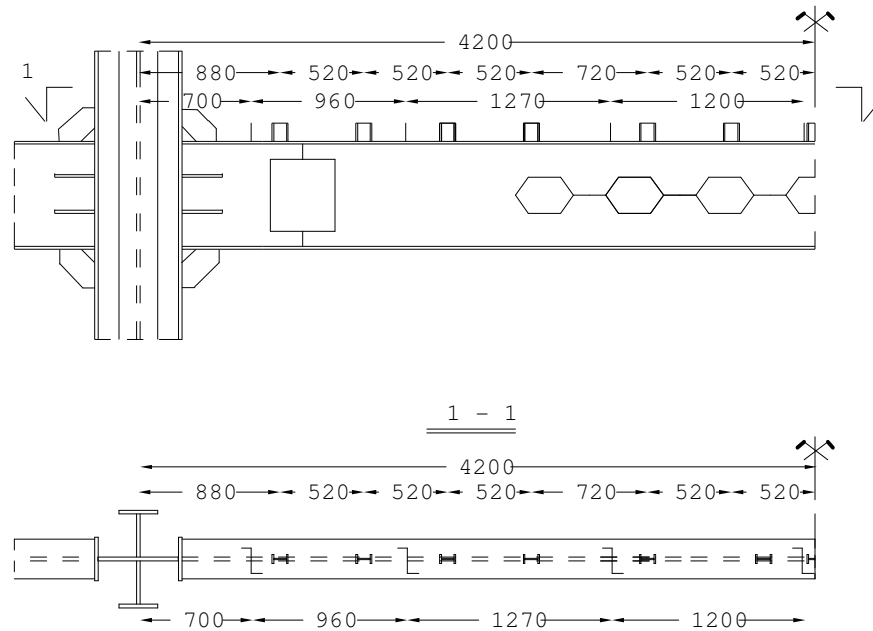


Figure 2.4 Beam connectors

For the inner space between the main beams a rectangular simply supported steel grid was provided. The secondary beams were realised as composite beams, too. The steel part of the secondary beams is represented in Figure 2.5.

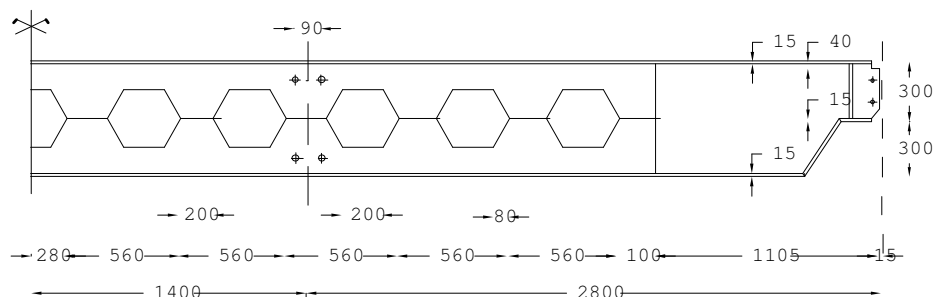


Figure 2.5 Typical secondary steel beam

The bracing diagonals, made up as I steel section, are connected by welding to the gusset plate, and located in the web plane of the beam, respectively at the corner joint.

The cross sectional characteristics, as can be seen in Table 2.1, were determined accordingly

to the stress design values.

Table 2.1. A/U ratio for the structural elements

ELEMENT	Frame beams	Secondary grid beams	Braces
A/U (m)	100-165	160-240	115-160

The floor system was realised by precast reinforced concrete slabs monolithically connected at the upper part of the supporting beams.

The columns were designed and made as steel-concrete composite section, using Eurocode 4 [2.2] code (Commission of the European Community). A typical detail of the column structural steel is represented in Figure 2.6 and of composite one in Figure 2.7.

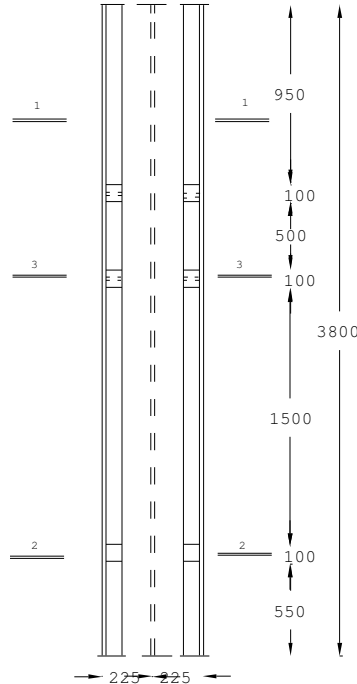


Figure 2.6 Typical structural steel for composite column

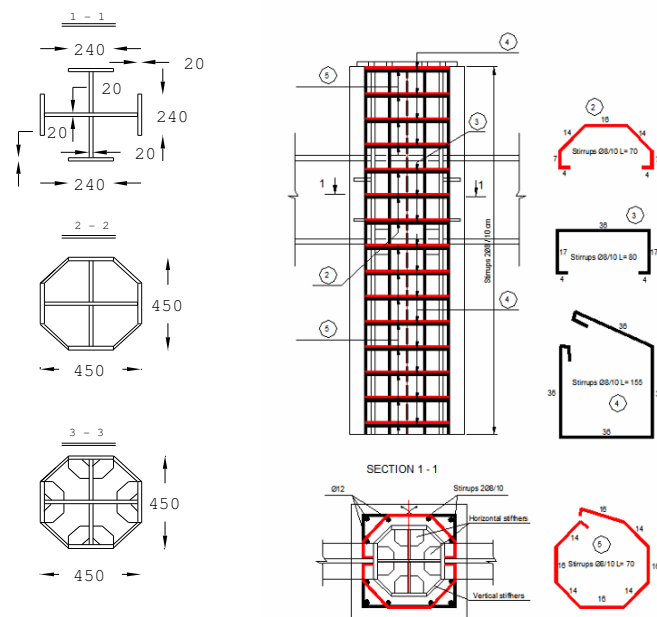


Figure 2.7 Details of composite column and joint

The structural solution imposed the construction technology. Thus, the first phase was the erection and the welding of the structural steel components; forming a steel skeletal structure using steel welded vertical elements for the columns. Continuity joints between rigid reinforcement were provided in the minimum moment section on the level height. As a result a space steel skeletal structure was realised (Figure 2.8). The steel structure was anchored with anchor bolts embedded in concrete.



Figure 2.8 Structural skeleton under construction



Figure 2.9 View of structural steel for composite joint

The vertical reinforcement of the composite column is also anchored in the concrete zone. The anchorage zone for the structural steel is considered at the middle height of the underground level. This solution was provided for several reasons, such as: incompatible dimensions of the anchorage zone with the column section, to avoid creating a shear sensitive section at the structure base, inconsistent provisions for the composite steel-concrete column base sections, difficulties for the detailing design in these sections and insufficient knowledge of the behaviour of these connections. Then a second phase in which elastic reinforcement for columns followed. The third phase consists in cast in place concrete using column form work. Finally, the reinforced concrete slabs were placed over the steel beam girder.

2.2.2 Structural system

The multistorey building of 9, partially 12 levels is placed in a seismic zone with $a_g=0.16g$, according to Romanian Seismic Code (Figure 2.10).

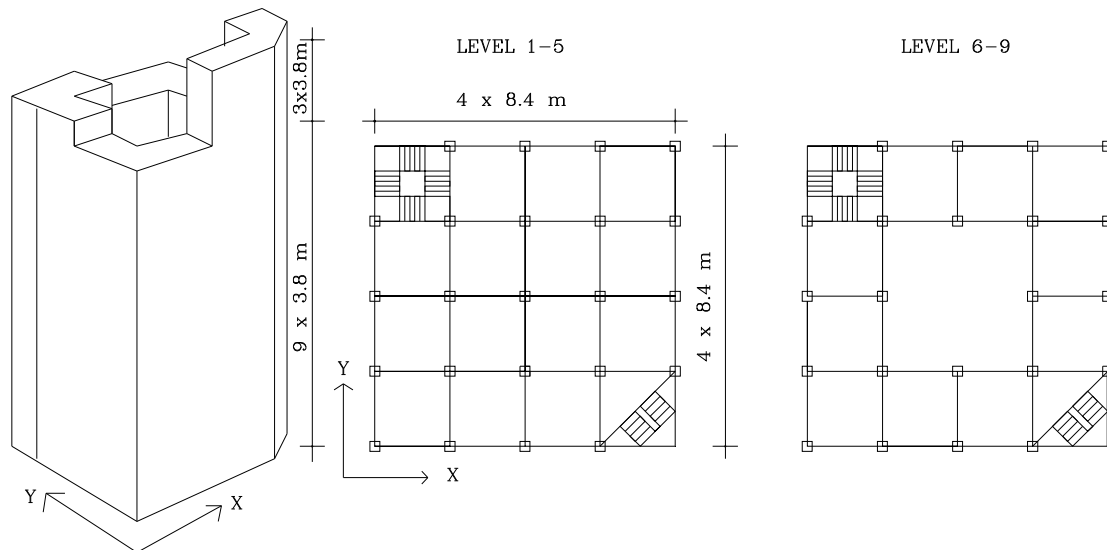


Figure 2.10 The building structural system

The structural system consists of a stiff spatial reinforced concrete box as infrastructure, in which there are embedded the component elements of the structure. The columns and the beams of the spatial skeleton of the structure are designed as steel-concrete composite elements.

2.2.3 Structural stiffening

The structure is stiffened with eccentric braces made from steel diagonals, placed between the bottom end of the column-beam joint and the bottom part of the cross section of the beam frame at the next level.

In order to stiffen the structure due to the effect of the horizontal loads, two variants of braces positioning were studied:

- A variant - at which the braces are placed on the exterior part of the building in two consecutive spans on each side (Figure 2.11A);
- B variant - at which the braces are placed in the four corners of the exterior part of the building (Figure 2.11 B).

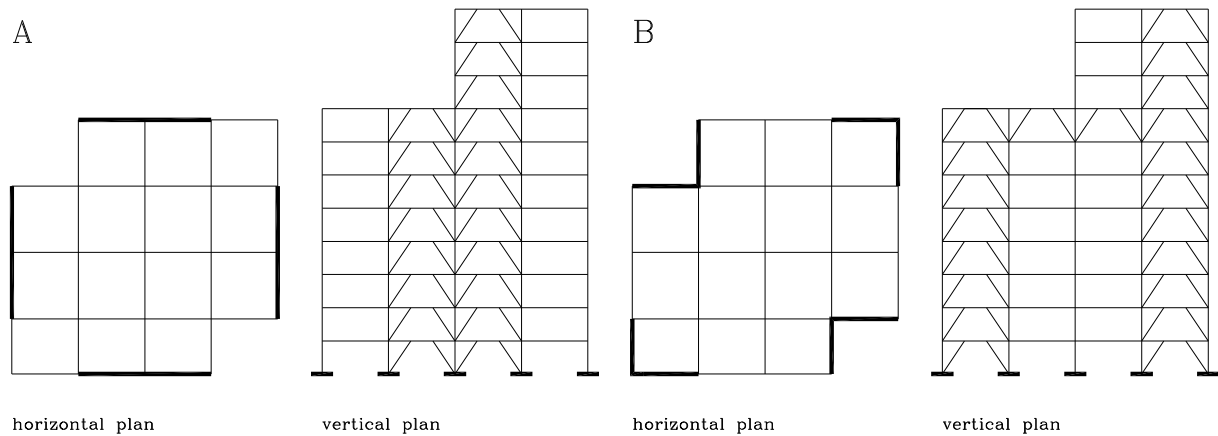


Figure 2.11 Braces positioning

In both two variants the braces consist of diagonal bars subjected to axial forces. Therefore, the modal response of the structure, lateral displacements and the relative level stiffness are affected by the number of braces rather than by their position (Table.2.2).

Table 2.2. Structural modal response

PERIOD (s)	1	2	3	4	5	6
VARIANT A	1.48	1.43	1.12	0.55	0.54	0.40
VARIANT B	1.53	1.47	1.37	0.55	0.53	0.48

Modal response of the structure and axial forces in the columns are highly dependent by the braces position, as shown in Table 3.

Table 2.3. Displacements, horizontal forces and stresses

VARIANT	A			B		
	1_y	1_x	1_{teta}	1_y	1_x	1_{teta}
d_x (mm)	-2	34	-7	-9	24	-23
d_y (mm)	34	2	6	23	22	14
teta (rad)	0.0003	-0.0002	-0.002	0.0014	-	-0.002
					0.0004	
F_x (kN)	-630	10760	-570	-2460	7340	-5370
F_y (kN)	10830	840	500	5710	6470	3170
M_{teta} (kNm)	15740	16340	53690	72320	-7600	-86140
M_{maxsup} (kNm)	-320	874	86	-690	690	-90
M_{maxinf} (kNm)	1099	-2443	-358	19400	-1755	303
N (kN)	-4506	-1024	702	940	-3556	1050
M_{minsup} (kNm)	352	82	-52	340	140	-140
M_{mininf} (kNm)	-1854	-314	282	-1529	-835	367
T_{max} (kN)	209	-422	-73	336	-286	57
T_{min} (kN)	-395	-61	61	-311	-181	59

The dynamic analysis reveals that the structure has a geometrical and mechanical symmetry toward one of the diagonal axis. This direction becomes the principal inertial direction in the second mode. Due to the little mass inertia moment at all levels, the general torsional moment is not very high, and the structural response being uncoupled (Figure 2.12).

As a conclusion, the effect of the braces can be studied on a plane frame.

The square form of the building plane admits as symmetry axes both the sides and the diagonal. These axes will be found in modal analysis as principal axes, thus:

- side: if it will be accentuated the stiffness upon the side (variant A);
- diagonal: if it will be placed corner braces (variant B) and eccentrically mass positioning. In

this situation the dynamic structural response is coupled.

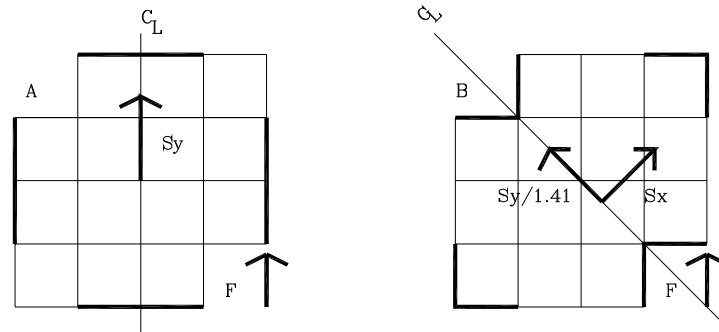


Figure 2.12 Principal structural axes

Based on these conclusions the local effect of the braces positioning was analyzed on a plane frame. As a conclusion, it is obviously that providing the braces in the central spans (variant A) has an advantage in the distribution of the axial forces due to horizontal loads (Figure 13).

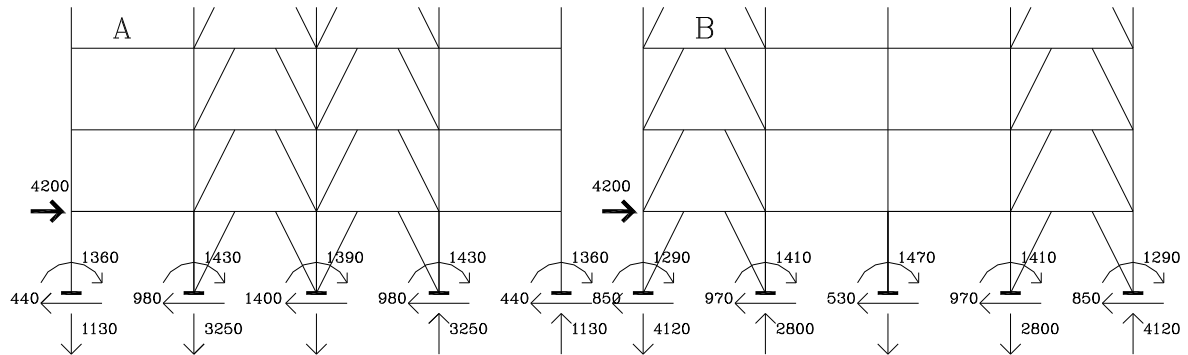


Figure 2.13 Axial force distribution in a plane frame

Variant B gives a coupled dynamic response of the structure and determines a bigger general torsional moment.

Absolute and relative displacements reflect the monotonic character of the structure, with different values at the top levels (Table 2.4).

Table 2.4. Extreme relative structural displacements

VARIANT	A	B
d_{rmax}/H_{level} (mm/m)	10.356	22.372
d_{rmin}/H_{level} (mm/m)	3.3	3.48

2.2.4 Seismic analysis

The modal analysis was performed using SAP software for the space frame model as it is shown in Figure 2.14, in which the typical plane frames and floor plane models are represented, too. The eccentric braces are provided on the perimeter of the space structure.

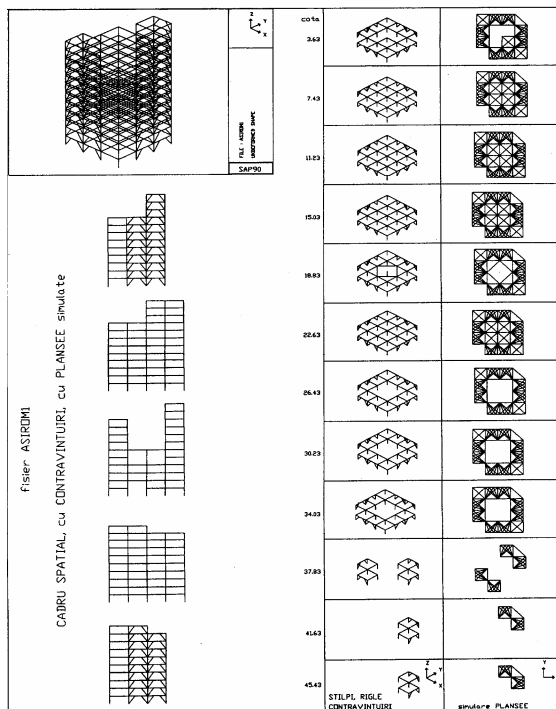


Figure 2.14 Space frame model

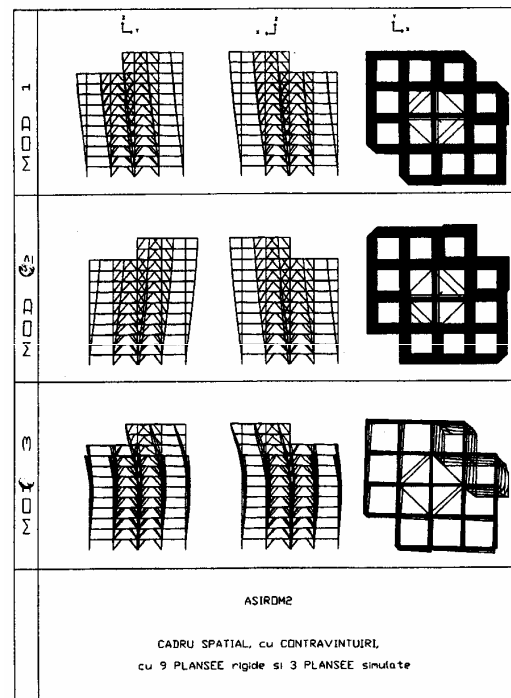


Figure 2.15 The first three mode shapes

The first three mode shapes are represented in Fig. 15. The structural behaviour shows that the eccentric highest levels have no significant influences over the general behaviour. Also, the holes at the several floor levels do not affect the floor stiffness or the overall behaviour; the floor systems at all levels being in the small deformation domain.

The characteristic aspects of the structural behaviour are the followings:

- the inertia principal axes are the diagonals of the rectangular plan. Therefore the mode shapes are coupled and the columns are subjected to biaxial eccentric compression;
- the torsion general effect is not important and can be neglected.

This assumption is accepted also due to the fact that the structure has structural and dynamic double symmetry having small inertia moment, the structure was provided with identical beam span on both directions and columns with square section. All these particularities induce a general seismic response similar to the response of a plane frame. The floors were modeled as rigid in their own plane. The first three fundamental mode shapes are two coupled translations upon the floor plane diagonals, followed by the torsion mode shape. The fundamental three periods are $T_x=1.49s$, $T_y=1.48s$, $T_\theta=1.15s$. The maximum drift was 0.00572. The superior mode shapes are under $T=0.60s$.

In the Table 2.5, the shear level forces for the first level are presented.

Table 2.5. Shear level forces at first level

LEVEL	ID	DIR	1	2	3	4	5	6
			ϵ	η	θ	ϵ	η	θ
1	level 1	X	-749.95	778.47	56.09	123.02	-32.93	-46.94
2	level 1	Y	742.38	786.41	-55.53	-122.69	-133.31	46.44
3	level 1	θ	2371.6	-0.43	5352.85	-2099.87	3.28	-1885.31

2.3 Theoretical Study on Steel – Concrete Composite Joint

The used composite steel-concrete joint is conceived as a space structure (with horizontal stiffeners between the web and the corresponding flanges and vertical stiffeners between the column flanges) being embedded in concrete which is “confined” with ties around the reinforcement and the structural steel of the column, as it can be seen in Figures 2.16 and 2.17

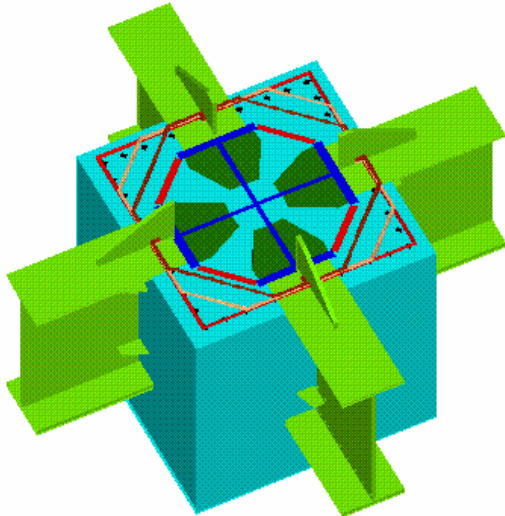


Figure 2.16. Steel – concrete composite joint



Figure 2.17. Details of constructional work for composite column and joint

Due to the technological process, a composite structure is initially a steel structure. After placing the reinforcement and the concrete casting, the structure becomes a composite one.

The entire structure was built as a steel-concrete composite construction. The structural type is a space skeleton bar structure using plane frames placed on two orthogonal directions, being connected through the floor slabs.

The structural solution is justified by the span width with unexaggerated cross sectional dimensions for the columns, adequate lateral stiffness and cost effective fire protection, due to the presence of the concrete. The general view of the composite joint is presented in Figure 2.16. Few relevant aspects from the constructional site are represented in Figure 2.17.

As it is known, the structure becomes a composite one after the longitudinal reinforcement and the transversal reinforcement are placed on site and the concrete are cast into the column mould.

The composite steel-concrete joint which was tested belongs effectively to the composite steel-concrete structure already erected and finished.

The reasons which for the joints as composite element were studied were based on the following aspects, revealed into the design process:

- the contribution of the reinforced concrete floor slab at the cross section of the beams was neglected into the overall stiffness evaluation of the space frame;
- the cross section of the composite beam is composed by a reinforced concrete precast slab and steel I profile. The connectors were provided only along the steel beam, but not into the joint zone;
- in the joint zone, the continuity of the reinforced concrete slab was interrupted due to the technological process, thus the reinforced concrete precast slab as part of the floor system, was not provided as an continuous reinforced concrete element over the joint zone, and therefore was not considered as part of the composite joint.

The calculus of the experimental model was made for all components. Thus the design

moment was evaluated for beam, column and joint. It was important to evaluate the design capacity of the column and the beam because the aim of the experimental program was to study the behaviour of the joint and the failure mode. The aim of this study was to obtain the collapse in the joint panel rather than outside the joint. Initially, using the real dimensions used in practice, for the column and beam a numerical analysis was performed and we observed the tendency to have a plastic hinge at the exterior of the joint.

To evaluate the stresses in the structural steel web using the axial stress state relations is irrelevant, because the joint is in the Plane Stress State, the undeformed section hypothesis being nonrealistic. In such conditions, to consider the connection between the beam and column exclusively on the basis of the Eurocode 3 [2.1] as unstiffened joint, neglecting the presence of the stiffeners and the favourable effect of the confinement, is a simplified scheme, inadequate with the physical reality of the problem. In order to demonstrate that, the authors present in the paper a finite element analysis, comparing various cases of detailing and loading. Similar conclusions were drawn on the basis of nonlinear numerical analysis.

2.3.1 Structural steel joint analysis

The first analysis was performed for the structural steel joint (Fig. 2.18) to evaluate the strength and stiffness. The analysis was realised using the dedicated software SAP. The finite element mesh is represented in Figure 19.

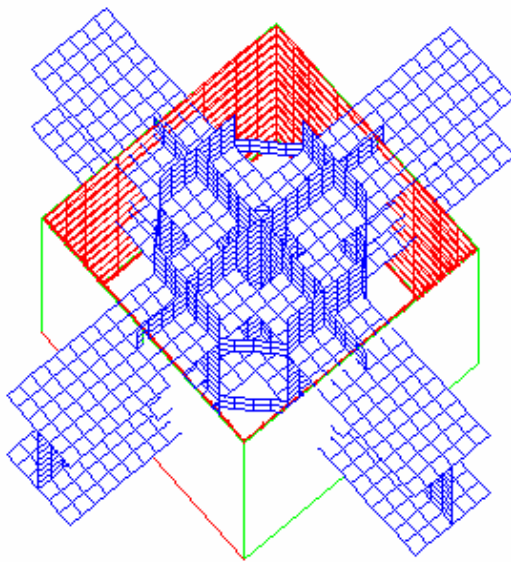


Figure 2.18 Structural steel elements of the composite joint

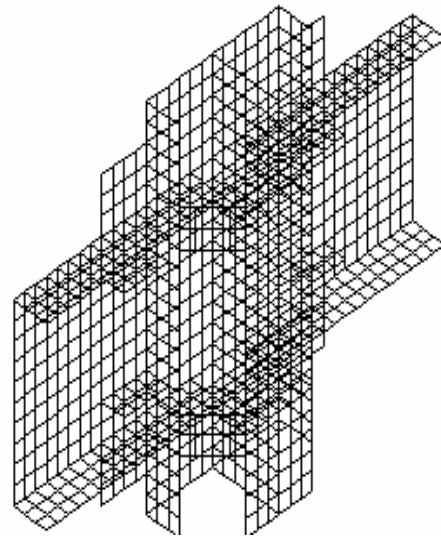


Figure 2.19 Finite element mesh of the structural steel joint (half part, one direction analysis)

Two load hypotheses were considered (at beams extremity):

- I- symmetrical vertical eccentric loads;
- II- asymmetrical vertical eccentric loads.

These two loads hypotheses simulate the permanent loads, and respectively the horizontal (seismic) loads acting on the structure and the corresponding joints.

The isostresses σ_{\max} are represented in Fig. 2.20 and 2.21.

There were analyzed three typical steel joints: author's joint (a), stiffened (b) and unstiffened (c).

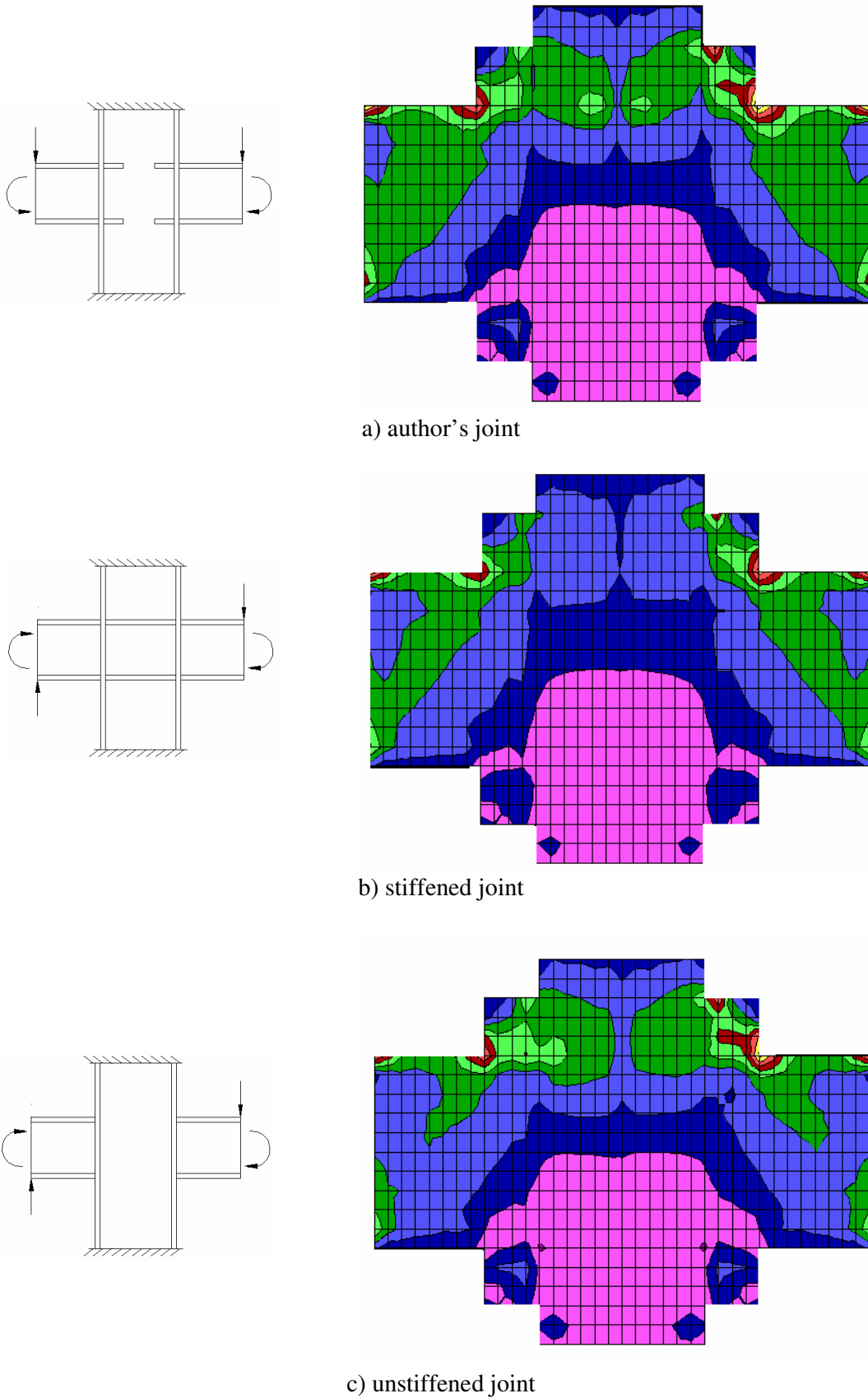


Figure 2.20 Isostresses σ_{max} in the structural steel joint- mid-plane view-symmetric load

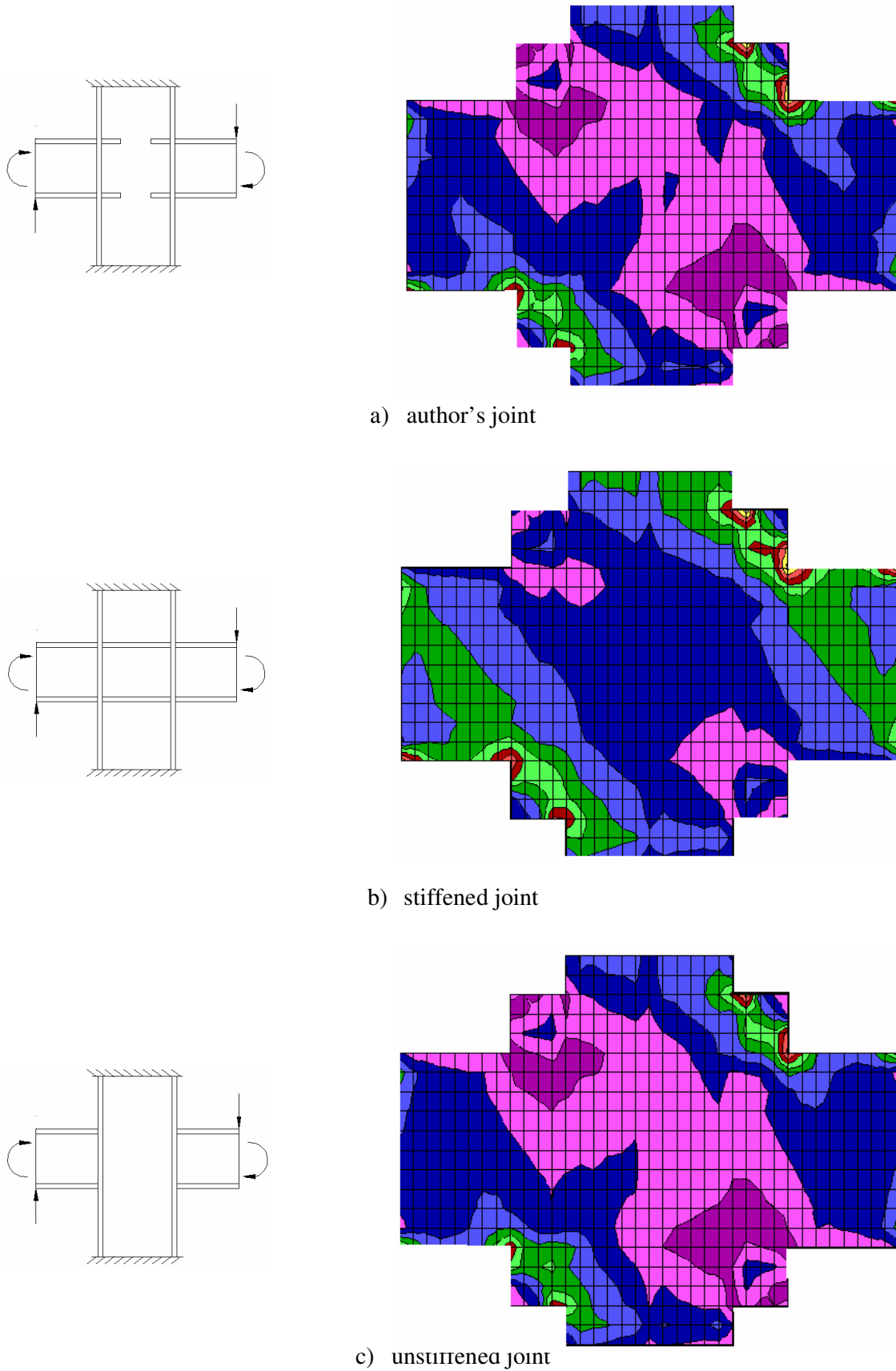


Figure 2.21 Isostresses σ_{\max} in the structural steel joint- mid-plane view- asymmetric load

The analysis of the joint Stress State reveals the following aspects:

- the finite element analysis of the structural steel joint shows that all the joint steel elements (web, flanges, stiffeners etc.) are loaded;
- the web buckling is avoided because the structural steel is realised as double symmetrical section;
- the results show that, in all the loading cases, the peak values for the stress were found outside the joint zone (exactly in the vertical stiffeners) not in the structural steel web;
- existence of horizontal and vertical stiffeners must not be neglected; due to the connection between these elements;
- stress level in the joint is lower than in the beam zone adjacent to joint;
- stress concentration in the joint web is located in a zone between the horizontal stiffeners and the perpendicular web, but the level stresses do not overpass the stress level in the beam web;
- the peak stress location is not near the flange because the joint is provided with stiffeners;
- plastic zones in the web structural joint ("b" zone accordingly to EC3) cannot be reached than after the yielding of the vertical stiffeners between the beam and column flanges;
- the stress level in the joint web, in an unstiffened joint, is quasi-equal with the stress level in the beam web. Therefore a possible plastic zone in the column web is not to be expected.
- in the case of asymmetrical loads (seismic case) the stress level is generally lower than in the case of permanent loads.

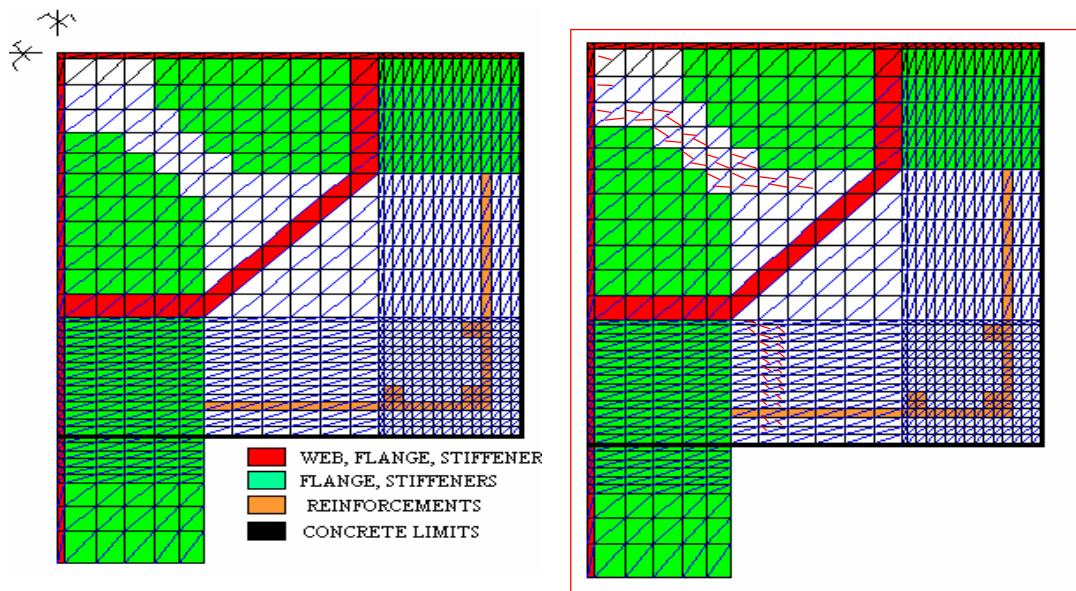
2.3.2 Composite steel-concrete joint analysis

Due to the technological erection process the structure is initially a steel structure, but after placing the reinforcement and the concrete casting becomes a composite one.

The simplified tendency to take into account only the structural steel is inadequate and cannot be sustained, due to the following considerations:

- There is a redistribution of the stresses between the concrete, reinforcement and structural steel;
- the connection between the structural steel flanges and the web is in a zone where the stress distribution must take into account the reinforcement and the concrete; the stress state is far from a pure steel stress state.

Similar conclusions can be stated using a non-linear analysis of the joint as reinforced concrete. The non-linear analysis was performed using BIOGRAF software for both horizontal and vertical section of the joint, using the assumption of the plane Stress State. The horizontal section was considered at the level of the beam flanges. The results were presented in Figure 2.22.



a) topology

b) crack distribution

Figure 2.22 Plane stress analysis for composite joint horizontal layer

It was revealed the same quasi-equal stress levels in the joint web as in the beam web. There were detected stresses in all the elements of the joint (structural steel, concrete, and reinforcement), i.e.: the joint behaviour is far from a simple steel joint. It is also obvious that the column concrete in the joint section avoids the web buckling.

Another nonlinear analysis was performed for the vertical section (Figure 2.23). As it can be seen in the Figures 2.24 and 2.25, the crack distribution is similar to those of a typical reinforced concrete joint.

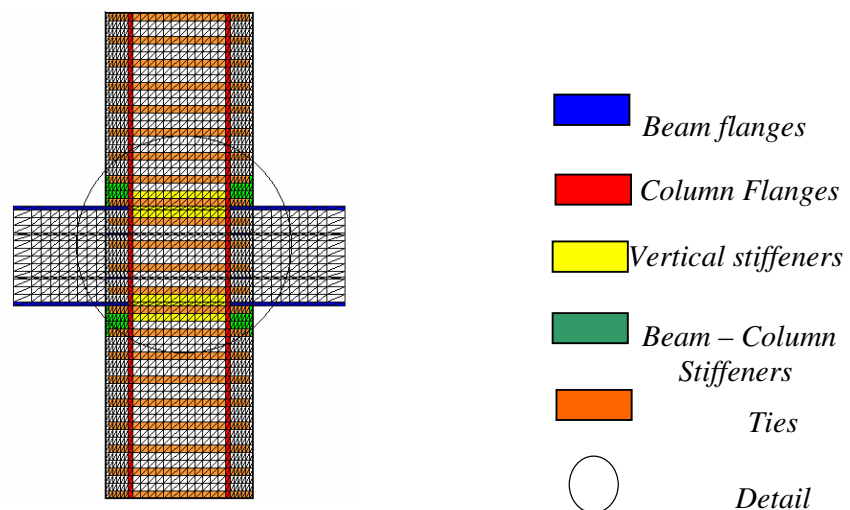


Figure 2.23 Mesh of analysed composite joint (vertical section)

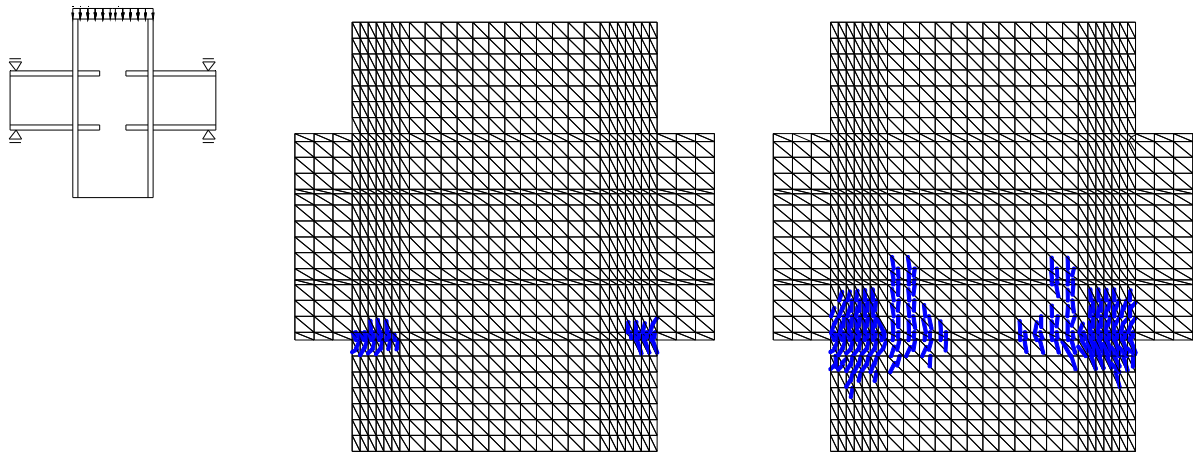


Figure 2.24 Evolution and distribution of cracks – symmetrical load

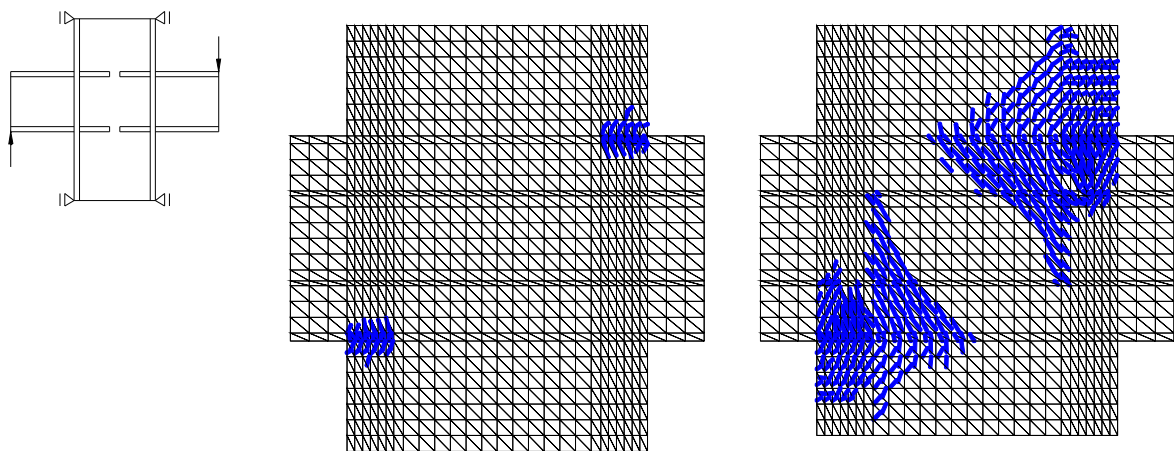


Figure 2.25 Evolution and distribution of cracks – asymmetrical load

The analysis revealed the plastic zone outside the joint in the steel beam section. The strain distribution in the vertical sections is represented in Figures 2.26 and 2.27.

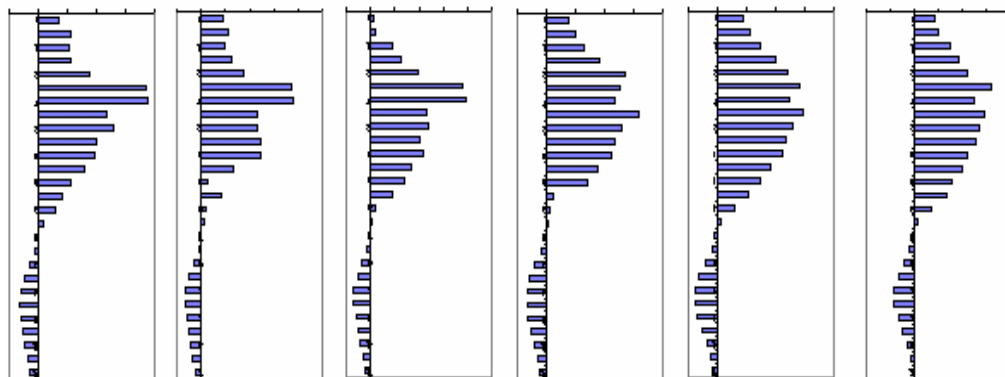


Figure 2.26 Horizontal strain distribution in the vertical section of the joint: symmetrical loads

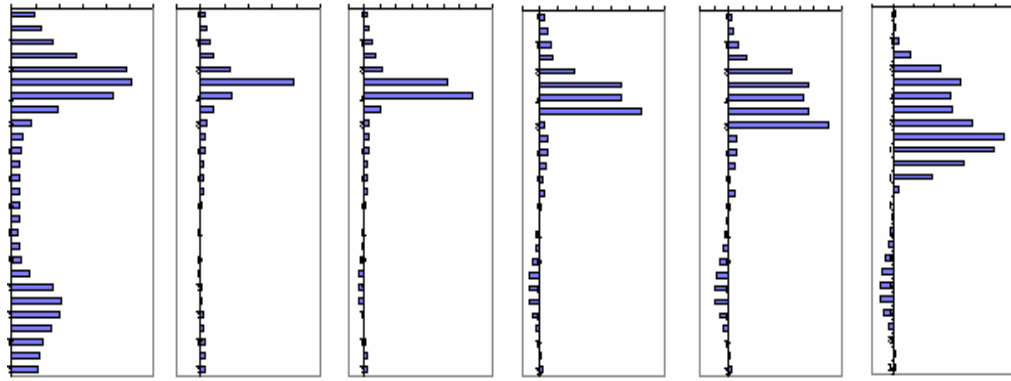


Figure 2.27 Horizontal strain distribution in the vertical section of the joint: asymmetrical loads

As it can be seen, the compressed zone represents about 30 % of the section height; using that value the design moment resistance $M_{j,Rd}$ is of 2059.37KNm. The nonlinear numerical prediction is 1920 KNm. The plastic moment in the beam cross section near the joints is $M_{pl,beam} = 1570$ KNm. It demonstrates that the plastic hinge will not appear in the joint or in the column.

All these conclusions validate the initial assumption that the joint must be understood and designed as a composite steel-concrete element, in spite of insufficient knowledge of the behaviour of such joints.

2.4 Experimental study on steel – concrete composite joint

An experimental testing program for the specific steel - concrete composite joint, used at the construction work of the administrative building, was developed at the "Politehnica" University of Timisoara. Starting with the joint type used, eight joints were considered as experimental specimens. The joints were initially analysed together with their connections – the beams and the columns in order to determine the dimensions of the joint components, thus, satisfying the desired collapse mechanism at the joint zone.

As it is known, in reality, the plastic hinges must appear outside of the joints into the beams. The aim of the study was to obtain the collapse in the joint panel rather than outside the joint, in order to compare the bending moment resistant of the steel joint with the bending moment resistant of the composite joint. Were also studied the failure mechanism of the steel joint and compared it with the composite one. Initially, the joint was design by using the Eurocode 4 [2.2] code. Then a numerical study was performed in the elastic and post elastic range. Finally, the experiment was performed using special testing equipment, and the international recommended testing procedures.

The calculus of the experimental model was made for all components. Thus, the design moment was evaluated for: beam, column and joint. It was important to evaluate the design capacity of the column and the beam because the aim of experimental program was to study the behaviour of the joint and the failure mode. The aim of this study was to obtain the collapse in the joint panel rather than outside the joint. Initially, using the real dimensions used in practice, for the column and beam a numerical analysis was performed and we observed the tendency to have a plastic hinge at the exterior of the joint. Because the purpose of the testing was the study of the joint failure mode and the checking of its bearing capacity, in the situation presented above, it was suggested the increase of the beam bearing capacity by increasing its flange width and its web as well, and by maintaining the column section and the height of the beam, respectively.

2.4.1 Calibration of the experimental joint. Numerical analysis

In order to evaluate the stress state in the joint and the behaviour study of the dimensioning element, on the geometrical dimensions basis, some numerical analyses have been done using the finite element method. In the first stage, the SAP 2000 numerical analysis programme was used, the modeling been done by type SHELL finite elements, for the structural steel in the joint.

To have a clearer view of the stress state in the joint, the model analysed was done according to the testing mode. Taking into consideration the possibility of making an experimental test, we drew the conclusion that the instruments, which we had at our disposal, allow the loading of the column and the mounting of some joint supports, at the extremity of the two beams that concur in the structural joint. In fact this loading type simulates the real situation when the loading is actually on the beams. The schematization of the testing mode and of the actual loading is presented in Figure 2.28.

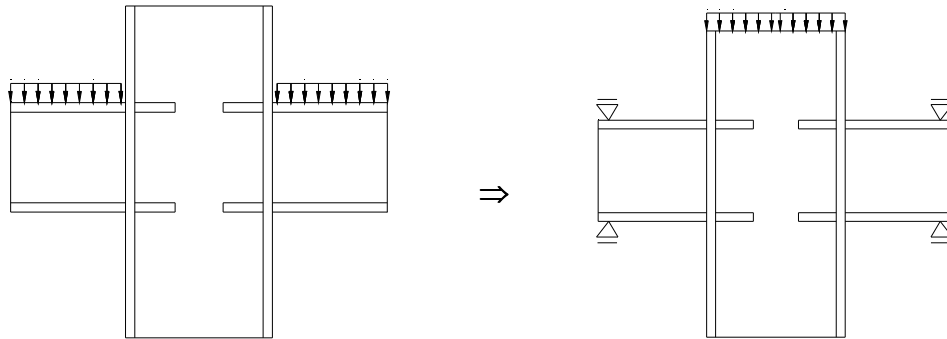


Figure 2.28 Schematization of the real load case and experimental testing

The results of the numerical analysis on the structural steel of the experimental element, obtained initially as a result of the design, are presented in Figure 29.

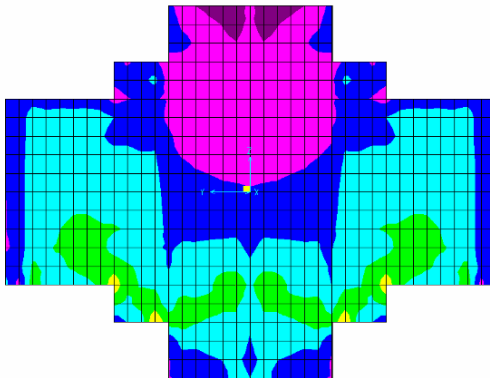


Figure 2.29 Stresses σ_{\max} for steel joint (mid-plane view)

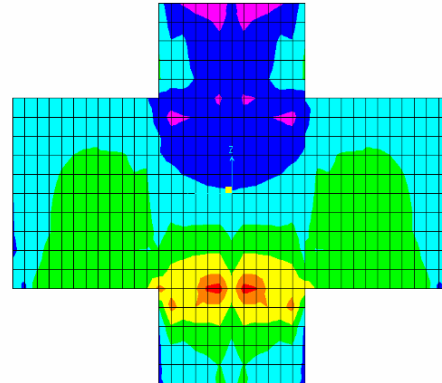


Figure 2.30 Isostresses σ_{\max} for the steel joint (mid-plane view)

By the analysis of the diagrams of the efforts in the joint, we can observe that there is a concentration of stresses in the vertical stiffeners which connect the beam to the column. The value of the maximum stresses in the stiffeners is of 450 N/mm^2 , and in the web of the column or in the beam of $\sim 300 \text{ N/mm}^2$.

These observations lead to the idea that in case of an experimental testing on a model, made up as above, there is the possibility of tearing outside the joint, starting from the vertical stiffeners and continuing with the beam.

Because the purpose of the testing was the study of the joint failure mode and the checking of its bearing capacity, in the situation presented above, it was suggested the increase of the beam bearing capacity by increasing its flange width and its web as well, and by maintaining the column section and the height of the beam respectively.

The purpose of the testing being also to obtain information on the stress state inside the joint and thus to cause the failure in the joint, the decision was to eliminate the vertical stiffeners, which became useless in this case. The vertical stiffeners are useful in real structures because they increase the bearing capacity in the joint zone, the plastic hinge taking place in the beam and not in the joint.

The vertical stiffeners are useful in real structures because they increase the bearing capacity in the joint zone, the plastic hinge taking place in the beam and not in the joint.

In Figure 2.30 there are presented the isostresses, obtained for the proposed experimental specimen (symmetrical load), after the elimination of the stiffeners. Starting with the geometrical dimensions obtained at the previous analysis for the asymmetrical load cases (Figure 31) the new numerical analysis on the structural steel of the experimental element was performed. The results obtained are presented in the Figure 32.

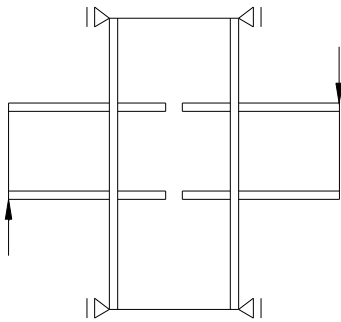


Figure 2.31 Schematization of the experimental test asymmetrical loads

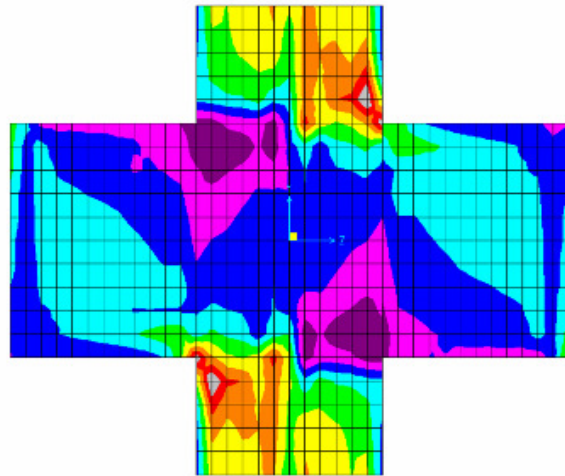


Figure 2.32 Isostresses σ_{\max} for the steel joint asymmetrically loaded (mid-plane view)

2.4.2. Experimental Tests on Steel and Steel Composite Joints under Symmetrical and Asymmetrical Loads

All the experimental tests were performed using the procedure indicated by ECCS [2.21]. For the symmetrical load case, the load was applied at the top of the column for each tested element.

For the asymmetrical load case, the load was applied at the top and at the bottom of the beams flanges of the tested element. The tests were controlled using the displacements devices of the hydraulic jacks. In order to record the behaviour of the tested joints a basic instrumentation was used for both elements. The instrumentation consisted in displacement transducers, inclinometers and strain gauges (Figures 2.33 and 2.34).

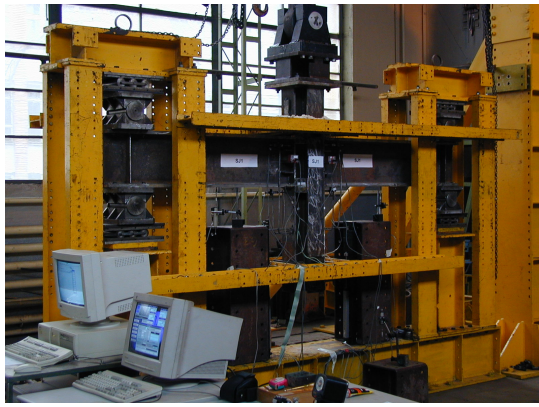


Figure 2.33. General view of testing equipment for symmetrical load



Figure 2.34. General view of testing equipment for asymmetrical load

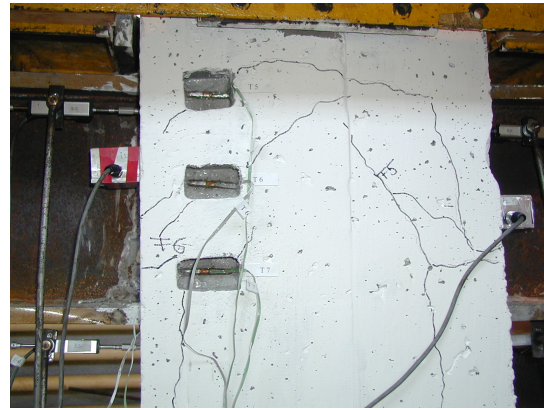
Using the recorded data from the monotonic displacement increase tests made on the steel joint and the composite joint there were evaluated the limit of the elastic range F (kN) and the corresponding displacement e_y (mm).

2.5 Comparative study concerning the behaviour of the structural steel and steel-concrete composite joint under symmetrical and asymmetrical loads

In the pictures shown in Figures 2.35 ÷ 2.36 it can be observed a comparative study between the failure mechanism of steel joints and the steel-concrete composite joints.



a. Front view of steel joint during test



a. Distribution of cracks at the composite steel concrete joint during test



b. Tearing of vertical stiffener



c. Large crack in the joint panel

Figure 2.35. Failure mechanism of steel joint symmetrical load



b. Tearing of vertical stiffener



c. Small crack in the joint panel

Figure 2.36. Failure mechanism of steel-concrete composite joint, symmetrical load

The joints behaviour under symmetrical loads were similar, the failure mode was practically the same. The failure mechanism consists in tearing of the vertical stiffener from beam to column flanges and the cracking of the joint panel at the end of the horizontal stiffeners.

As we expected, in the case of the composite joint, the crack length and the opening in the joint panel were smaller than in the steel joint, due to the presence of the concrete and of the stirrups into the joint.

The comparative study between the experimental elements is based on the moment rotation characteristic diagram recorded at the lateral face of joints. In the Figure 37 it is represented the moment rotation diagram for the steel and the steel concrete composite joint under symmetrical load.

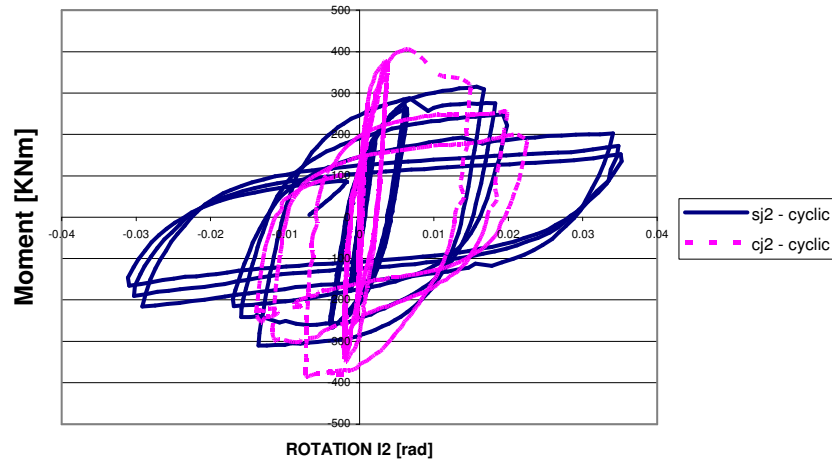


Figure 2.37. Comparative moment – rotation diagram for steel and composite joints under symmetrical loads

The comparative diagrams represented in Figure 2.37 shows a similar behaviour of the joint under symmetrical load, but with different initial value of the stiffness.

Table 2.6. Basic parameters for cyclic tests

	Steel joint (SJ2) / Cyclic test		Composite joint (CJ2) / Cyclic test	
Maximum bending moment [kNm]	+315.5	-310.39	+405.	-382.8
Maximum displacement [mm]	+41.17	-36.8	+27.3	-25.51
Ultimate rotation [mrad]	+35.2	-29.3	+22.3	-13.8
Elastic limit e_y [mm]	6.18		6.38	
Experimental bending moment (elastic limit) [kNm]	+201.4	-215.8	+273.	-284.9

The comparative study between the behaviour of the steel joint under monotonic SJ1 and under cyclic loads SJ2 (symmetrical case load) was performed using the diagrams presented in the Figure 2.38.

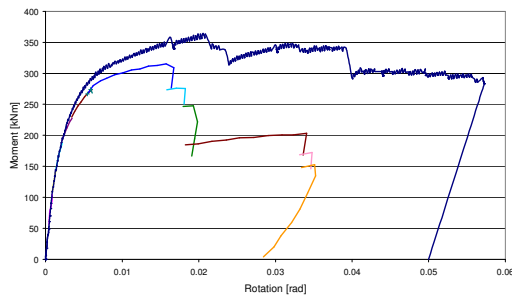


Figure 2.38. Comparative study between the monotonic and cyclic tests (envelope curve) – steel joint symmetrical load

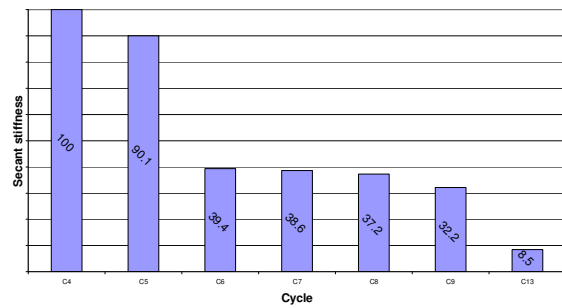


Figure 2.39. Degradation of stiffness during cycles steel joint SJ2

The degradation of the secant stiffness function of the cycles for the steel joint SJ2 is presented in the figure 16. If the initial stiffness is considered as 100%, at the last cycle performed the value of stiffness decrease until 8% from the initial.

A similar comparative study was performed for the composite joint (figure 2.40).

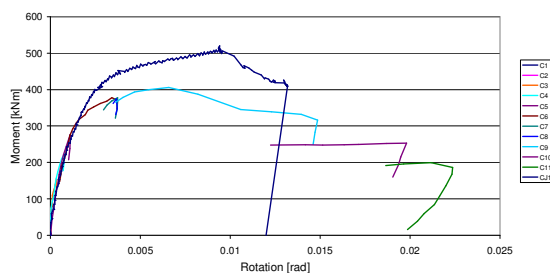


Figure 2.40. Comparative study between the monotonic and cyclic tests (envelope curve) – steel concrete composite joint symmetrical load

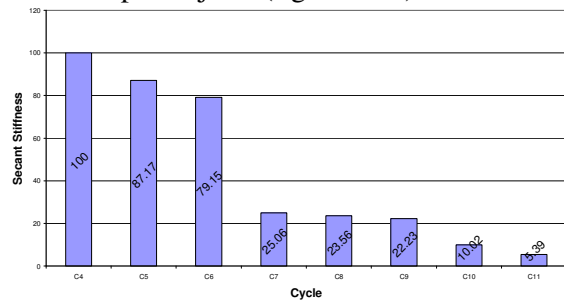


Figure 2.41. Degradation of stiffness during cycles steel concrete composite joint CJ2

The degradation of the secant stiffness function of the cycles for the steel concrete composite joint CJ2 is presented in the Figure 2.41. If the initial stiffness is considered as 100%, at the last cycle performed the value of stiffens decreases until 5.3% from the initial.

The presented diagrams indicate the dissipative behaviour of the tested joints.

In the pictures represented in Figures 2.42 ÷ 2.43 it can be observed a comparative study between the failure mechanism of the steel joints and the steel-concrete composite joints under asymmetrical loads.



a. General view of steel joint – asymmetrical load



a. Distribution of cracks at the composite steel concrete joint during asymmetrical load test



b. Tearing of vertical stiffener



c. General view of joint at failure

Figure 2.42. Failure mechanism of the steel joint asymmetrical load



b. Distribution of first cracks in joint and column



c. Cracks distribution at failure

Figure 2.43. Failure mechanism of the steel concrete composite joint asymmetrical load

The comparative diagrams represented in Figures 2.44, 2.45 show a similar behaviour of steel and composite joints under symmetrical and asymmetrical loads, but with a different initial value of the stiffness. For both tested joints (steel and steel concrete composite joint) the rotation capacity of the joint under symmetrical load is smaller than the joint under asymmetrical load.

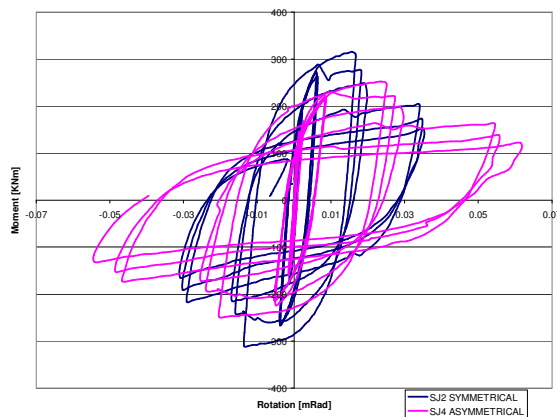


Figure 2.44 Comparative moment – rotation diagram for steel joints under symmetrical and asymmetrical load

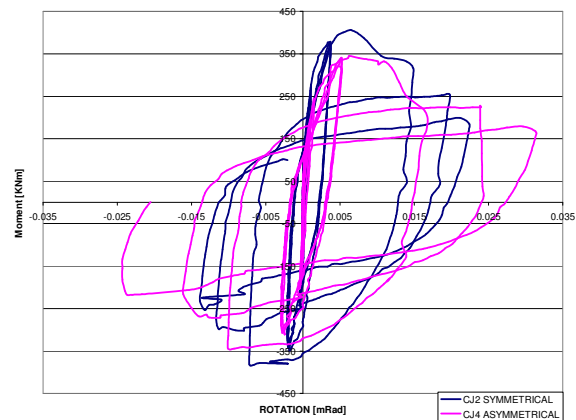


Figure 2.45 Comparative moment – rotation diagram for composite joints under symmetrical and asymmetrical load

The diagrams presented indicate the dissipative behaviour of the tested joints in both load cases, symmetrically and asymmetrically. The variation of the total dissipated energy during the tests is presented as comparative diagrams in Figures 2.46 ÷ 2.47.

As it can be observed the dissipated energy is increasing from one cycle to another but the total energy dissipated at the composite joint CJ2 after 11 cycles is smaller with 35 % than that at SJ2 joint, for symmetrical load case.

For asymmetrical load case the total dissipated energy for steel joint is greater than the total dissipated energy for composite joint. At the end of test, cycle 11, the total energy dissipated by steel joint is double in comparison with the steel concrete composite joint.

The diagram presented in Figure 2.48 shows the differences of total dissipated energy for steel joint under symmetrical and asymmetrical load. The total energy for symmetrical load case is greater for steel joint than composite one.

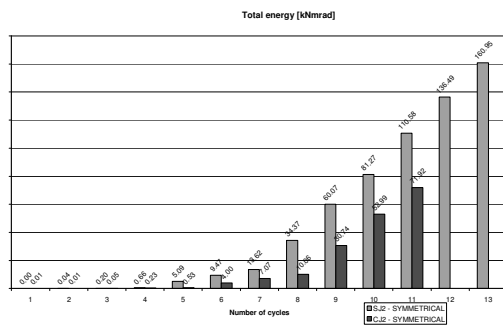


Figure 2.46 Total dissipated energy for steel an steel composite joint under symmetrical load SJ2 - CJ2

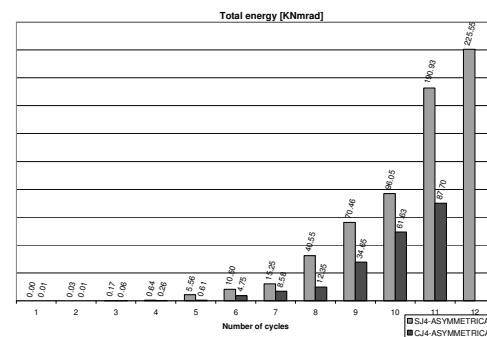


Figure 2.47 Total dissipated energy for steel an steel composite joint under asymmetrical load SJ4 – CJ4

For asymmetrical load case the variation of total dissipated energy of steel concrete composite joints during cycles shows the dissipative behaviour of tested elements.

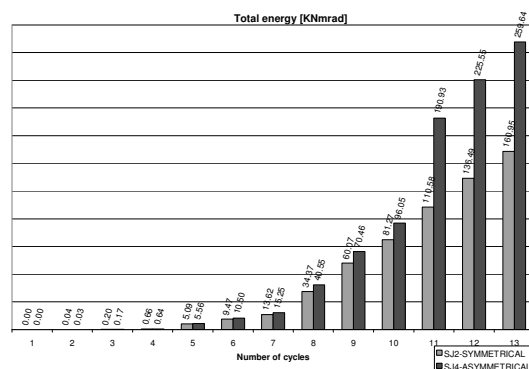


Figure 2.48 Total dissipated energy for steel joint under symmetrical and asymmetrical load SJ2 – SJ4

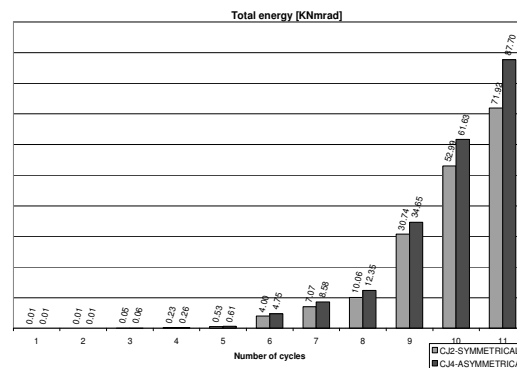


Figure 2.49 Total dissipated energy for steel concrete composite joint under symmetrical load CJ2 – CJ4

Related to the total energy dissipated by steel concrete composite joint we can observe similar values of dissipated energy under symmetrical and asymmetrical load for first cycles but at the end of tests the recorded energy for asymmetrical load case is greater with 22 % than in symmetrical load case (Fig. 2.49).

2.6 Conclusions

Using the results from the theoretical study and the experimental tests the following conclusions were formulated for the specific steel concrete joint:

- the results of the numerical analysis were confirmed during the testing process;
- the tested joints are dissipative;
- due to the technology of the welding the vertical stiffeners cannot be weld by complete penetration; it is considered that the vertical stiffeners play a significant role in the increase of the joint bearing capacity, the weak point being the welding section at the column flanges;
- the behaviour of the steel joint under symmetrical and asymmetrical load is different;
- the behaviour of the steel and composite joint under symmetrical loads is similar;
- the cracks distributions on numerical analysis are similar with the experimental distribution of the cracks;
- the concrete inside the composite joint after testing is crushed; at the exterior face the concrete shows only smeared cracks;

- for the composite joint the crack distribution of concrete is similar to those of a typical reinforced concrete joint;
- the failure mechanism for symmetrical loads starts by the tearing of vertical stiffeners between column and beam flanges, then continues by the buckling of the compressed vertical stiffeners and by the tearing of the joint panel;
- for the tested elements under symmetrical loads, the stiffness of the composite joint increases with 30% due to the presence of the concrete;
- the presence of the concrete in the joint has the effect of increasing the load bearing capacity of the joint;
- as it can be observed, the tested joints are dissipative, with different values of energy dissipation.

As perspectives studies the connection between concrete and structural steel at the joint level can be an interesting subject and finding new technological solution who can assure technological condition to fulfil the joint with casted in place concrete.

3. Theoretical and Experimental Study on Composite Steel-Concrete Shear Walls with Vertical Steel Encased Profiles

3.1 Introduction

The design and the detailing requirements for reinforced concrete ductile flexural walls are based on the capacity design philosophy developed by Park and Paulay (1975) to ensure that significant flexural hinging can occur without the formation of brittle failure modes which is characteristic to shear. This design philosophy is nowadays present in the design codes for reinforced concrete structures and stipulates that the value of the capable shear force associated to a possible shear failure ($V_{R,sh}$) must be higher than the shear force corresponding to the flexural capacity (V_f). This important design philosophy was marked out by the last two decades earthquakes when some examples of shear failure of reinforced concrete wall structures were reported. It is well-known that the good seismic performance of reinforced concrete shear walls is attributed to the concrete compression diagonal; able to transfer the lateral loads from top to base, but sometimes these compression forces, in default of some severe designing details, can produce the crushing of concrete which can produce a structural damage. On the other hand, in the tension zone, the development of the tension cracks in the case of reversed cyclic loading, could lead to a stiffness reduction and higher displacements that could possibly cause damages to non-structural elements and sensitivity to P- Δ effects.

To study the behavior of concrete walls reinforced by vertical steel sections, a theoretical and experimental program was proposed and developed in the Civil Engineering Department at the Politehnica University of Timisoara, Romania. The presented work below was supported by CNCSIS – UEFISCSU project number PNII - IDEI ID_1004, Contract 621/2009, entitled “Innovative Structural Systems Using Steel-Concrete Composite Materials and Fiber Reinforced Polymer Composites”[3.1].

The overall objective of this research project was to investigate the feasibility of reinforced concrete shear walls after the replacing of the boundary reinforcements with structural steel boundary elements having adequate shear connection to the reinforced concrete. The reversed cyclic loading performances of this new type of element are compared with the performances of the concrete shear walls with conventional reinforcement details.

This idea arises from structural reasons but also from technological ones if we are thinking to the congestion of reinforcements which often appear in the boundary regions of reinforced concrete walls subjected to lateral loads. Taking into account the shape and the position of the structural steel encased element, a good confinement of the concrete could be obtained in the boundary region. If we look at the shear walls as the primary lateral load resisting systems in a high rise building, the encasement of the structural steel profiles in concrete could improve the connection between the wall and another structural system, designed to carry out and to transfer the gravitational loads, such as: transfer beams and outrigger beams. Also, the possibility to connect composite steel concrete composite walls by steel or composite coupling beams and the connection between composite walls and moment resisting steel frames or braced frames could be improved.

An experimental program for testing 1:3 scale composite shear wall specimens was undertaken to obtain information on the nonlinear behavior of the elements, including the interface connection between the reinforced concrete wall panel and the boundary members. In order to compare the seismic responses of the steel concrete composite shear walls with the response of the reinforced concrete ductile flexural wall, all the walls were subjected to the same reversed cyclic loading pattern and the tension capacity of the boundary reinforcement was the same for all tested specimens. Secondly, considering two finite element programs specialized in the analytical evaluation on reinforced concrete, numerical modelling of the composite systems, able to predict the behavior of elements, were performed and its accuracy assessed in comparison with the experimental test data.

3.1.1 International literature review in the field of composite shear walls

Composite constructions can correspond to many different structural typologies or systems, as long as concrete and steel are combined. The complete understanding of all the aspects of the seismic behavior of all the types of composite structure requires years of research efforts [3.2].

Composite shear walls originated as reinforced concrete shear walls with encased flat steel bars, steel trusses and steel plates (Tall Building Committee A41, 1979). The research program showed that the deformation capacity of the composite walls obtained by encasing steel truss and steel plate in the reinforced concrete walls was higher compared to traditionally reinforced concrete walls. The use of the composite construction resulted in greater ductility with the load-carrying capacity being limited by the buckling of the concrete-encased steel.

Composite lateral load resisting systems incorporating moment-resisting steel frames with an infill of reinforced concrete were also studied. Chrysostomou (1991) pointed out the importance of composite shear connection between the infilled concrete and the steel boundary elements. Without adequate shear connection, the shear force is primarily resisted by the compression struts in the concrete panel. This compressive strut has finite width and is aligned with the corners of the panel. In contrast, frames with adequate shear connection are able to resist the shear with a field of diagonal compression in the concrete rather than one single strut.

An important research on the field of composite walls was performed by B. Tupper in 1999 [3.3]. He investigated alternative construction techniques for shear walls incorporating structural steel boundary elements, interconnected to the reinforced concrete web of the wall by welding the horizontal bars to the steel profiles. Three experimental tests were performed, two on composite walls and one on traditional reinforced concrete wall. The aspect ratio height/width of the experimental elements was 3.9 and the thickness of the elements was 152 mm. The concrete compressive strengths varied between 25.8 and 38.7 N/mm², while the yield strength of the reinforcements varied between 381 and 487 N/mm². The yield strength of the steel encased profiles was between 377 and 402 N/mm². The axial load level n , defined as the ratio between the axial compression load and the gross concrete strength, was approximately 11% of gross concrete strength. All of the walls were designed to have equivalent flexural capacities and displayed similar ductility and cumulative energy dissipation. The wall specimens were tested to reversed cyclic lateral loads and constant axial loads. The author concluded that the hysteretic responses of the walls with boundary elements were very similar to that of the typical reinforced concrete ductile flexural wall. It was also concluded that the welding of the transverse reinforcing bars directly to the hollow structural steel profiles provided excellent shear connection enabling the full development of the yielding of the boundary elements.

In 2002, A. Astaneh-Asl finalized a report in which there are presented information about the cyclic behavior and the seismic design of composite shear walls made of steel plate and of reinforced concrete encasement walls connected to each other to act as a composite element [3.4]. The test program consisted of subjecting two specimens of traditional and innovative composite shear wall to cyclic storey shear. The innovation consisted in a 32 mm gap provided between the concrete wall and the boundary steel columns and beams. The test specimens were 1:2 scale, three stories and one bay structure. The aspect ratio height/width of the experimental elements was 2 and the thickness of the elements was 75 mm. The concrete compressive strength was 28 N/mm², while the yield strength of the reinforcements varied between 330 and 400 N/mm². The yield strength of the steel plates was between 248 and 345 N/mm². The reinforcement ratio in each direction was 0.92%. The elements were not axially loaded. The research program summarizes that the behavior of traditional and innovative composite shear walls that were tested, indicated that both are excellent systems for lateral load resisting capable of exceeding inter-storey drift values of 4% without reduction in their shear strength. In addition, both specimens were able to reach inter-storey drifts of more than 5% and still maintain, at least, 80% of their maximum strength reached during the tests. In the innovative composite shear wall,

the concrete wall remained essentially undamaged up to inter-storey drift values of about 3% while bracing the steel plate wall, preventing it from buckling and enabling it to reach yielding.

J.F. Hajjar et. al. performed a research program on the cyclic behavior of a composite structural system consisting of partially-restrained steel frames with reinforced concrete infill walls. The composite interaction was achieved through the use of the headed stud connectors along the steel frame–infill interfaces so that the two main components of the system share in the resistance of lateral shear and overturning moment [3.5]. The experimental specimen was one-bay, two-storey of approximately 1:3 scale. Each story was 2.18 m wide and 1.22 m height, measured center-to-center of the steel members. The RC infill wall was 89 mm thick, cast using high-slump concrete. The reinforcement ratio was 0.51% in both the horizontal and the vertical directions. The infill wall was connected to the steel frame using 9.5 mm diameter headed studs at 102 mm spacing. Two special detailing approaches were adopted in the specimen so as to optimize the economy and the energy dissipation capacity of the entire structural system. First, partially restrained connections were used to join the columns and girders to ensure that plastic hinges formed in the partially restrained connections, instead of in the columns or girders, at the state of the incipient collapse. Second, the confining steel cages were provided at the steel–concrete composite interfaces to increase the strength and deformation capacity of the headed stud connections. The specimens were tested to reverse the cyclic loading. The study summarizes that the system has the potential to offer the appropriate strength to resist the lateral forces from earthquakes and adequate stiffness to control the drift. Redundancy is also exhibited through alternate load paths occurring at different levels of loading, including shear stud–infill interaction, steel frame–infill strut interaction, and deformation of the steel frame.

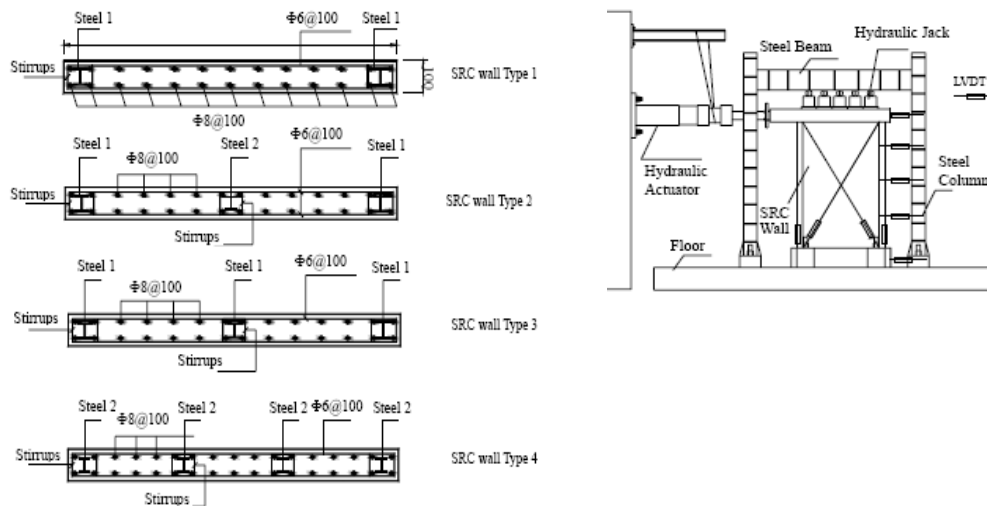


Figure 3.1 Wall specimens and test set-up. Xilin Lu & Yuguang Dong

In 2005, Xilin Lu and Yuguang Dong performed an impressive study on 16 steel reinforced concrete wall specimens. Different parameters such as: height-width ratio, axial compression ratio, concrete strength, and steel volume ratio of stirrup were tested under cyclic loading and the effect of these parameters on the steel reinforced concrete walls was evaluated [3.6]. During the tests the effect of the concrete strength on the seismic behavior of the SRC wall was considered using three different grades of concrete such as: 28.5 N/mm², 50.4 N/mm² and 64.3 N/mm². In addition, the specimens with height/width ratios of 3.75, 2, 1.5, 0.8, and axial compression ratios of 0.095, 0.102, 0.197 and stirrup steel volume ratios 0.0062, 0.0110, 0.027 were analysed, respectively. At last, the SRC walls with different position of steel (showed in Figure 3.1) were studied to find more feasible scheme to improve seismic property of SRC walls. No connection devices were provided between the steel profiles and concrete.

One of the conclusions drawn from this research program was that the height to width ratio affects the seismic behavior of SRC wall remarkably, and with increase of height to width ratio, seismic behavior of SRC wall will be improved significantly. Also, it was concluded that SRC walls with additional intermediate steel skeleton have better seismic behavior than those without.

In 2009 Lin-Hai Han et. al. conducted an experimental investigation including four test models on circular CFST columns and RC shear wall mixed structures subjected to constant axial load and cyclic lateral load. The test parameters included axial load level in the composite column and height/width ratio of the RC shear wall. The effects of these parameters on the strength, ductility, rigidity and dissipated energy of the specimens were investigated [3.7]. The specimens are one-bay, one storey specimens, as shown in Figure 3.2 and are the idealized representation of the bottom storey of the prototype structure.

The specimens were designed to investigate the effects of changing the following parameters: the axial load level in the CFST column, and the height/width ratio of the RC shear wall. For comparison purposes, the height, thickness and reinforcement ratio of all RC shear walls were kept the same.

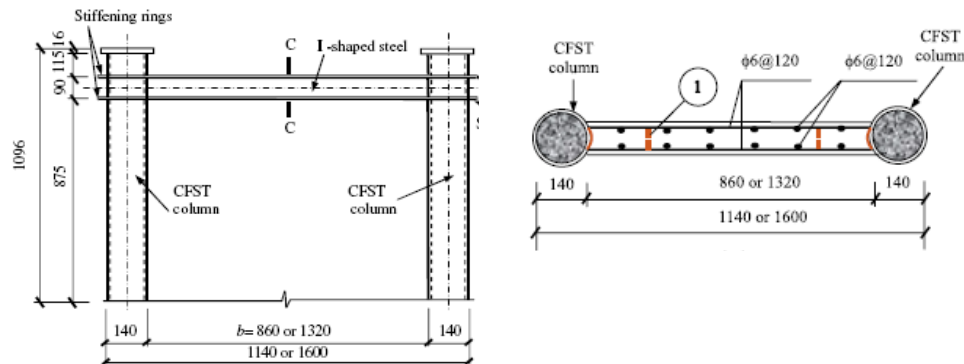


Figure 3.2 Wall specimens. Lin-Hai Han et. al. [3.7]

All the walls had a height of 820 mm and a thickness of 85 mm. Both the horizontal and the vertical reinforcing steel bars of an RC shear wall consisted of two layers of 6mm diameter bars spaced at 120 mm. The sectional dimension of the circular CFST columns was $D/t=140/2$ mm. The connection between the RC wall and the CFST column was assured by welding U-shaped connectors to the steel section and to the horizontal bars. All specimens were tested under combined constant axial load and cyclically increasing lateral load. The conclusions that were drawn from this research study are that the circular CFST columns and RC shear wall mixed structures showed a shear-dominant failure mode in the current tests. After the RC shear wall deteriorated gradually, the CFST columns could still resist part of the lateral load and considerable axial load. The CFST columns and RC shear wall have reliable connections and can work together by using the U-shaped connectors. The lateral load carrying capacity increases with the increase of the axial load level, whilst the effects on the ductility and dissipated energy are just the reverse. A lower height/width ratio tends to induce more inclined-compression failure characteristics for the specimens, resulting in the improved ultimate strength and the reduced ductility and energy dissipation capability.

Another research program conducted by Lin-Hai Han et. al. in 2009 is similar with the one presented above. It is related to the experimental investigations of six shear wall models, including three RC shear walls framed with SRC columns and three counterparts framed with RC columns, conducted under constant axial load and under cyclic lateral load [3.8]. The specimens were designed to investigate the effects of changing the following parameters: the type of boundary column (SRC or RC column), the height-width ratio of RC wall, h/b ($=0.62$ and

0.95), the axial load level of boundary column, n ($=0.26$ and 0.52). For comparison purposes, the height, thickness and reinforcement ratio of all RC walls were kept the same. The RC columns, which had a sectional dimension of 170×170 mm and were reinforced with four 16 mm diameter longitudinal bars, were designed as having an approximately same flexural strength to the SRC columns. All specimens were tested under a constant axial load and a cyclically increasing shear load. The research program summarizes that the RC shear walls framed with SRC columns showed a shear-dominant failure mode in the current tests. The specimens attained their ultimate strengths when the diagonal cracks of both wall and column interconnected, and after that spalling and crushing of the concrete occurred in RC wall and SRC columns. The lateral load carrying capacity of RC shear walls framed with SRC columns increased with the increasing of the axial load level and the decreasing of the height-width ratio, while the effects to the ductility and energy dissipation were reverse. The ductility and energy dissipation capacity of a RC shear wall framed with SRC columns are superior to those of a RC wall framed with RC columns.

In 2010, X. Ji, J. Qian and Z. Jian performed an experimental study on an innovative composite shear wall, named the steel tube-reinforced concrete (ST-RC) composite wall [3.9]. Steel tubes were embedded at the boundaries of the elements. The steel tubes and concrete cores act compositely as concrete-filled steel tubes (CFST), which offer the ST-RC wall a higher bending strength and a larger lateral deformation capacity. A series of quasi-static tests were carried out to examine the composite walls. The tested walls were designed with higher axial force ratios and relatively larger aspect ratios (over 2.0). The studied parameters were the effects of the steel tube/CFST ratio, axial force ratio, and transverse reinforcement at the boundary elements on the lateral load-bearing capacity, the deformation capacity, and energy dissipation capacity. Seven walls fabricated at approximately 1:3 scale were examined, one was a conventional RC wall, and the others were ST-RC composite walls. The overall geometries of the tested walls were 2600 mm tall, 1300 mm wide and 160 mm thick, and had an aspect ratio height/width of around 2.0, showing flexure-dominated behavior. Each wall was designed with six 8 mm diameter vertical and horizontal web reinforcements. Six 12 mm diameter steel rebars were placed as the vertical reinforcement at the boundary elements. The measured cubic compressive strengths at the time of testing varied between were 40.1 and 49.8 N/mm². The nominal yield stress of the reinforcing bars was $f_y = 335$ N/mm². The circular steel tubes included two sizes respectively of $D/t = 113/3.36$ mm and $88.5/3.5$ mm. All tubes were fabricated by steel with the nominal yield stress, $f_y = 235$ N/mm². The steel tube and concrete core acted compositely as a CFST. The conclusions drawn from this study were that the ST-RC walls showed a larger crack load, yield load, maximum load capacity, and ultimate deformation capacity relative to the conventional RC wall. The load-carrying capacity and deformation capacity increased with the increase of the steel tube/CFST ratios. After the maximum load, the ST-RC specimens slowly deteriorated in strength, because the CFST could still resist the vertical load after the compressive strength of concrete outside of the steel tubes was degraded. The wall specimens finally failed because of concrete crushing at the wall bottom. Under the design axial force ratio of 0.73 and the confined boundary element's stirrup characteristic value of 0.20, the rectangular ST-RC wall had an ultimate drift ratio of 0.012, which was larger than the story drift limit. Considering the reliability of the design, rectangular ST-RC walls that were adopted in severe earthquake-prone regions were suggested under a design axial force ratio, no greater than 0.65, and a confined boundary element's stirrup characteristic value, no less than 0.2.

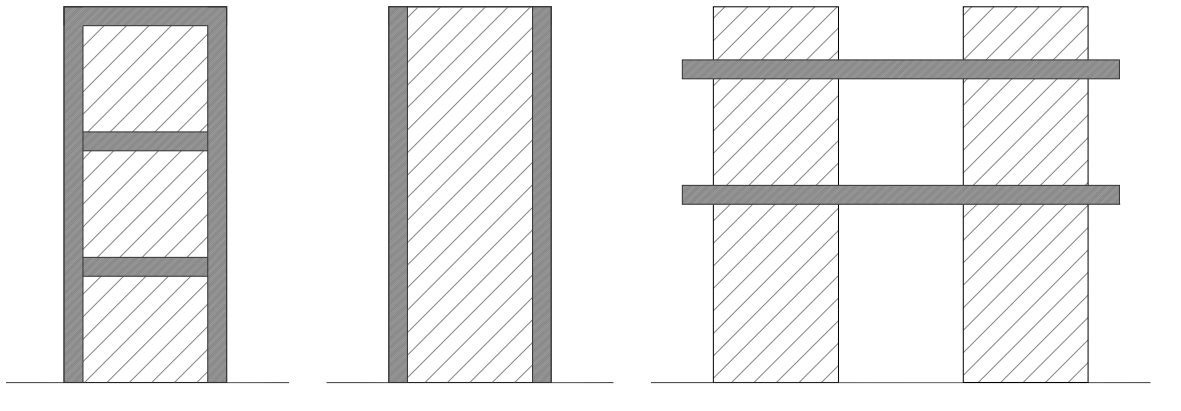
Other research activities on different types of composite shear wall systems have been conducted by Chen et al. [3.10], Saari et al. [3.11], Hossain and Wright [3.12], Astaneh [3.13], Guo [3.14], Greifenhagen et al. [3.15], Su and Wong [3.16].

The presented literature review was prepared during the research program, PNII - IDEI ID_1004, Contract 621/2009, entitled "Innovative Structural Systems Using Steel-Concrete Composite Materials and Fiber Reinforced Polymer Composites" [3.1], part of that being included in the general report [3.1] and the Ph.D. thesis [3.17].

3.2 Theoretical study and the design of the specimens

3.2.1 Design of the experimental specimens

To study the behavior of the concrete walls reinforced by vertical steel sections, a theoretical and experimental program was developed in the Civil Engineering Department at the Politehnica University of Timisoara, Romania. In Eurocode 8 part 7.10 [3.18] three types of composite structural systems are defined and presented (fig. 3.3). The studied walls belong to Type 2.



Type 1 – Steel or composite frame with concrete infill

Type 2 – Concrete walls reinforced by vertical steel sections

Type 3 – Concrete shear wall coupled by steel or composite beams

Figure 3.3 Composite structural systems with shear walls

For this type of structural walls, the Composite Steel Reinforced Concrete Wall (CSRCW) notation will be used in the followings. The experimental program consists of six 1:3 scale elements (CSRCW1 to 6), designed using the principles from the existing codes (Eurocode 2, Eurocode 4 and Eurocode 8) applied to composite steel-concrete elements [3.19], [3.20]. A typical CSRCW experimental element scaled 1:3, simulating the lower three story of one composite wall from a multistory building is presented in Fig. 3.4.

The design details of all the six types of composite steel-concrete shear walls are shown in Fig. 3.5.

Special provisions for composite structures subjected to earthquake loads, of Eurocode 8 were used in the specimen design.

Special provisions for composite structures subjected to earthquake loads, from Eurocode 8 [3.18] were used in the specimen design. As it is known, the behavior of the structural elements subjected to seismic loads has to be ductile. To avoid the brittle failure of specimens to shear, the design process must respect the following steps: first the bending design, then the shear design to a value associated to the capable bending moment.

The specimens were designed and conceived to investigate the effects of the following parameters on the behavior of the composite walls: the type of vertical side reinforcement, i.e. reinforcement bars or structural steel, the position of the structural steel in the cross section, the structural steel shape. All the specimens had the same tension capacity of the steel from the edges. The structural steel profiles were connected with the concrete web by headed shear stud connectors with $d=13$ mm diameter and $h=75$ mm length. The specimen CSRCW3 had a supplementary steel encased profile placed in the middle of the cross section. The parameters of the steel sections used in CSRCW specimens are presented in Table 3.1.

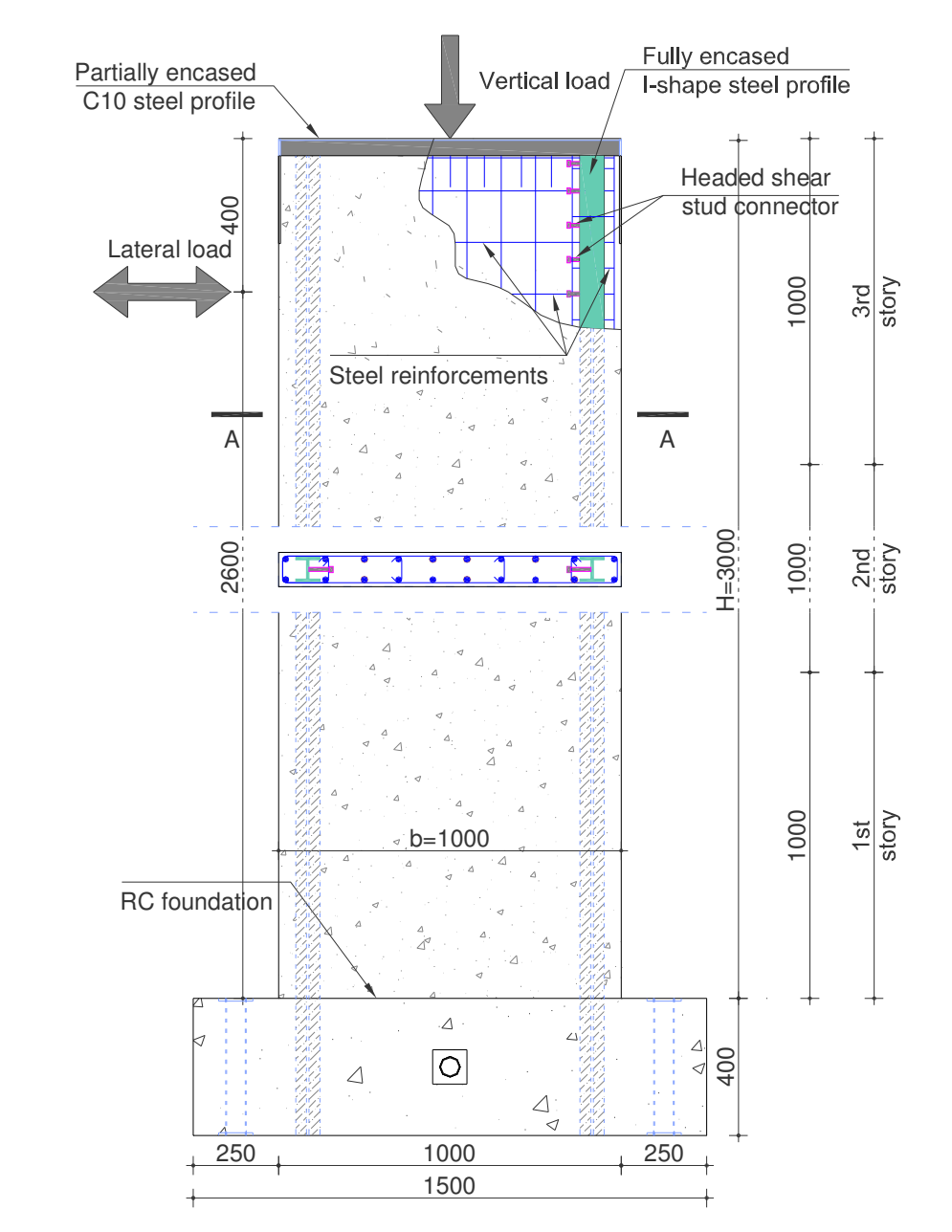


Figure 3.4. Composite steel-concrete experimental element [mm]

Table 3.1 The parameters of experimental specimens

Specimen label	No and steel shape	Encasement degree	Steel ratio δ	Axial load N (kN)	Normalised axial level v_a
CSRCW1	2□	fully	0.20	100	0.018
CSRCW2	2H	fully	0.23	100	0.021
CSRCW3	3H	fully	0.26	100	0.015
CSRCW4	2H	fully	0.20	100	0.016
CSRCW5	2I	partially	0.22	100	0.015
CSRCW6	—	—	—	100	0.016

For all specimens the reinforcements of the RC web panel consist of $\text{Ø}10/100$ mm vertical bars and $\text{Ø}8/150$ mm horizontal bars. The vertical and the horizontal reinforcements were placed on both faces of the wall and were connected together with $\text{Ø}8/400/450$ mm steel ties. In specimen CSRCW5, the horizontal bars were welded on the steel profiles.

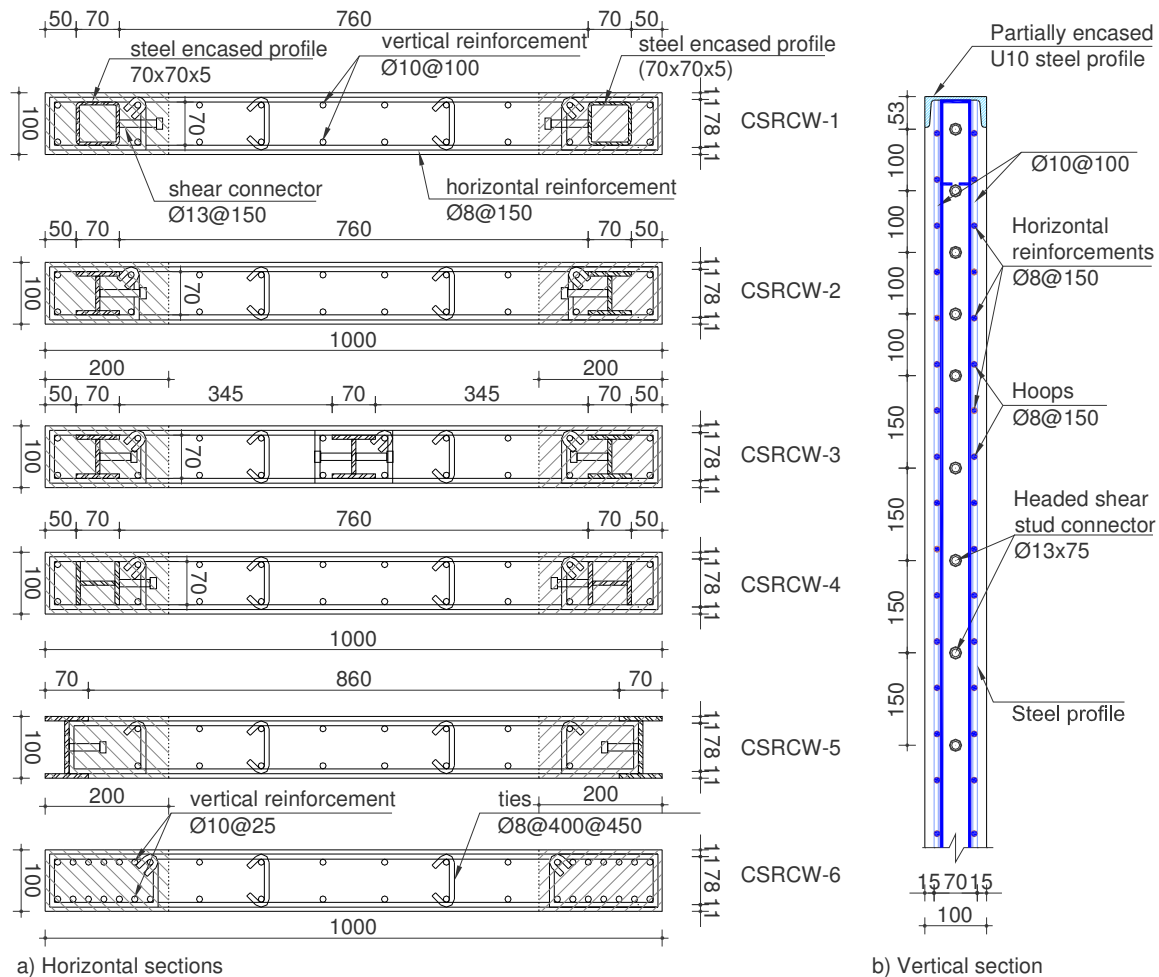


Figure 3.5. Details of the composite steel-concrete walls

The parameters of the specimens are presented in Table 3.2. The reinforcement ratio and the total steel ratio were evaluated by taking into account the total concrete section of the specimens. The edge steel ratio was evaluated taking into account the hatched concrete section from Figure 3.4.

Table 3.2. Numerical analysis results for proposed specimens

Point specimen	Element yielding		Limit stage		Plastic moment resistance $M_{pl,Rd}$ (kNm)
	P_y (kN)	Δ_y (mm)	P_{max} (kN)	Δ_{max} (mm)	
CSRCW1	250.4	19.9	324.9	126.5	974.7
CSRCW2	223.5	19.3	312.1	114.7	936.3
CSRCW3	235.1	21.5	355.1	116.4	1065.3
CSRCW4	228.9	19.26	322.5	113.0	967.5
CSRCW5	249.7	20.9	333.1	117.9	999.3
CSRCW6	198.5	18.1	263.1	106.5	789.3

The steel contribution ratio is determined according to Eurocode 4 [3.20] as the ratio between the structural steel capacity and the plastic resistance to compression of the member.

3.2.2 Specimen fabrication

The specimens were manufactured in a specialized construction company. The manufacturing process of the specimens started with the fabrication process of I steel shapes, the welding of the studs and the shaping of the steel bars. The square hollow sections were provided as cold-formed steel tubes. The studs were welded with special equipment, using additional ceramic rings. All welds had 3 mm in thickness. The steel profiles and the vertical reinforcement bars were embedded into the RC foundation block to assure the anchorage. Special steel pieces were welded on the steel profiles in order to obtain the required anchorage into the foundation. At the top, each element was provided with a supplementary horizontal C-shape steel profile partially encased in concrete, stiff enough to distribute on the element width the vertical and horizontal applied forces. The concrete was cast and vibrated in the mould. The specimens were cast in horizontal position together with the foundation block, in order to avoid the formation of casting joints. The foundation block was reinforced with steel rebar. Circular holes were provided for the anchorage bolts. After 48 hours each element was removed from the mould and placed upright to air dry. Some aspects related to the manufacturing processes and particular details are presented in Figure 3.6.



Reinforcements cage in mould

Anchorage of steel profiles

Figure 3.6 Manufacturing process aspects

3.2.3 Numerical analysis and calibration of experimental specimens

It is well-known that the behaviour of RC in bending is nonlinear. In the case of the composite steel-concrete shear walls, the nonlinearity is due to the nonlinear behavior of the concrete and steel, to the shear stud behavior, and also to the connection between the steel and the concrete [3.21].

Therefore, the software ATENA-2D was used to analyze the proposed experimental elements in order to have a general overview related to the expected behavior during the experimental tests. The software is capable to analyze the reinforced concrete and also the composite steel-concrete elements in a plane stress state. The two dimensional non-linear analysis is performed using the incremental-iterative procedure. The incremental approach is adequate in such cases to describe the transition from one stage to another (load history analysis) while within each loading step an iterative procedure is being used [3.22]. The finite element mesh uses triangular elements; the composite elements have the same thickness.

Both the reinforcements and the steel encased elements are modelled as distinct finite elements. In Figure 3.7 there are represented: the stress-strain law and failure criterion for reinforcement, the structural steel and the concrete used by ATENA 2D software. For the

structural steel, the material called 3D Bilinear Steel Von Misses was used. This material uses the Von Misses yield criterion for the description of plasticity. A bilinear stress-strain law, elastic-perfectly plastic was used both for reinforcement and steel. The material model SBETA was used for concrete. The material model SBETA includes the following effects of concrete behavior: non-linear behavior in compression including hardening and softening, fracture of concrete in tension based on the nonlinear fracture mechanics, biaxial strength failure criterion, reduction of compressive strength after cracking, tension stiffening effect, reduction of the shear stiffness after cracking (variable shear retention), two crack models: fixed crack direction and rotated crack direction. The formulas used for determining the material parameters for SBETA constitutive model of concrete are taken from the CEB-FIP Model Code 90 [15]. In the numerical analysis the bond between steel and concrete was assumed as a full connection as well as in the design process. During the manufacturing process the wall panel was full embedded in the foundation. In the numerical analyses as boundary conditions, all the degrees of freedom for the bottom nodes of the specimens were blocked.

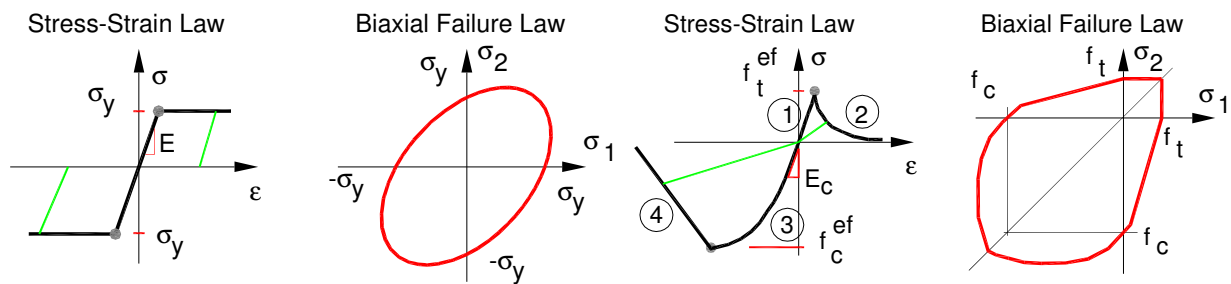


Figure 3.7 Stress-strain and failure laws for materials

The numerical analysis was performed to predict the nonlinear behavior, the stress distribution in the cross section of the elements, the crack distribution, the structural stiffness at different load level and the load bearing capacity of the composite steel-concrete shear walls. Those results will later be compared with the experimental values. The results from the numerical analysis are the values of the displacements, the stresses and strains in the concrete, in the reinforcements and in the structural steel. They also provide the crack distribution in concrete.

In Figure 3.8 there are represented the analytical load displacement curves for the specimens.

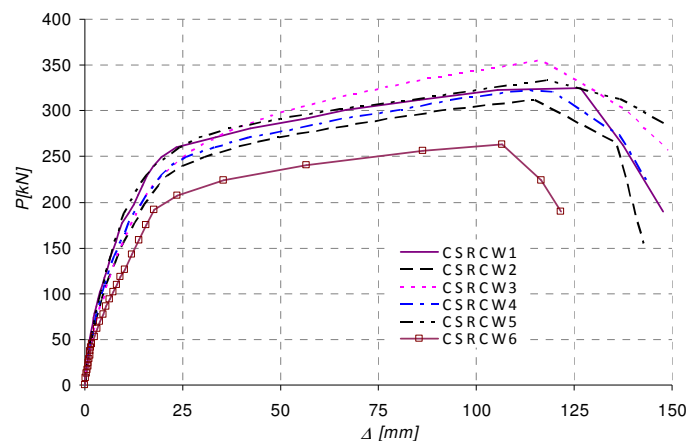


Figure 3.8. Analytical P - Δ curves

In Table 3.3 there are presented the results obtained from the numerical analysis.

Table 3.3 Numerical analysis results for proposed specimens

Point specimen	Element yielding		Limit stage		Plastic moment resistance $M_{pl,Rd}$ (kNm)
	P_y (kN)	Δ_y (mm)	P_{max} (kN)	Δ_{max} (mm)	
CSRCW1	250.4	19.9	324.9	126.5	974.7
CSRCW2	223.5	19.3	312.1	114.7	936.3
CSRCW3	235.1	21.5	355.1	116.4	1065.3
CSRCW4	228.9	19.26	322.5	113.0	967.5
CSRCW5	249.7	20.9	333.1	117.9	999.3
CSRCW6	198.5	18.1	263.1	106.5	789.3

3.2.4 Material properties

The designed concrete quality was C20/25 class, the reinforcement S355 steel and the structural steel Fe510. The steel profiles were manufactured by welding the steel plates. Cold formed steel tubes were used for the structural steel, too. Tensile tests on steel samples were done to determine the yield strength (f_y), ultimate strength (f_u), modulus of elasticity (E_s). The average experimental results related to steel properties are given in Table 3.4. The concrete used to fabricate the specimens was obtained using the mix proportions as follows: Cement: 370kg/m³ Water: 181kg/m³ Sand: 855kg/m³ Aggregate: 1025kg/m³ Additive 50g/m³. The properties of the fresh concrete were the following: Slump flow (mm): 300; Concrete temperature (°C): 20.

Table 3.4 Material properties of steel

Type / Steel thickness	Rebar diameter (mm)	f_y	f_u	E_s	
			(N/mm ²)	(N/mm ²)	(N/mm ²)
d8-1	8	483	616	2.09x10 ⁵	
d8-2	8	484	616	2.05x10 ⁵	
Steel rebar	d8-3	8	471	617	2.01x10 ⁵
	d10-1	10	526	626	2.10x10 ⁵
	d10-2	10	559	624	2.15x10 ⁵
	d10-3	10	558	616	2.09x10 ⁵
I-shaped steel	s-01	7	328	515	2.00x10 ⁵
	s-02	7	324	513	2.01x10 ⁵
	s-03	7	331	521	2.05x10 ⁵

For each element, three sample concrete cubes were provided for further compression strength tests, made on the day of the test of the composite walls. At the age of the tests, the Young's modulus and the average cube strength of concrete had the values presented in Table 3.5. Though the same materials and the same mix proportion were used, the material properties of the resulting concrete were slightly different from one element to another. This can be explained by the fact that separate mixes were successively prepared.

Table 3.5 Properties of the concrete elements

Element Type	No. of samples	f_{cm}	E_{cm}
		(N/mm ²)	(N/mm ²)
CSRCW1	3	54.7	36628
CSRCW2	3	46.0	34773
CSRCW3	3	65.1	38591
CSRCW4	3	62.0	38031
CSRCW5	3	65.6	38680
CSRCW6	3	63.5	38305

3.3 Experimental investigation

3.3.1 Testing methodology and test set-up

The testing procedure consists in quasi-static reversed cyclic horizontal loads performed on 1:3 scaled composite steel-concrete wall specimens. Six shear wall specimens have been tested: one reinforced concrete (CSRCW6) and five composite steel-concrete (CSRCW1 to 5). All specimens were tested under constant vertical load and cyclically increasing horizontal (lateral) loads. The lateral loads were applied alternatively from left and right. The test specimens were placed in the same plane with the loading frame and were anchored into the reaction floor. The loading frame consists in two steel braced frames, placed symmetrically. The alternate horizontal force was applied using two 400 kN hydraulic jacks, whereas the vertical force was realized by a 250 kN hydraulic cylinder. Initially, a constant vertical load of 100 kN was applied to the specimen and was maintained during the test. The vertical force was provided in order to obtain the normalised axial force v_d between 0.015 and 0.025. These values are obtained in low and medium rise structures, where the composite walls are used for the stiffened core of the building.

The hydraulic cylinder induced the vertical force using a pair of steel rods anchored into the foundation of the wall. The foundation of the element was anchored with steel bolts into the laboratory reaction floor. The horizontal forces were applied at 400 mm below the top of the elements, thus providing sufficient anchorage length above the load application level for the reinforcing bars and steel profiles. A transverse brace system was used in order to avoid any out of plane displacements of the specimens.

The recommended ECCS short testing procedure [3.24] was used, as it defines the loading levels as submultiples and multiples of the elastic displacement. According to ECCS the short testing procedure is used when the yield load and yield displacement are not known at the beginning of the test. The test should be performed with increments of displacement, sufficiently small to ensure that at least four levels of displacement are done before the yield displacement is reached. The elastic limit is defined by the intersection point of the tangent line in the origin at first cycle curve and the tangent to the envelope curve of the cycles with a 0.1 slope from the first tangent line, Figure 3.9.

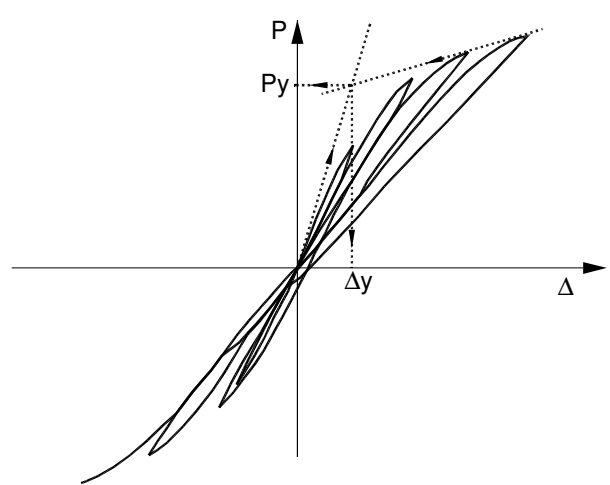


Figure 3.9 Determination of the elastic limit of specimens

The tests were performed using the displacement control. After the elastic limit, for each displacement level, three cycles were performed. The horizontal forces were applied under

controlled cyclic displacements until the strength of the specimens decreased to 85% of the peak horizontal load, as in reference [3.25].

The behavior of the experimental specimens was monitored by pressure transducers, displacement transducers (D), strain gauges glued on the reinforcement bars and on the structural steel (G), and by optical measurements for stress and strain distribution on concrete surface using a non-contact measurement equipment Aramis 3D. The test set-up of the tested elements is presented in Figure 3.10. The cyclic loading speed was 2 mm per minute. Each cycle was followed by a few minutes stop to record the crack development in the specimens.

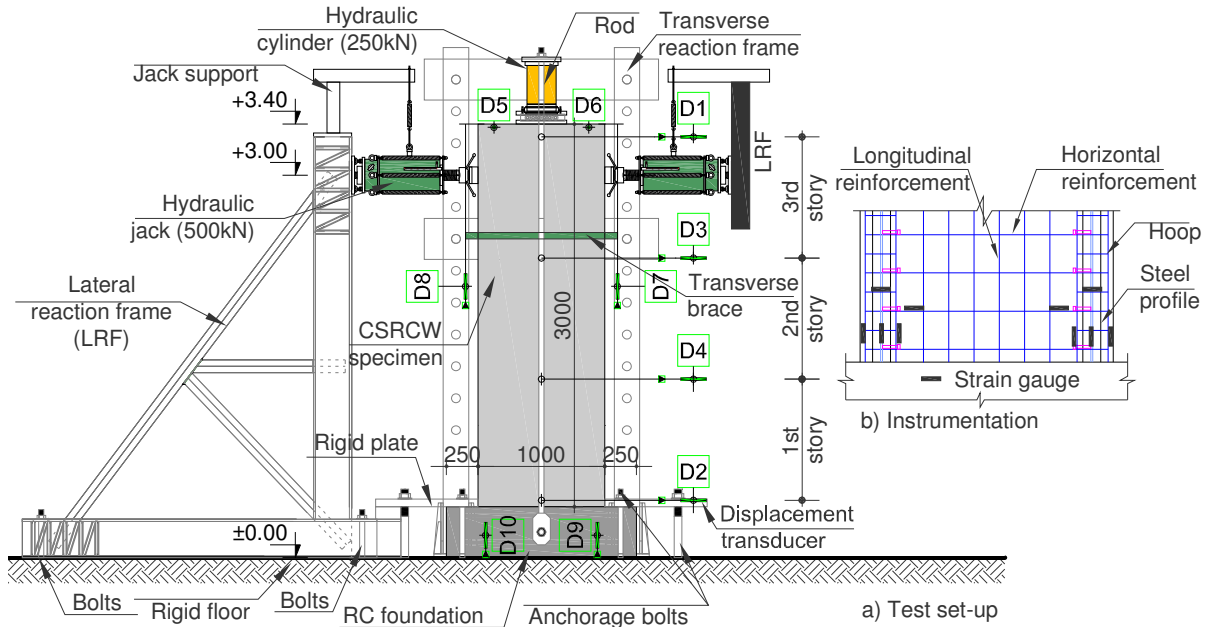


Figure 3.10 Test set-up

The loading history and instrumentation scheme are presented in Figure 3.11.

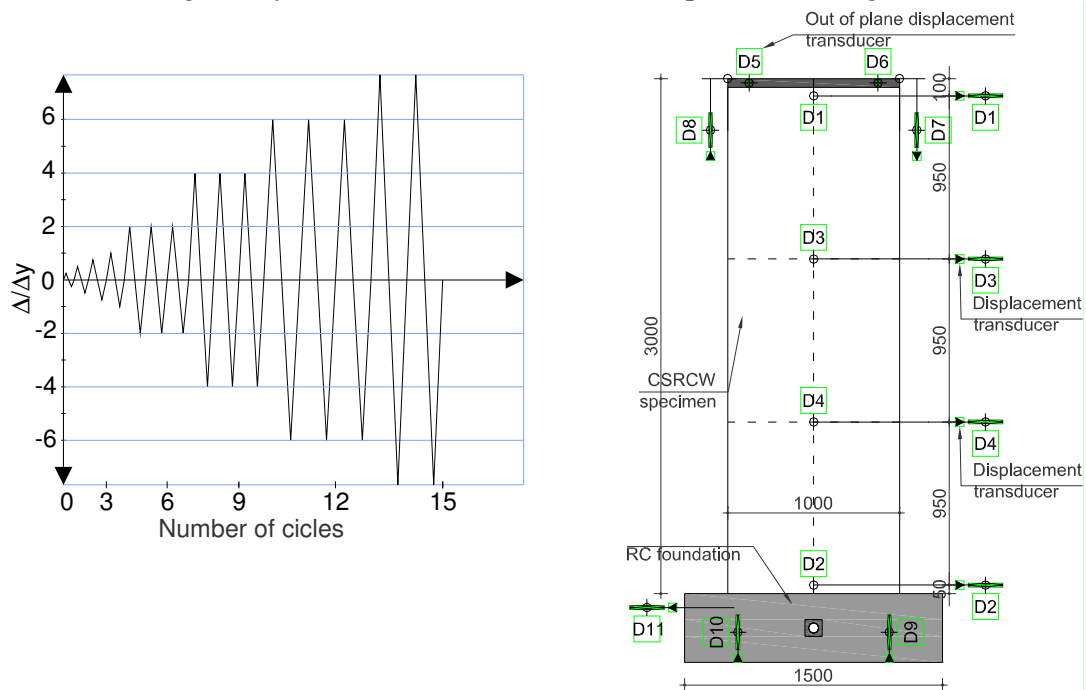


Figure 3.11 Loading history and instrumentation

3.3.2 Experimental observations

As a general conclusion the experimental tests have shown similar behavior of the tested elements. The typical curves of horizontal load P versus horizontal displacement Δ and the experimental observations at the characteristic points A, B, C and D of the P - Δ curve are presented in Fig. 3.12 for the CSRCW1 specimen.

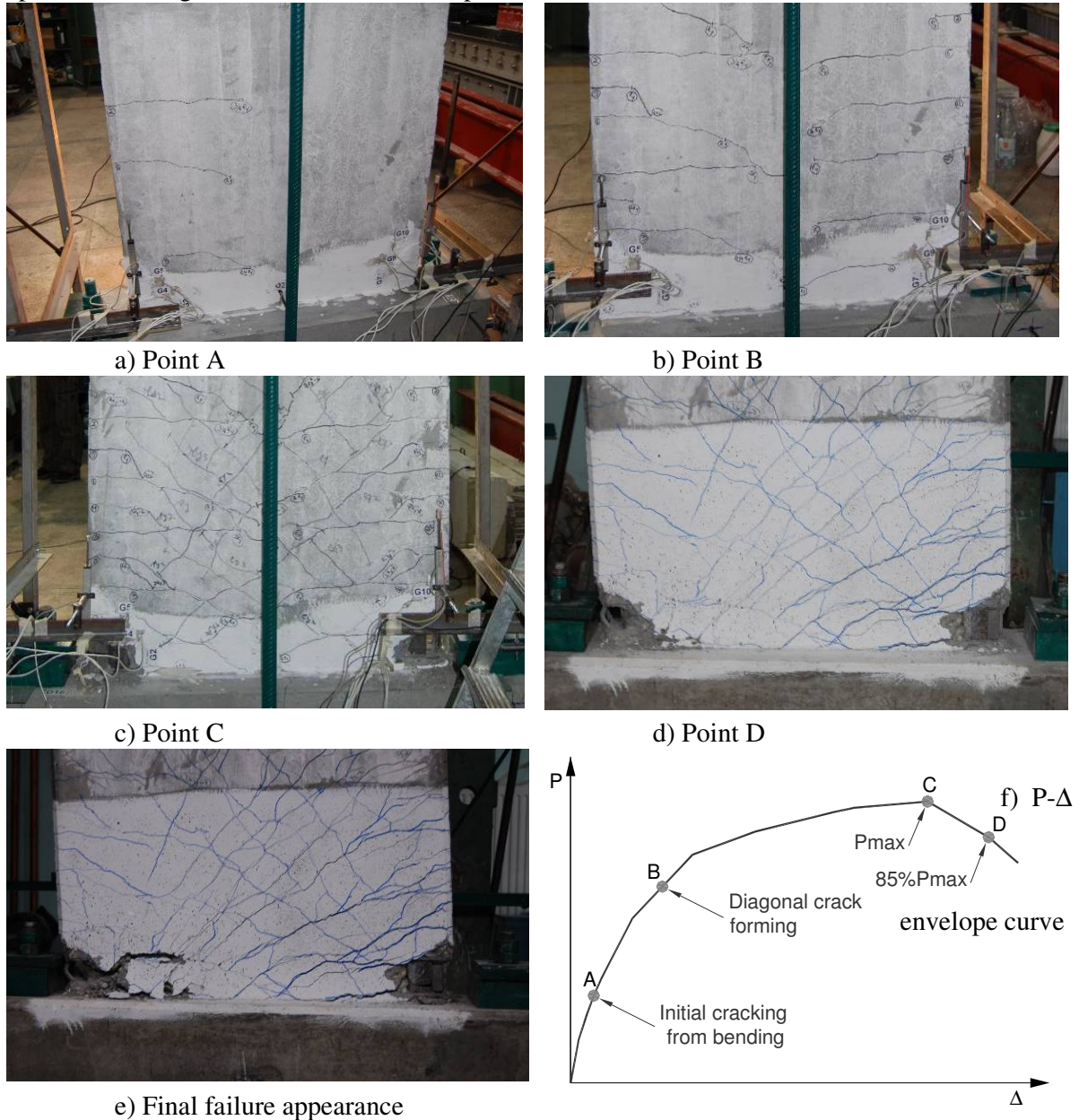


Figure 3.12 Typical P - Δ envelope curve and failure mode for (CSRCW1) specimen

As designed, the failure starts with horizontal cracks which appeared in the tensioned zone (Point A), as shown in Figure 3.12a. This crack is caused by the transfer of the stresses from the steel profile to the concrete. The first crack appeared approximately at 0.8 m from the bottom line. After that, new horizontal cracks and the extension of the existing ones were observed upon further loading. The diagonal cracks appear in the cycle $+\Delta_y$, and developed until practically the entire surface was separated into a series of rhombic concrete blocks by pairs of

intercrossing inclined cracks. The measured strains indicated yielding of the vertical reinforcing bars located at the extremities and yielding of the steel profiles, too.

The main diagonal cracks, crossing the entire width of the specimen from the bottom corner to the opposite side at approximate 45 degrees (Point B), are shown in Figure 3.12b. At this moment, in the compression zone, no visible damages occurred. For the cycle $+3\Delta y$, the specimen attained its ultimate strength P_{max} (Point C), and is shown in Figure 3.12c. Then after the lateral load decreased, the diagonal cracks developed and, finally, the collapse occurred with the buckling of steel profile and the crushing of concrete in the compression zone, simultaneous with the tearing of tensioned steel profile.

During the testing process, the connection between the steel profiles and the concrete was monitored and no visible separation at the interface was observed.

All tests performed showed an expected behavior in accordance with the design process. The tested composite shear walls with steel encased profiles showed a bending failure mode, with the crushing of the compressed concrete and the tearing of the tensioned steel. The vertical reinforcement, placed at the extremity of the elements, yielded in tension, but never failed. In the compression zone the local buckling of the steel profile occurred after the concrete crushing. Generally, the failure of the specimens can be divided into four stages: initial cracking stage from bending, diagonal cracks forming stage, limit stage and failure stage.

The characteristics of the failure stages of the specimens can be summarized as follows:

Initial cracking stage: This stage lasts from the starting load to the occurrence of the first crack. During the $\pm 1/2\Delta y$ cycles, horizontal cracks were observed and they were probably caused by the stress transfer from the steel profile to the concrete. The width of first crack varies between 0.05-0.15mm. The load intensity at the initial cracking (P_{cr}) is between 77 kN for CSRCW1 to 94.6 kN for CSRCW4. In this stage, the specimens were generally kept in elastic range though their stiffness deteriorated slightly.

Main diagonal cracks forming stage: After the initial cracking stage, the horizontal cracks developed through the middle axis of the wall and new inclined cracks appeared. For all the tested elements the inclinations of the diagonal cracks were between 35 and 65 degrees. The horizontal cracks width increased upon further loading and yielding occurred in the vertical reinforcing bars. The encased steel profiles also yielded in this stage. After the yielding of the reinforcements and of the steel profile, the stiffness of the element decreased continuously during the three cycles performed at every displacement level.

Limit stage: This stage was defined as starting with the formation of inclined cracks to the point where the lateral load attained the ultimate capacity value (P_{max}). In this stage the widths of horizontal and diagonal cracks developed quickly, also smeared cracks appeared in the compression zone and small parts of concrete split.

Failure stage: The composite steel-concrete shear wall reaches this stage after the peak horizontal load P_{max} has been attained and when the horizontal load decreases to 85 % of the maximum load. The load-bearing capacity of the specimens was decreasing in this stage. During the cycles performed in this stage, the compressed concrete crushed and the steel profile in compression buckled simultaneously with the yielding of the steel profile in tension. The collapse occurred when the compressed concrete is crushed and the steel profile tears off.

3.3.3 General behavior of the specimens

As it is known the behavior of RC in bending is nonlinear. The nonlinearity is due to the nonlinear behavior of the concrete and of the steel, to the shear studs behavior, and, of course, to the connection between the steel and the concrete [3.26]. All performed tests showed an expected flexure-dominant behavior in accordance with the design process, with the crushing of the compressed concrete and the tearing of the tensioned steel profile. The high concrete class and the confinement provided by the stirrups at the ends of the elements section assured the yielding

of tensioned steel and increased the ductility of tested specimens. The concrete class was designed according to the principle of having the equilibrium between the tensioned steel and the compressed concrete section. The vertical reinforcement, placed at the extremity of the elements, always yielded in tension, but never failed. In the compression zone, the local buckling of the steel profiles and vertical reinforcements occurred after the concrete crushing. Generally, the failure of the specimens can be divided into four stages: initial cracking stage from bending, diagonal cracks forming stage, limit stage and failure stage. The values of force and the corresponding displacements at these characteristics stages are presented in Table 3.6.

Table 3.6 Force and drift at different characteristic stages

Stage	Initial cracking		Element yielding		Limit stage		Failure stage	
	P_{cr} (kN)	Δ_{cr} (%)	P_y (kN)	Δ_y (%)	P_{max} (kN)	Δ_{max} (%)	$P_{85\%}$ (kN)	Δ_u (%)
Specimen								
CSRCW1	80.5	0.264	228.2	0.929	354.4	4.39	301.5	4.75
CSRCW2	80.6	0.264	204.7	0.901	311.2	4.04	262.1	4.56
CSRCW3	91.6	0.263	209.2	0.884	357.8	3.72	304.2	4.76
CSRCW4	94.6	0.265	238.6	0.926	324.8	4.13	275.4	4.81
CSRCW5	84.0	0.175	258.3	0.923	357.3	4.04	303.7	4.74
CSRCW6	77.0	0.260	185.8	0.863	279.6	3.79	237.6	4.14

The distribution and the evolution of cracks, for all the mentioned stages, are presented in Fig. 3.13. The crack evolution is presented related to the total drift of the specimens. The crushing and the spalling zones of the concrete at failure are distinguishably marked for all the specimens. In the initial stage, performed until the elastic limit in the initial four cycles, horizontal cracks appeared in the tensioned zone due to the transfer of the stresses between the steel profile and the concrete. As it can be observed, there are some differences between the elements related to the distribution and density of the cracks, their openings and lengths, more visible at 0.7% total drift. For elements CSRCW1, CSRCW3 and CSRCW5 the cracks that appeared in this stage are mostly horizontal. At the lateral extremities, two alternative series of cracks occurred. The first series is developed, more or less up to the middle axis, and the second series of cracks, parallel and alternative with the first one, developed until 120 mm from the elements edges. The first series of horizontal cracks appeared along the horizontal bars while the second series appeared in the sections where the connectors and stirrups are disposed. After the elastic limit was attained, corresponding to total drift cycles between 0.64% and 0.75%, new horizontal and diagonal cracks appeared. The diagonal cracks developed from the horizontal small cracks. The developed cracks formed a typical diagonal cracking pattern crossed by horizontal cracks. It is important to mention that the diagonal cracks developed from the horizontal small cracks became diagonal only after the section where the steel profiles are located. The main diagonal cracks, crossing the entire width of the specimen from the bottom corner to the opposite side at approximate 45 degrees, can be seen for the specimens at 1.4% total drift. The specimens reached their maximum lateral strength during the 3.65% and 4.31% total drift cycles, with the spalling and the crushing of the concrete in the compression zone. At collapse, the buckling of steel profile occurred simultaneously with the tearing of tensioned steel profile. In the failure stage, at the bottom part of the specimens, more horizontal cracks parallel with the foundation block can be observed. After the crushed concrete was removed, the buckling of the steel encased profiles was visible for all tested elements. It must be mentioned that for the specimen CSRCW6, which has only rebars at the extremities, the failure occurred when the compressed concrete crushed and the vertical reinforcement buckled. For this element the vertical reinforcements in tension did not tear. The connection provided by shear studs between the steel profiles and the concrete was monitored and no visible separation at the interface occurred during the transfer of stresses between the steel encased profiles and the concrete. For element CSRCW2, the connection between the steel and the concrete failed in

tension at 2% drift cycle due to a missing shear stud, probably fractured in the manufacturing process.

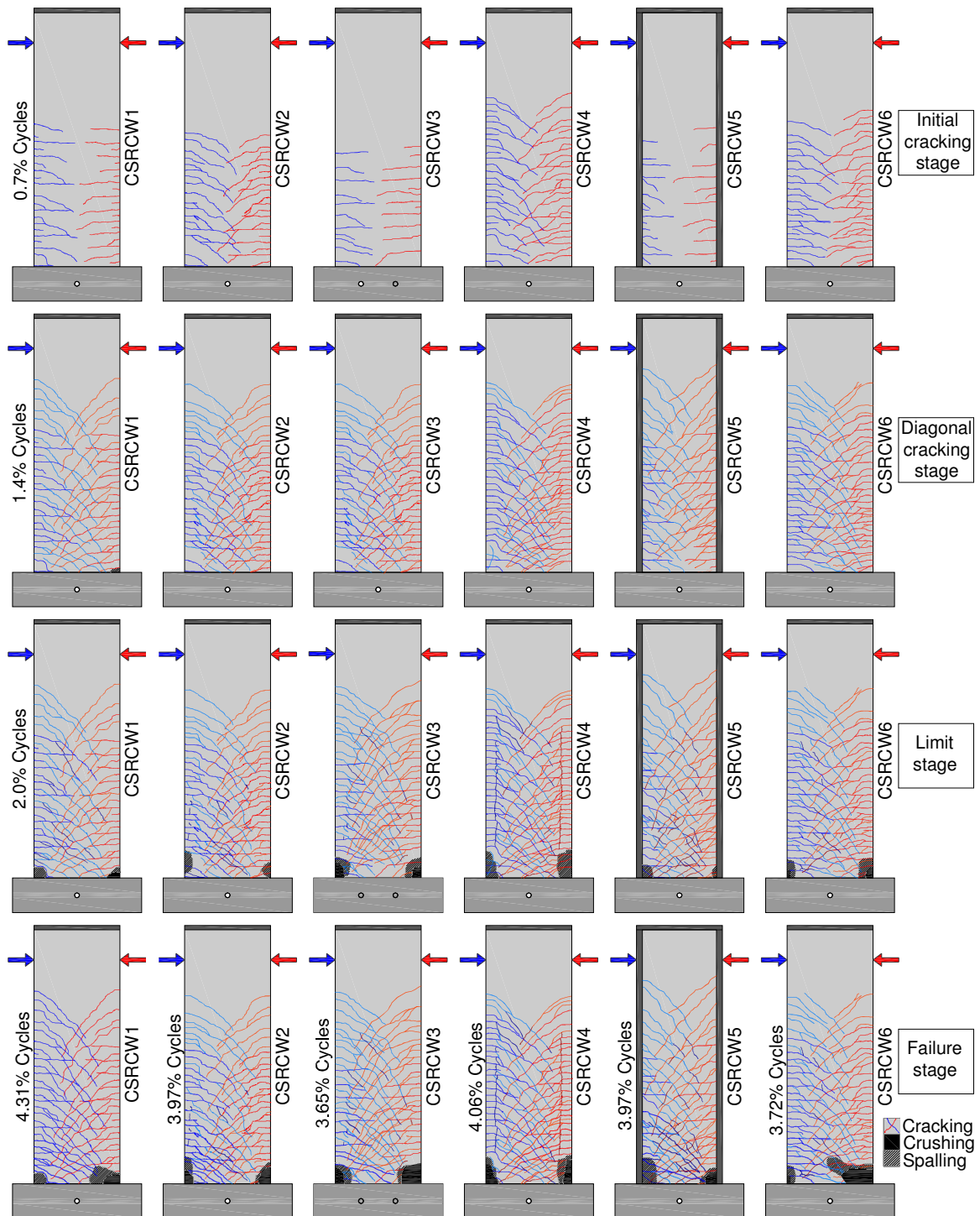


Figure 3.13 Cracking and crushing patterns

The details of the failure modes of the tested elements are presented in the Figure 3.14.



a) CSRCW1



b) CSRCW2



c) CSRCW3



d) CSRCW4



e) CSRCW5



f) CSRCW6

Figure 3.14 General view of specimens at failure stage

In Table 3.7 the recorded values for horizontal loads and displacements at the characteristic points are presented.

Table 3.7 Force and displacement at different characteristic points

Specimen	Initial cracking		Element yielding		Limit stage		Failure stage	
	P_{cr} (kN)	Δ_{cr} (mm)	P_y (kN)	Δ_y (mm)	P_{max} (kN)	Δ_{max} (mm)	$P_{85\%}$ (kN)	Δ_u (mm)
CSRCW1	80.5	7.54	228.2	26.5	354.4	125.1	301.5	135.4
CSRCW2	80.6	7.53	204.7	25.7	311.2	115.0	262.1	130.0
CSRCW3	91.6	7.52	209.2	25.2	357.8	106.03	304.2	135.7
CSRCW4	94.6	7.56	238.6	26.4	324.8	117.75	275.4	137.2
CSRCW5	84.0	5.00	258.3	26.3	357.3	115.1	303.7	135.2
CSRCW6	77.0	7.41	185.8	24.6	279.6	108.1	237.6	118.2

The P- Δ envelope curves, characterizing the behavior of the tested elements, connect the peak point of each loading cycle on the hysteretic curves. The horizontal load (P) versus lateral displacement (Δ) envelope curves is shown in Figure 3.15. The maximum horizontal load (P_{max}) was attained by element CSRCW3 and represents 127% of the ultimate lateral load of the reinforced concrete wall CSRCW6. Note that the steel encased sectional area from the extremities of the wall has the same value as the vertical reinforcement area of the reinforced concrete element. It can be mentioned that composite wall had a higher initial stiffness than the reinforced concrete wall. The value of the element stiffness prior to failure is higher for the composite wall than for the reinforced concrete wall. The diagrams presented in Figure 3.15 show symmetrical behavior of the tested elements until the mentioned cycles. The differences between the values obtained for positive and negative directions of loading, are due to the testing methodology. After the third cycle at $3\Delta_y$ performed in both directions, all the specimens were tested up to failure in the positive direction only.

The comparative study between the analytical values and experimental results reveals some differences between the characteristic values P_y and Δ_y . The horizontal displacement at the yielding stage is higher into the experiments, due to the nonlinear phenomenon which occurred into the reinforced concrete and has not been taken into account for the analytical model. At the limit stage, the values of the ultimate force and ultimate displacement are quite close.

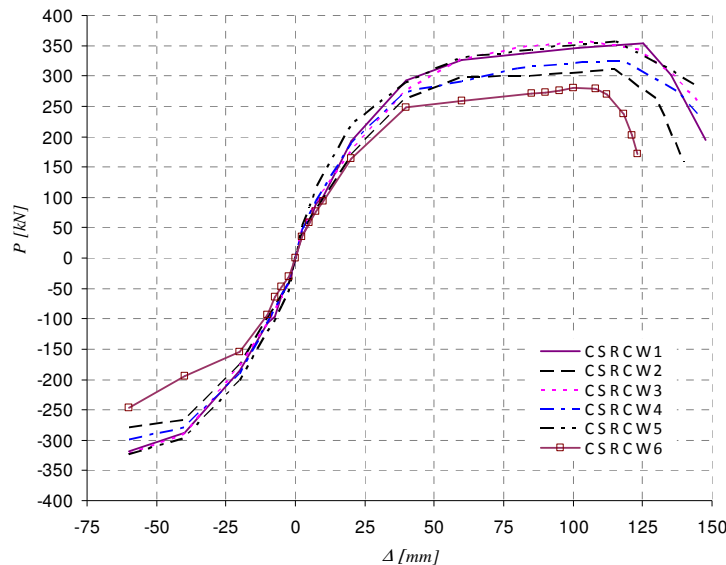


Figure 3.15 Comparative experimental P - Δ curves

3.4 Test results and discussions

The lateral loads versus the total drift diagrams for all specimens are presented in Figure 3.16. The hysteretic energy dissipation was small during the initial cracking stage performed practically until the elastic limit. The specimens behaved approximately elastically within the range 0.64% - 0.75% of the total drift cycles.

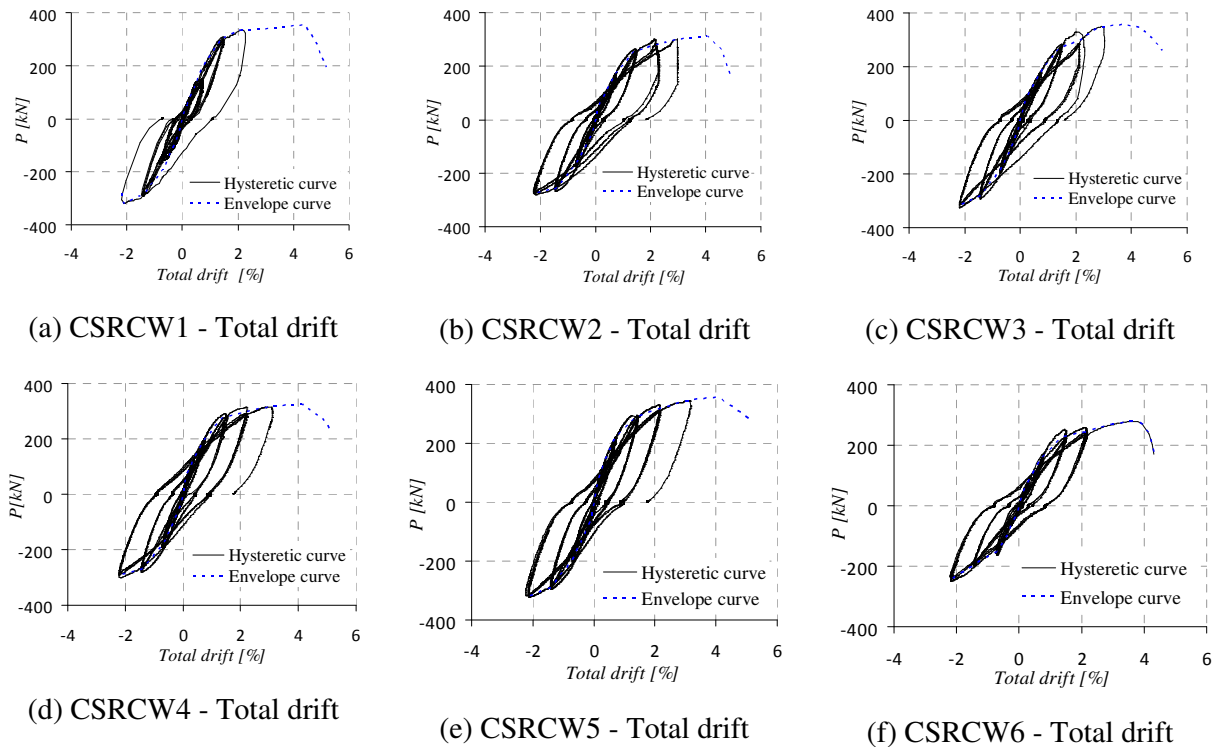


Figure 3.16 Total drift versus horizontal load of specimens

The hysteretic curves show a ductile behavior for all the elements. Figure 3.16 shows the relationship between the lateral load and the interstory drift of each story for CSRCW2. Each story considered is presented in Figure 3.4. The interstory drifts are represented up to 2.1% total drift only, due to the limitation of the displacement transducers. After this limit, during the testing processes, only the total drift was recorded and monitored. For all the tested elements, similar values were recorded for the interstory drifts (Fig. 3.17).

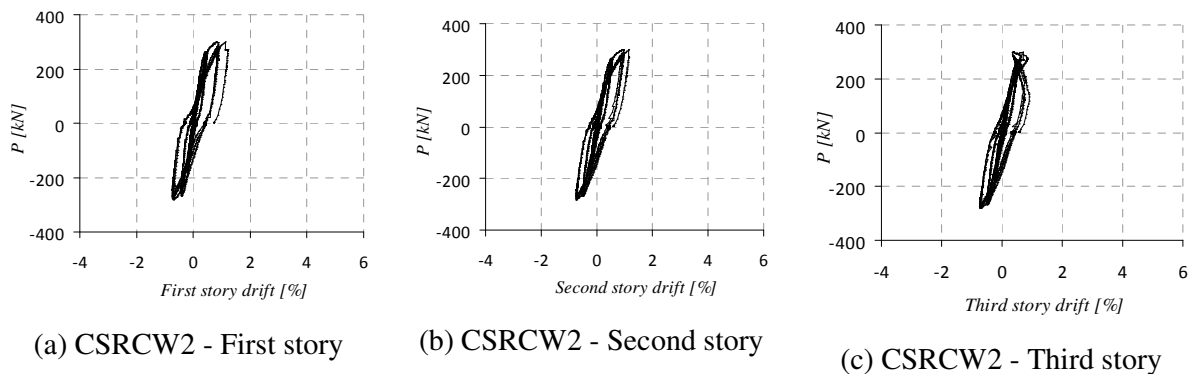


Figure 3.17 Interstory drifts versus horizontal load

3.4.1 Dissipated energy

The dissipated energy (E_i) in each cycle was evaluated from the horizontal load (P) versus horizontal total drift hysteretic curves, as the area bounded by hysteretic loop of each cycle. Figure 3.18 shows the energy dissipation of the tested specimens during the loading process. It can be seen that the energy dissipation of all composite steel reinforced concrete walls with steel encased profile is higher than that of the common reinforced concrete wall (CSRCW6), provided with the same reinforcement area by means of classical bars in the sectional extremities. It is important to mention that the major part of the energy dissipation of the specimens occurs until 2.5% drift cycles, which is the displacement limit for ULS. It can be noticed that the evolution of dissipated energy is similar for CSRCW2, CSRCW4 and CSRCW5. The initial stiffness of the tested CSRCW elements is almost the same. The stiffness degradation was almost the same for all the elements in the preliminary loading stages; after that more severe stiffness degradation occurred. The composite steel concrete shear walls with steel encased profiles and the common RC wall have shown gradual stiffness degradation during the cycles performed.

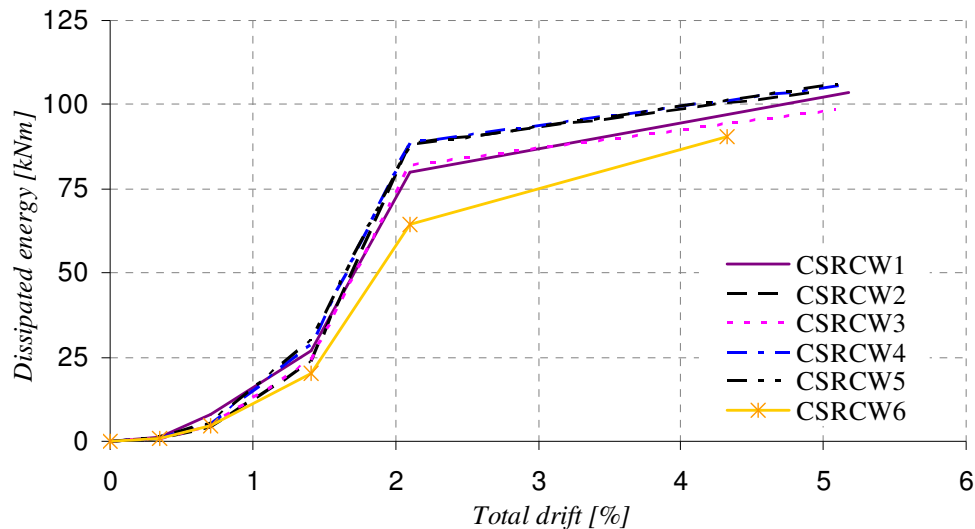


Figure 3.18 Dissipated energy - total drift relations

A comparison between the total dissipated energy (E_{total}) within each test performed is presented in Figure 3.19.

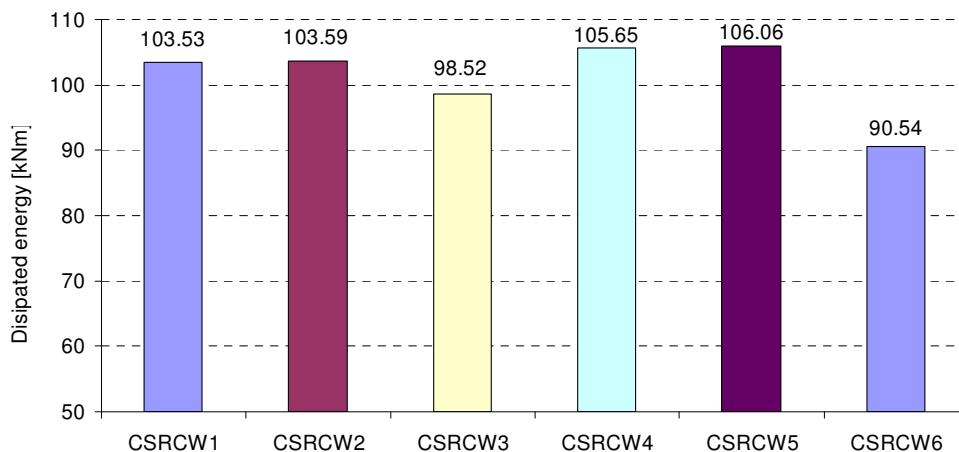


Figure 3.19 Comparative dissipated energy (total)

It can be concluded that all tested composite steel reinforced concrete walls dissipated more energy than the usual reinforced concrete wall, provided with the same reinforcement area in the sectional extremities. It is important to mention that the influences of different values of concrete strength have also been taken into consideration.

3.4.2 Capacity degeneration

The capacity degeneration coefficient evaluates the stability of the shear capacity of specimens during the cyclic loading. It was evaluated as:

$$\lambda_i = \frac{F_j^{i+1}}{F_j^i} \quad (3.1)$$

where F_j^{i+1} is the shear capacity of $i+1$ cycle at j load level; F_j^i is the shear capacity of i cycle at j load level.

After the elastic limit three cycles were performed for each displacement level. For each package of those three cycles the capacity degeneration coefficient are presented in Table 3.7. In this table λ_1 represents the ratio between the shear capacity in the second cycle and the shear capacity in the first cycle of the considered displacement levels. The value of λ_2 was evaluated as the ratio between the shear capacity in the third cycle and the shear capacity in the second cycle at the same displacement levels. It can be noticed that a stability of shear capacity of the tested elements was observed until a 2.11% total drift cycle. After that, the load was applied in one direction only, monotonic until failure and no capacity degeneration coefficient could be calculated.

Table 3.7. Capacity degeneration coefficient

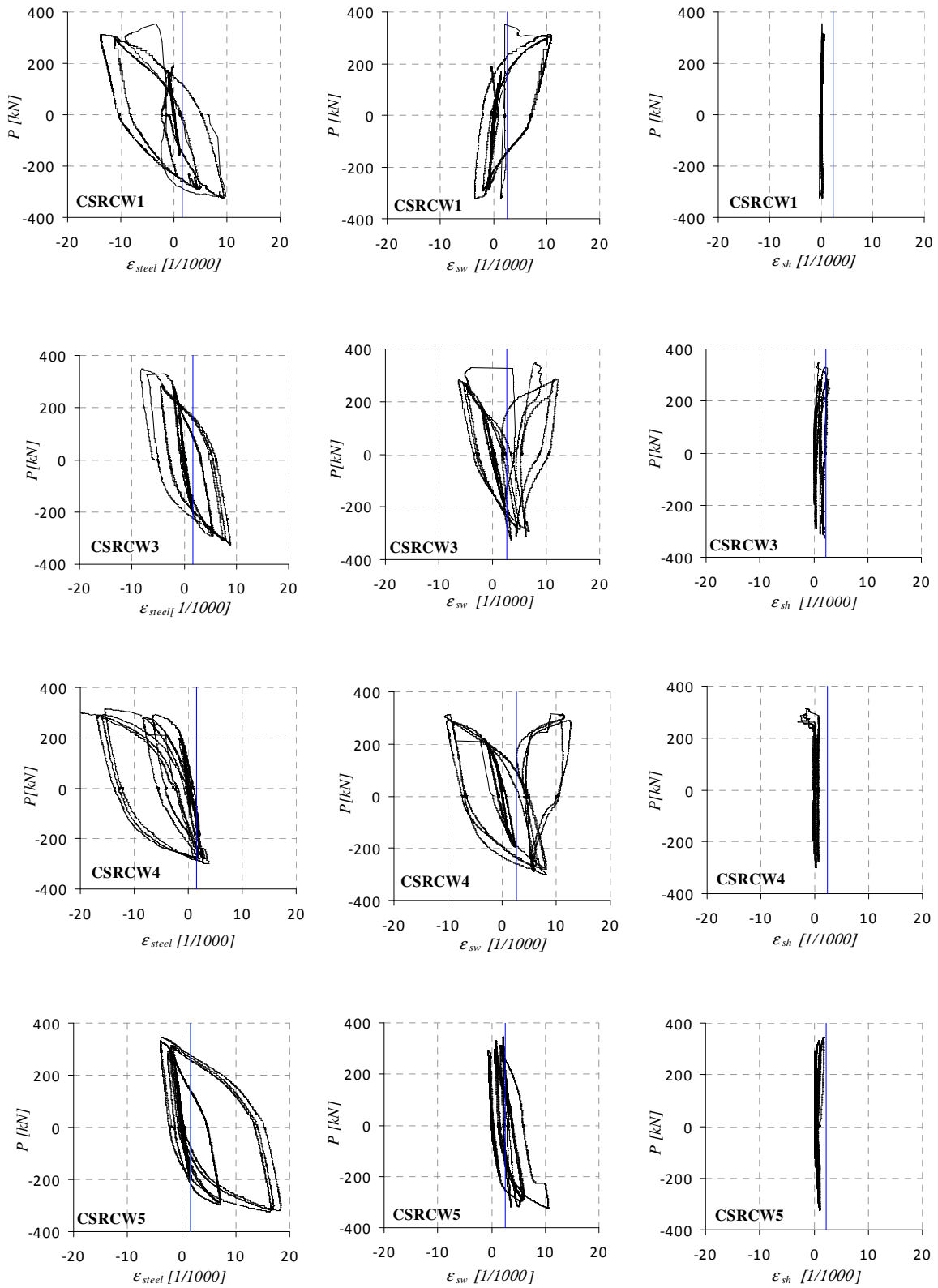
Drift %	CSRCW1		CSRCW2		CSRCW3		CSRCW4		CSRCW5		CSRCW6	
	λ_1	λ_2										
0.70	1.03	0.99	0.97	0.98	1.01	0.97	0.97	0.98	0.98	0.98	0.94	1.03
1.40	0.99	0.97	0.96	0.97	0.96	0.98	0.95	1.00	1.00	0.98	0.93	0.98
2.11	0.98	0.97	0.95	0.95	0.91	0.98	0.94	0.98	0.96	0.99	0.95	0.98

3.4.3 Strain analysis

During the experimental tests, the strains were measured using strain gauges placed along the longitudinal direction of the reinforcing bars and on the steel encased profiles. Figure 3.20 presents the diagrams of the lateral load (P) versus strain (ϵ) on the steel profiles, vertical and horizontal reinforcements for four selected specimens.

Figure 3.20(a) represents the typical relation between lateral loads (P) versus longitudinal steel strain (ϵ_{steel}) for steel encased profiles of different specimens. The strain gauges were placed on the web of the steel profile for CSRCW5 specimen and on flanges for specimens CSRCW1, CSRCW3 and CSRCW4. The relation between P and ϵ_{steel} is a linear one until the diagonal crack develops in concrete. After that phase, ϵ_{steel} increases more rapidly, and the yield strain is attained at total drift values between 0.55% and 0.74%. For element CSRCW3 the yield strain in the steel encased profile, placed in the middle of the cross section of the specimen, was attained at a total drift of 1.62%. This is due to the fact that part of the shear force carried by RC wall is transferred to the steel profile after the concrete cracking. It is important to mention that with the exception of element CSRCW4, when yielding occurred in the same time for vertical reinforcements and vertical steel encased profile, it occurred first in steel encased profiles and

after that in the vertical reinforcements. The maximum strain recorded on structural steel encased profile was between 9.8 to 19.8‰. Fig. 3.20(b) presents the ϵ_{sw} strain, measured on the first layer



a) Steel profiles

b) Vertical rebars

c) Horizontal rebars

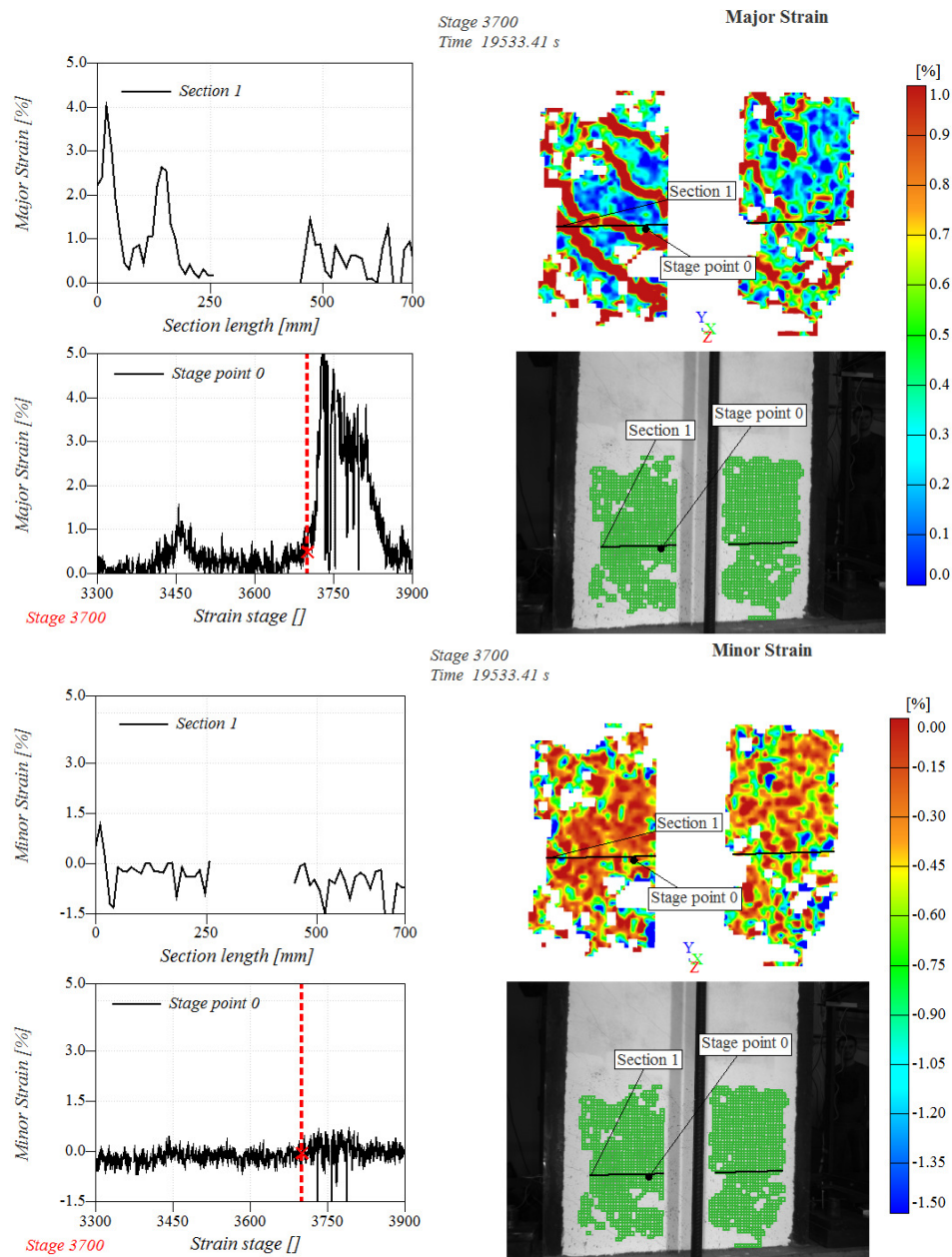
Figure 3.20 Lateral load (P) versus steel strain (ϵ)

of the vertical bars located near the steel encased profile, at the extremity of the element. For all specimens the strain increases slowly at lower load levels, whereas at higher load levels, when diagonal cracks appeared in concrete and the shear force was transferred to vertical reinforcements, the strain increased rapidly. The yield strain for the vertical rebars is attained for total drifts between 0.69% and 0.97%. The value of 0.97% drift corresponds to specimen CSRCW5 where the vertical rebars are located on the inner side of the steel profile. Fig. 3.20(c) presents the ε_{sh} strain, measured on the horizontal rebars placed on the second row from the bottom of the specimens.

The strain increased due to the development of diagonal cracks in the specimens, which intersect the rebar. Excepting element CSRCW3 in which yield strain is attained at a total drift of 1.94%, the yield strain was not reached in the horizontal rebars of the elements. The local strain on the concrete surface of the CSRCW elements was measured during the experimental tests with a non-contact measurement equipment Aramis 3D. The system consists of two high resolution cameras, a computer and software for testing procedure definition and the post processing of the recorded data. A stochastic high contrast dot pattern is applied to the surface of the object. Aramis system allocates points/coordinates to the reference image by dividing the digital image in facets of $n \times n$ pixels. During the test further images are recorded with the deformation surface, and Aramis recognizes the positions of the individual facets on the new images by considering their trace. The system calculates the displacements of the central points of the facets in the new stages compared to the reference stage. From these displacements, the surface strain components are calculated. The strain measuring range for Aramis system is from 0.05 up to >100%, whereas the strain measuring accuracy is up to 0.01%, obtained from the calibration procedure. Because of the concrete surface degradation due to cracking during the testing procedure, some facets disappear. Therefore, after computation, these are parts of the surface in which no results are represented.

Figure 3.21 presents two Aramis reports with the distribution of the main strains on the concrete surface, recorded on element CSRCW5 at stage 3700, which corresponds to the beginning of the first cycle on 2.1% total drift from the testing procedure, at a force value of 282 kN and a total drift of 1.4%. The two reports are composed by a point strain versus time (stage) diagram, a strain distribution along the section length diagram, a recorded image with one of the two systems cameras and an image with the strain distribution on the concrete surface.

The selected section plane is positioned at 250 mm from the bottom of the element and the selected point is located on the section plane at 200 mm from the left edge of the element. From these reports, it can be observed that at lower load level the strain distribution on the selected point is linear. At an increasing of a total drift from 1.4% to 2.1% the major strain increases about three times, from 1.5% to 5%, while the increasing of the minor strain is from 0.75% to 1.5%. At the selected section the major strain distribution at 1.4% total drift is not a linear one, some peaks appearing along the vertical rebars position due to the stress transfer between the steel and concrete.



3.4.4 Ductility coefficient

The ductility of the specimens was evaluated by the displacement ductility coefficient μ , which is evaluated as $\mu = \Delta_u / \Delta_y$, where Δ_y is the lateral displacement at yield, determined according to ECCS procedure, and Δ_u is the corresponding horizontal displacement when the horizontal load value falls to 85% of the maximum horizontal force (P_{max}). The value of the ductility coefficient μ for each tested specimen is represented in Figure 3.22. It was concluded that all CSRCW with encased profile have a higher ductility than the common reinforced concrete wall CSRCW6.

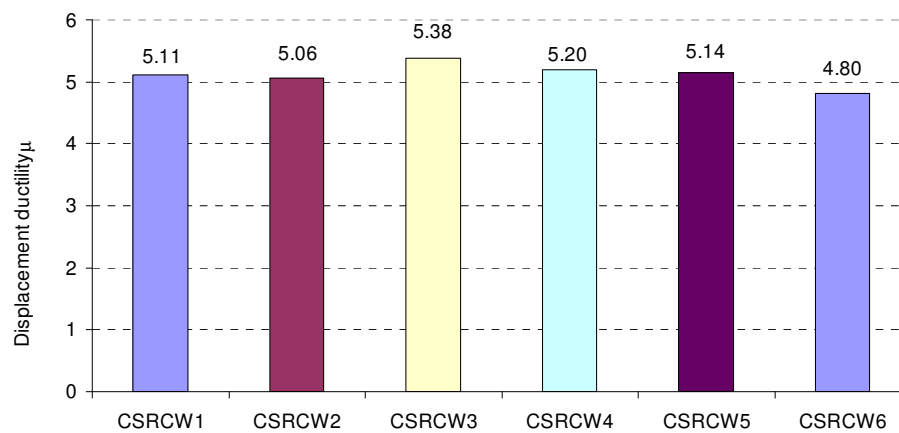


Figure 3.22 Comparative ductility coefficient

3.5 Conclusions

The following conclusions were derived from the theoretical and experimental results within the limitation of the current research:

The tested CSRCW behavior was governed by the bending moment up to collapse, with no major influence of the shear effects. The failure mode is characterized by the crushing of the compressed concrete and the tearing of the tensioned steel. The vertical reinforcing bars, placed in tension side yielded, but they never failed. On the compression side after concrete crushing, local buckling occurred. These concrete walls reinforced by vertical steel sections (type 2 as are defined in Eurocode 8), can have a good seismic behavior. They open a possibility to achieve walls with greater resistance and ductility than simple RC walls, needed to improve the lateral resistance of the buildings located in earthquake regions.

In order to assure a dissipative behavior of CSRCW, a high class of concrete has to be used to avoid the failure in compression before the yielding of the steel section. For all specimens the failure in compression was avoided before the steel yielding, so ductility was provided. The obtained results, in terms of resistance and ductility, are lightly higher in comparison with simple RC walls. The dissipated energy of the tested elements is significant and the stiffness degradation during the cycles performed is gradual. A higher confinement of boundary edges using more dense stirrups could improve the results by reducing the concrete degradation. For element CSRCW5 the local buckling of steel flanges appeared in the limit stage and developed quickly in the failure one. The deformation capacity of CSRCW recommends these types of structural elements for buildings placed in seismic zones, where the dissipation of energy is very important.

The shear failure of CSRCW can be avoided if the composite elements are designed to bending and shear at the associated shear force of the capable bending moment. This structural system can offer lateral strength and adequate stiffness for controlling drift. The shear capacity of the tested specimens during the cyclic loading is stable.

From the general behavior observation it can be concluded that the difference of the concrete compressive strength between the specimens does not lead to different crack patterns.

Further studies are needed to extend the range of the test data and to investigate other variables that have not been investigated. The influence of the axial load ratio must be taken into account for the buildings elements placed in seismic areas. More experiments are required to be conducted with greater axial load ratio to investigate the threshold between the bending and the shear behavior. The experimental work presented in this paper provides a basis for the development of theoretical models necessary in the design process of composite reinforced concrete walls with steel encased profiles [3.27, 3.28].

3.6 Retrofitting solutions for damaged composite steel concrete walls

3.6.1 Introduction

The use of the composite steel concrete shear walls with steel encased profiles CSRCW can be one of the alternative solutions for a lateral load resisting system. This system can provide, during earthquakes: lateral stiffness, high shear and flexural capacity, ductility and energy dissipation.

Due to the large number of earthquakes produced in the last decade, the researchers have studied possible solutions for retrofitting structural elements affected by the seismic action. Since, in many cases, the solutions must be conceived to assure the same distribution of the seismic loads, no major stiffness changes are allowed in the existing structures. Otherwise, the deformation capacity and the load bearing capacity of the element have to be re-evaluated after the repairing and the strengthening of the damaged element. If the initial ductility factor “q” is maintained in the retrofitted structure design process, the designers have to assure the required local ductility, for the repaired and strengthened structural members. Unless this condition is assured, the failure mechanism of the structure can be unexpected and the local brittle fracture of such members can produce the collapse of the entire building.

The reinforcement effectiveness of the fiber-reinforced polymer (FRP-EBR) externally bonded is widely used, either to increase the shear strength of the reinforced concrete members or to provide the critical region confinement of the members. Recent research on reinforced concrete walls strengthened with FRP composites were conducted by Li and Lim [3.29], Antoniadis et al. [3.30, 3.31], Demeter et al. [3.32], Kitano et al. [3.33], Lombard et al. [3.34], Hiotakis et al. [3.35], Ghobarah and Khalil [3.36]. Other research presented by Li and Pan [3.37], Wei et al. [3.38], Hatami et al. [3.39], showed the ability to restore the initial performances of the structural members repaired and strengthened with FRP composites.

A theoretical and experimental research program on the behavior of the composite steel concrete walls with steel encased profiles was conducted in the Civil Engineering Department at the Politehnica University of Timisoara, Romania. Five possible solutions of composite walls (called CSRCW1 to 5) and one for a reinforced concrete typical shear wall (CSRCW6) were designed and laboratory tested [3.27, 3.28]. The tests were performed under constant axial compression and cyclic lateral loads. Out of these five composite specimens, two were tested prior to failure (CSRCW2 and CSRCW4), retrofitted with CFRP composites and retested. Since the solution of using steel profiles at the boundary of shear walls is relatively new, there is no experimental research literature on the retrofitting solution for this type of post damaged elements.

The research performed aims to comprehend the seismic performances of CSRCW retrofitted with FRP composites. The most important issues related to the seismic performance, i.e. lateral stiffness, horizontal displacement (drift), ductility and energy dissipation capacity are presented and discussed for CSRCW_R elements in comparison with the CSRCW reference elements.

3.6.2 Experimental tests on seismically damaged CSRCW retrofitted with CFRP

Two specimens (CSRCW2 and CSRCW4) were selected for retrofitting with CFRP composites, from the previous experimental program presented in chapters 3.1 ÷ 3.3. These elements were tested both prior to failure and after retrofitting, to investigate the strengthening effect and the seismic behavior efficiency. The retrofitted elements CSRCW2_R and CSRCW4_R are referred to with an “R” suffix to the original specimen names.

The experimental specimens had: 3000 mm height, 1000 mm width and 100 mm thickness. The wall panels were fixed in reinforced concrete foundations of 1500 mm length, 400

mm height and 350 mm width. The structural steel profiles connected in the concrete web with headed shear stud connectors with $d=13$ mm diameter and $h=75$ mm at 150 mm interval. The reinforcements of the reinforced concrete (RC) web panel are made with: $\text{Ø}10$ mm vertical bars (1.57% steel ratio), $\text{Ø}8/150$ mm horizontal bars (0.67% steel ratio) and horizontal stirrups (0.67% steel ratio). The configuration of the two specimens selected for retrofitting is presented in Figure 3.23.

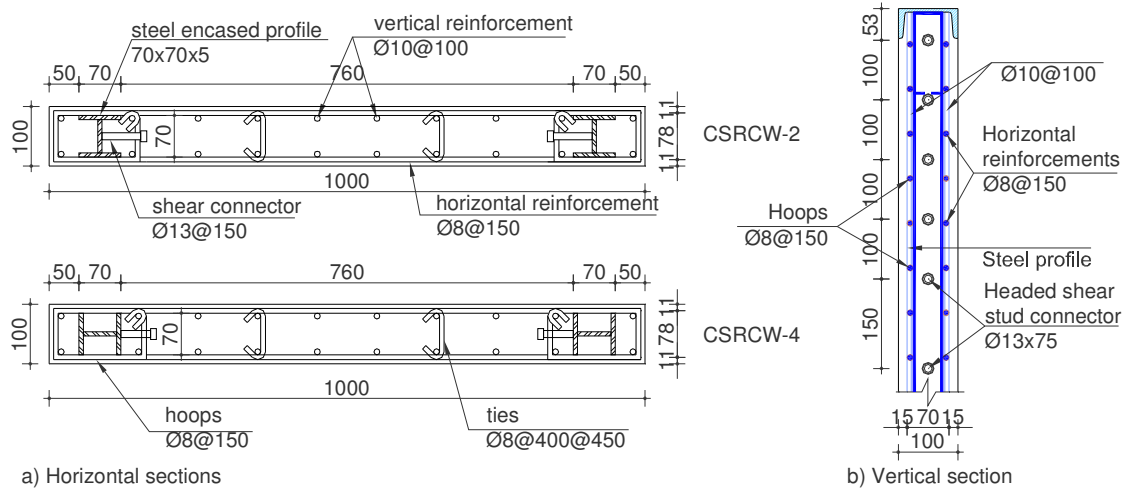


Figure 3.23 Reference elements configuration [mm]

The steel and the concrete characteristics are presented in Chapter 3.2.4. Unidirectional carbon fiber sheets, in form of strips and plates, were used as CFRP-EBR for retrofitting the specimens. The epoxy system used was made of resin and hardener, mixed in the ratio 2:1. Table 3.8 summarizes the geometrical and mechanical properties of CF-fabrics/strips, epoxy resin matrices and the laminated FRP materials used for the specimen repairing and strengthening. The mentioned characteristics are based on manufacturer's data. The high strength mortar, used to replace the heavily damaged concrete, was Sika Repair 13, with a compressive strength at 7 days of $48\div 52$ N/mm², according to the product data sheet.

Table 3.8. Geometrical and mechanical properties of FRP system

Component/system	CF-fabric/strip	Resin matrix	CFRP plate
Product name	SikaWrap 230C	SikaDur-330	SikaWrap Composite
Thickness (mm)	0.131	n/a	1
Areal weight (g/m ²)	230	n/a	n/a
Tensile strength (MPa)	4300	30	350
Tensile modulus (GPa)	234	4.5	25
Elongation at break (%)	1.8	0.9	1.12

3.6.2.1 Behavior and results of reference elements

The tested composite shear walls with steel encased profiles showed a bending behavior in accordance with the design process. The failure occurred with the crushing of the compressed concrete and the tearing of the tensioned steel profile. Detailed data related to the tests set up, behavior and failure details of the elements are presented in Dan et al. [3.27, 3.28]. In case of elements CSRCW2 and 4, selected for retrofitting, horizontal cracks appeared in the tensioned

zone, in the initial loading stages, due to the transfer of the stresses between steel and concrete. Diagonal cracks appeared in the cycle, when the elastic limit of the element was attained, and developed in the specimens until a series of rhombic concrete blocks, separated by these inclined cracks, resulted. The measured strains indicated the yielding of the vertical reinforcing bars, located at the extremities, and the yielding of the steel encased profiles. In the case of these two selected elements, the test was stopped at a displacement level of approximate 85 mm (3% drift). At that moment, the compressed concrete crushed and the strains, in the vertical reinforcements and in the steel encased profile, attended 1.98%, respectively 1.62%. The load displacement curves of the two reference elements and the cracking patterns are presented in detail in Dan et al. [3.28]. The tested composite shear walls were able to develop their flexural and energy dissipation capacity in condition of lower values of normalized axial force. Other important theoretical and experimental research on the nonlinear behavior of shear walls with multi embedded steel section, presented by Lu et al. [3.40] and Zhou et al. [3.41], showed that the ductility and the energy dissipation of the composite shear walls (CSW) is improved with the decrease of the axial load ratio. Carrasco et al. [3.42] note that the strength of the enveloped laminar concrete (ELC) panels is higher than that of other wall panels, which is mainly due to the contribution of steel U-sections in the composed structural system.

3.6.2.2 Repair and strengthening of the specimens

The damaged specimens were repaired before retrofitting, by removing the heavily cracked and crushed concrete and by replacing it with non-shrink, high-strength repair mortar. The concrete lateral surfaces were roughened with a special grinder to achieve a fully smooth surface and the concrete edges of the wall panel were rounded at a radius of about 20 mm to assure the effectiveness of the confining solution made by CFRP-EBR stripes. Local drilling holes ϕ 18 mm were made in the wall panel to assure the anchorages of the confining strips. The vertical strips were steel angle anchored whereas the vertical plates were anchored in inclined holes drilled in the foundation block. Afterward the surface was cleaned with a vacuum-cleaning system and dried completely before wrapping. A local formwork was fabricated around the affected zone to ease the application of the repair mortar. The cracks were cleaned and filled superficially. The epoxy resin was applied with a steel trowel. No other injections were made for repairing the cracks.

The strengthening strategy was based on the behavior and failure mode, observed during the test performed on the reference elements, and divided in three directions in order to: restore the flexural capacity along the edges, provide local confinement and restore the shear capacity of the wall.

The specimen retrofitting was performed by Externally Bonded Carbon Fiber Reinforced Polymer Reinforcement (CFRP-EBR), symmetrical on both faces of the wall, in order to restore the initial load bearing capacity of the reference elements. Two types of CFRP composites were used i.e.: unidirectional carbon fiber sheets cut in form of strips with 150 mm and 200 mm width and plates of 50 mm width. The vertical externally bonded FRP composites served to restore the bending capacity and shift the failure of the wall toward a ductile behavior. Horizontal strips were provided to increase the shear capacity to avoid the shear failure of the specimens. The failure mode in bending was taken into account in the designing phase. Finally, the shear force associated to bending resisting moment was evaluated and verified to be smaller than the shear capacity of the retrofitted elements. Using this design philosophy it is expected that the brittle failure mode associated to the shear be avoided.

A description of the order, form, position and the application procedures of the retrofitting solutions for the specimens is presented in the followings. As shown in Figure 3.21, the vertical FRPs made of strips and plates were external vertically bonded, along the edges of the wall panel, to improve the flexural strength of the walls. The 150 mm width strips were

placed on the front and rear faces of the wall margins. The first layer was applied on the entire height of the specimen, while the second layer was disposed up to 2000 mm from the foundation block.

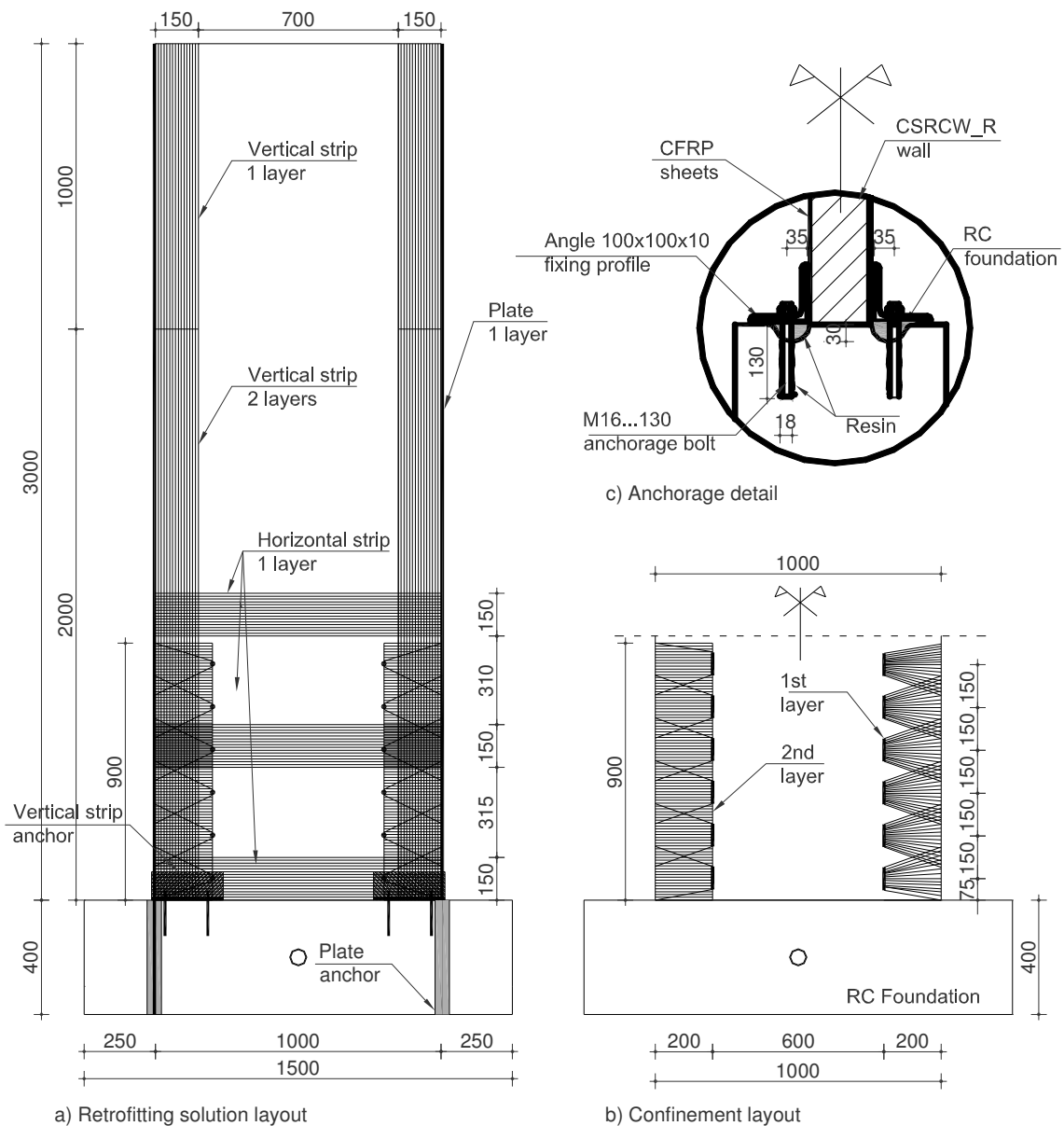


Figure 3.24 Retrofitting solutions of the composite steel-concrete walls [mm]

The plates were placed on the sides of the wall, in one layer, and on the whole height of the specimens. The strips were anchored with a steel angle profile and bolts, as depicted in Fig. 2b. The CFRP composite effectiveness for seismic retrofitting of RC shear walls, to improve or supply the load bearing capacity or ductility, is confirmed by Nagy-Gyorgy et al. [3.43], only if, to avoid debonding, this specific anchorage details are realized. The plates were anchored in an inclined hole created through the foundation, filled with epoxy resin. In the second step, the stirrup-like local confinement was realized by using 200 mm width strips. The fibers were drawn out through a hole and twice overlaid, thus closing the arms. For the enhancement of the shear strength of the walls, three FRP strips, at three levels from the lower part, were bonded to the wall, with the fibers orientated in horizontal direction. The shear strips were placed in one layer

only, anchored through superposing with 150 mm at the ends. Relevant aspects of the operations performed to repairing and retrofitting the specimens are presented in Figure 3.25.

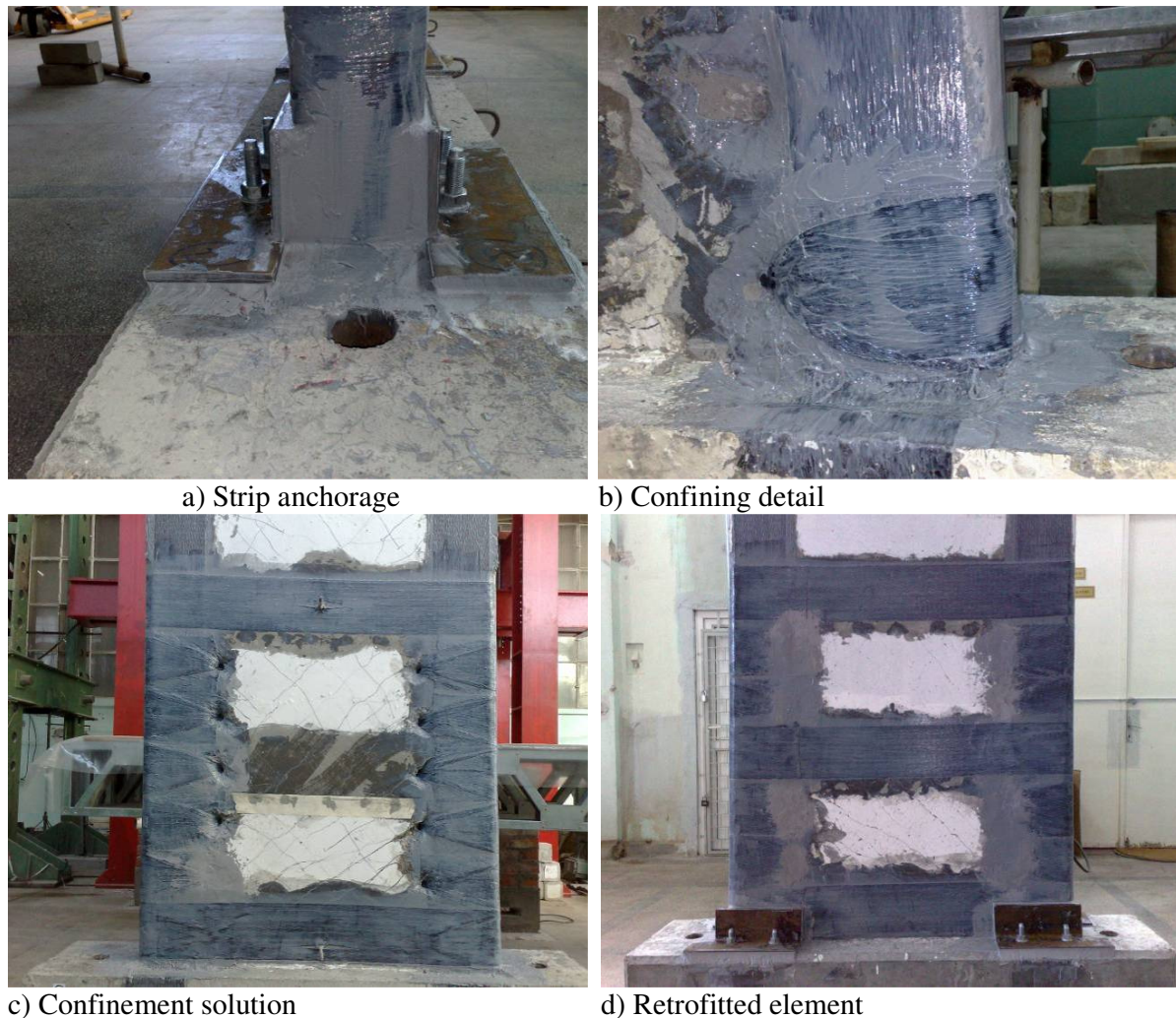


Figure 3.25 Retrofitting execution process aspects

3.6.2.3 Testing methodology and test set-up

The testing procedure consists in quasi-static reversed cyclic horizontal loads performed on the retrofitted wall specimens. Two retrofitted shear wall specimens were tested namely: CSRCW2_R and CSRCW4_R. The specimens were tested under constant vertical load and cyclically increasing horizontal (lateral) loads, by applying the recommended ECCS short testing procedure.

The testing procedure and the loading protocol were the ones used for testing the reference elements CSRCW2 and CSRCW4, presented in detail in Dan et al. [3.27]. The loading frame has two steel braced frames, placed symmetrically. The test specimens were placed in the same plane with the loading frame and anchored through the foundation block with steel bolts into the laboratory reaction floor, as depicted in Figure 3.25(d). It must be mentioned that, the specimens tested in this stage of the research program had the remaining displacement from the last cycle performed in the first phase of the research program. The sense of the first cycle induced was opposite to the direction of the remaining displacement, using the hydraulic jack of 400 kN, whereas the vertical force was realized by a 250 kN hydraulic cylinder. The induced normalized axial force v_d was maintained to 0.021 and 0.016 as for the reference tests, to be able

to compare the results. It must be mentioned that, these values are usually observed for low and medium rise structures, where the composite walls are used frequently for the stiffened core of the building.

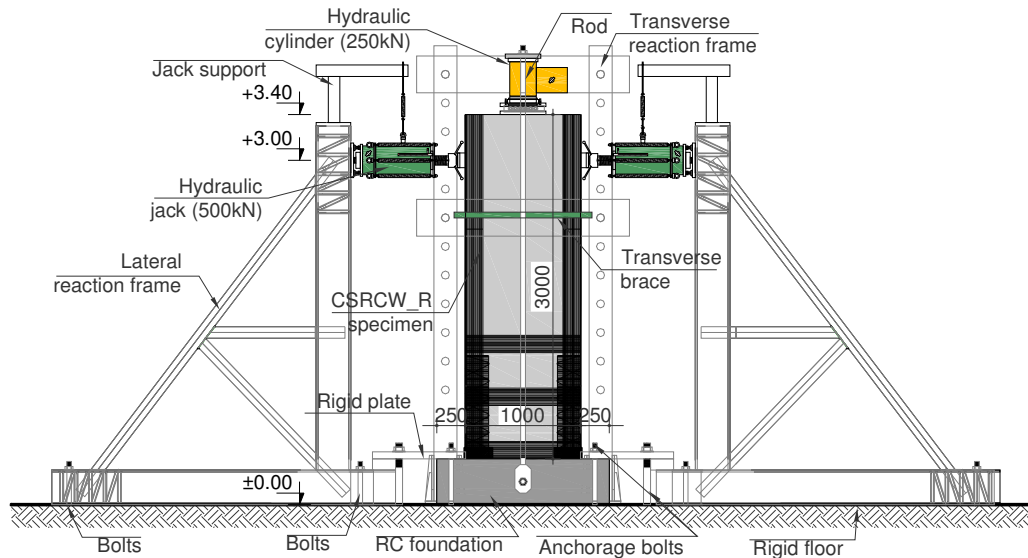


Figure 3.26 Test set-up [mm]

The behavior of the experimental specimens was monitored by: pressure transducers, displacement transducers (D), strain gauges glued on reinforcement bars, on structural steel and on CFRP plates and strips (G). The instrumentation of the tested elements is presented in Figure 3.27. The cyclic loading speed was 2 mm per minute. Each cycle was followed by a few minutes stop to record the crack development in the specimens.

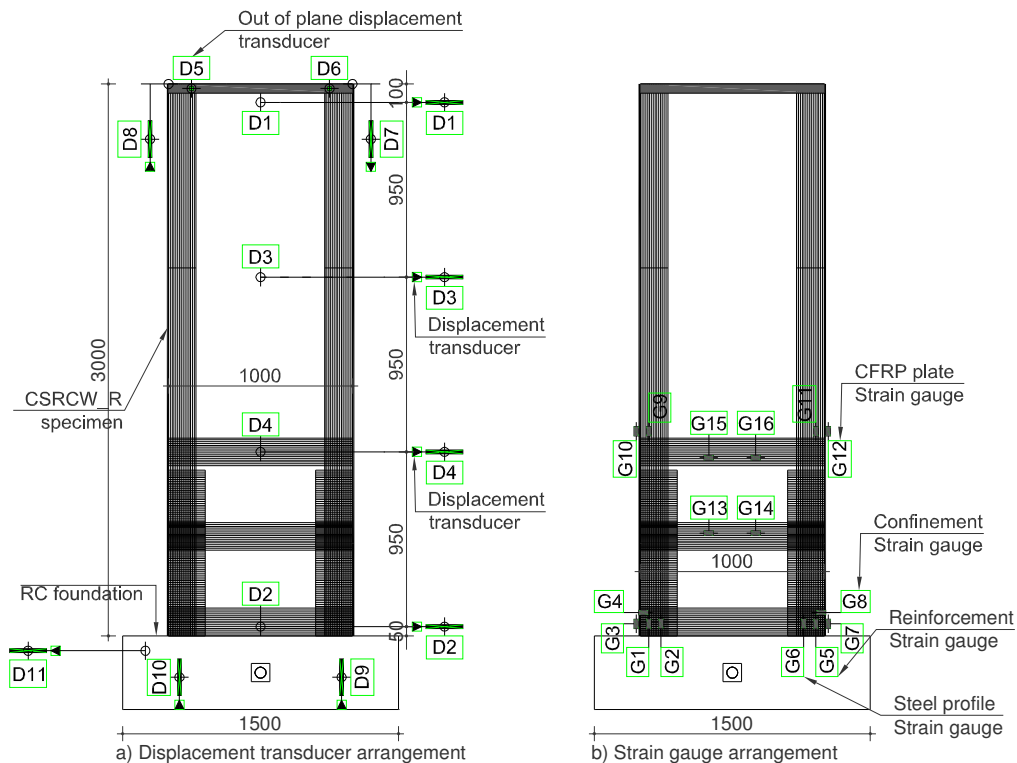


Figure 3.27 Instrumentation of the specimens [mm]

3.6.3 Experimental results and comparative study

3.6.3.1 General behavior and failure modes of FRP strengthened specimens

Generally, the behavior mode of a reinforced concrete wall subjected to in-plane lateral loading can be referred to as either flexural or shear. The flexural mode is characterized by horizontal cracks extending from the lateral edge in tension toward the opposite compressed side. The shear mode is marked by inclined cracks running across the web and/or straight sliding cracks at the linear joints. Nevertheless, it is quite frequent to observe cracks starting horizontally at the edge, and then sloping toward the compressed toe in the web; this situation can be regarded as flexural-shear behavior. The behavior of the two retrofitted and retested specimens CSRCW_R, under reversed cyclic lateral loads, showed an expected behavior, in accordance with the design process and the fracture of the confinement strips, followed by the crushing of the compressed concrete, while the tensioned steel and CFRP strips and plates fractured. Also the rupture of the tensioned reinforcements placed at the extremity of the elements edges occurred, but without the fracturing of the steel encased profile. The behavior of the tested elements was generally similar to the behavior of the reference elements, under similar loading conditions. The behavior aspects of the retrofitted elements are summarized in Table 3.9.

Table 3.9 Response characteristics of the specimens

Displacement stage Δ (mm)	Behaviour aspects
$\Delta < 10$	no visible cracks appeared
$10 < \Delta < 25$	old inclined cracks developed without producing damage on the CFRP strips
$25 < \Delta < 40$	locally debonding of the lower horizontal strip in central part
$40 < \Delta < 60$	new inclined cracks appeared delaminating the lower horizontal strip is important
$\Delta > 60$	horizontal crack appeared in the section near the foundation block through FRP strip fracture of CFRP confining strips in compression zones fracture of the tensioned vertical reinforcements, CFRP plate and strips concrete crushing and spalling

The cracking evolution recorded at the end of each performed displacement level and at failure is presented in Figure 3.25.

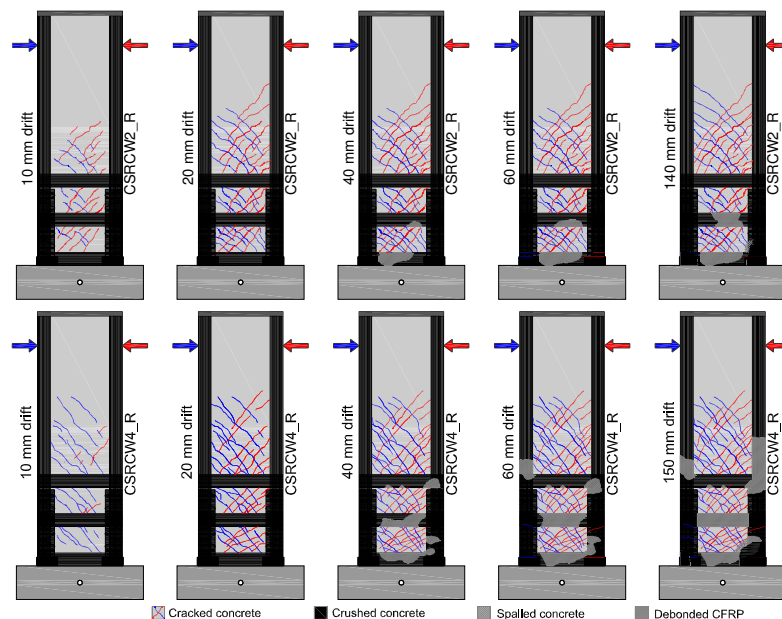


Figure 3.28 Crack evolution and distribution

The failure conditions of the two retrofitted and tested specimens are presented in Figure 3.29. The crack pattern and the hysteretic response diagrams show a flexural-shear behavior during the applied cyclic load. The anchorage provided for CFRP strips and plates were efficient, and no weakening of anchorage was observed during the tests.



Figure 3.29 Failure details

3.6.3.2 Load displacement response diagrams

For the two retrofitted elements, the obtained lateral loads (P) versus the lateral displacement (Δ) hysteretic response diagrams are presented in Figure 3.30 as a comparison with the same responses recorded on the reference elements. The hysteretic curves show that the retrofitted elements recovered the initial strength, in the positive loading cycle direction, and were stronger than the reference elements in the negative loading cycle direction. The increase of the strength in the negative loading cycle direction for element CSRCW2_R was 17%, whereas for element CSRCW4_R was 20%. In Table 4 the recorded values for horizontal loads and displacements at three characteristic stages are presented. As in the case of the reference

elements, a stable behavior was observed, during the cycles performed at each displacement level, with minor strength degradation.

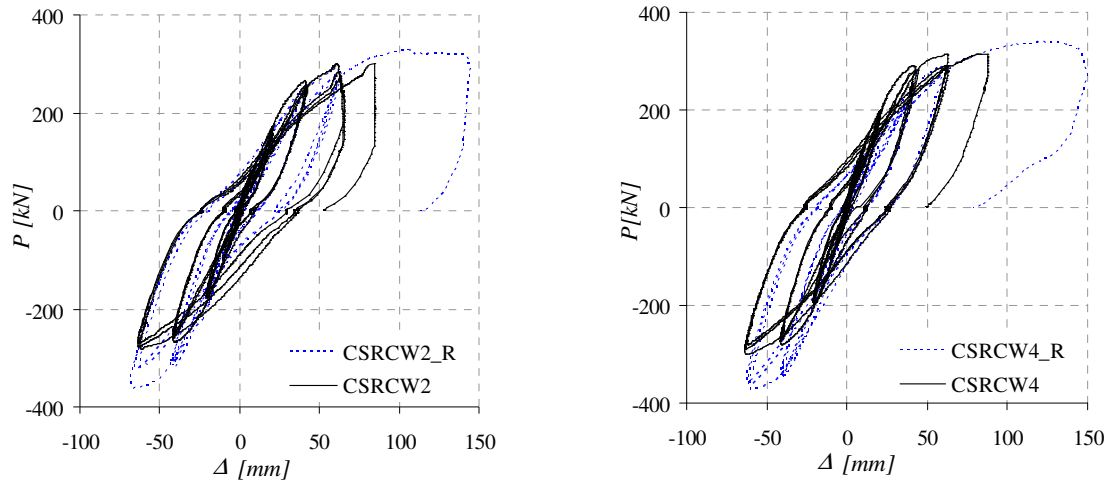


Figure 3.30 Comparison of horizontal load versus lateral displacement hysteretic curves

The behavior of the retrofitted elements was not so dissipative compared to the behavior of the reference elements. The envelopes of the cyclic load-displacement response were drawn in order to evaluate the ductility, the stiffness, the strength degradation and the ductility of the specimens. The cyclic response characteristics of the tested specimens can be revealed by the load-displacement envelope diagrams, which are presented in Figure 3.31, as a comparison with the same responses recorded on the reference elements. The retrofitted elements behavior is nonlinear like the recorded response for the reference elements. These can be attributed to the yielding of the steel encased profiles and the reinforcements that occurred due to the presence of FRP jacket which provides confinement for concrete, delayed concrete spalling and buckling of the reinforcements.

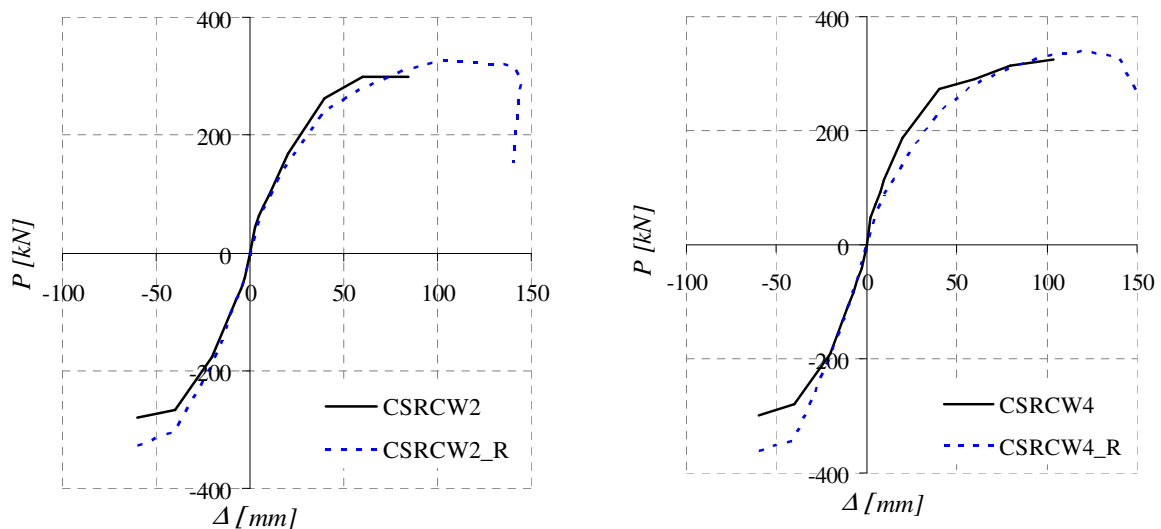


Figure 3.31 Comparison of horizontal load versus lateral displacement envelope curves

3.6.3.3 Stiffness analysis

The stiffness of the tested walls was estimated on the basis of its secant value, defined as the ratio between the load and the current displacement at each load cycle. The initial secant stiffness of each specimen was estimated from the first loading stage, at a displacement level of 2.5 mm, until the element behavior was elastic. In this paper, the stiffness degradation is presented in absolute values for each specimen (see Fig. 3.32 a) and relative to the stiffness of the reference element (Fig. 3.32 b). Table 3.10 presents the values of the initial stiffness for the tested elements and some parameters of stiffness degradation. It can be noticed that by using the retrofitting solution, neither the initial stiffness nor the stiffness at yielding were entirely recovered. It is observed that after 50 mm displacement, the stiffness values of the reference elements and retrofitted elements is equal and this trend is followed until failure.

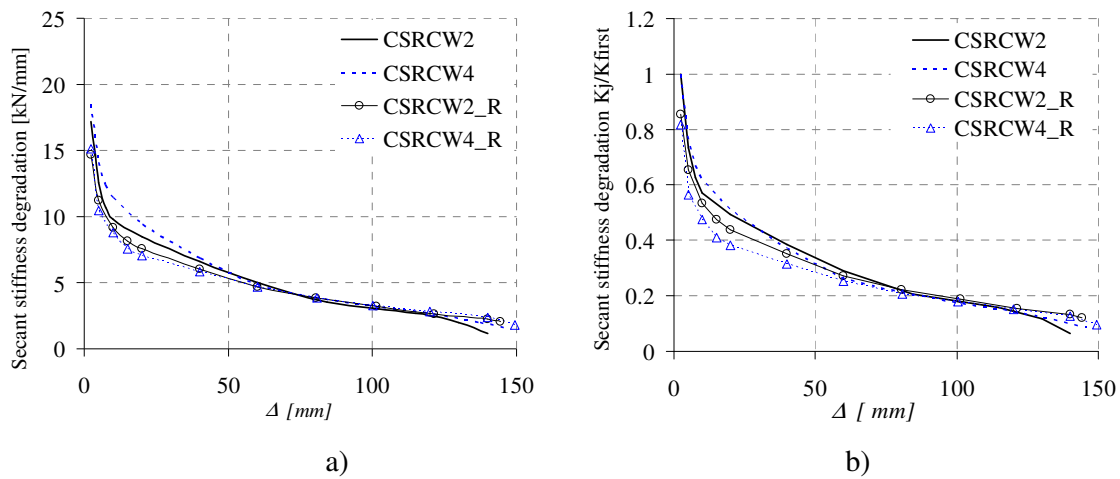


Figure 3.32 Stiffness degradation

Table 3.10 Stiffness degradation values

Stiffness	Initial	Yielding			
Specimen	K_{first} (kNmm)	K_y (kNmm)	K_y / K_{first}	$K_{first} / K_{first}^{ref}$	K_y / K_{first}^{ref}
CSRCW2	17.16	7.96	0.46	-	-
CSRCW2_R	14.65	7.03	0.48	0.85	0.41
CSRCW4	18.52	9.04	0.49	-	-
CSRCW4_R	15.12	6.82	0.45	0.82	0.37

3.6.3.4 Strain analysis

The strain measurements are fundamental in analyzing the response of an experimental element as it reveals precisely the local behavior. In the case of this experimental research, it was considered important to monitor the strains in the vertical and horizontal reinforcements, vertical steel profiles, vertical and horizontal CFRP strips and vertical CFRP plates applied at the edges. In Fig. 3.33(a) there are represented the typical relations between lateral loads versus longitudinal steel strain for steel encased profiles. The strain gauges were placed on the web of the steel profile for CSRCW4_R specimen and on flanges for specimens CSRCW2_R. Fig. 3.33(b) presents the relation between lateral load and ϵ strain, measured on the first layer of the vertical bars located near the steel encased profile, at the extremity of the elements. Fig. 3.33(c) presents the ϵ strain values in relation with the lateral load, measured on the vertical CFRP plates, placed on the side edges of the specimens. It can be noted that, in both cases the CFRP plates were activated from the beginning of the test and worked very well. In Fig. 3.33 (d) there

are presented the lateral load-longitudinal strain diagrams, measured on vertical CFRP strips placed on the front and rear sides, at the edges of the specimens.

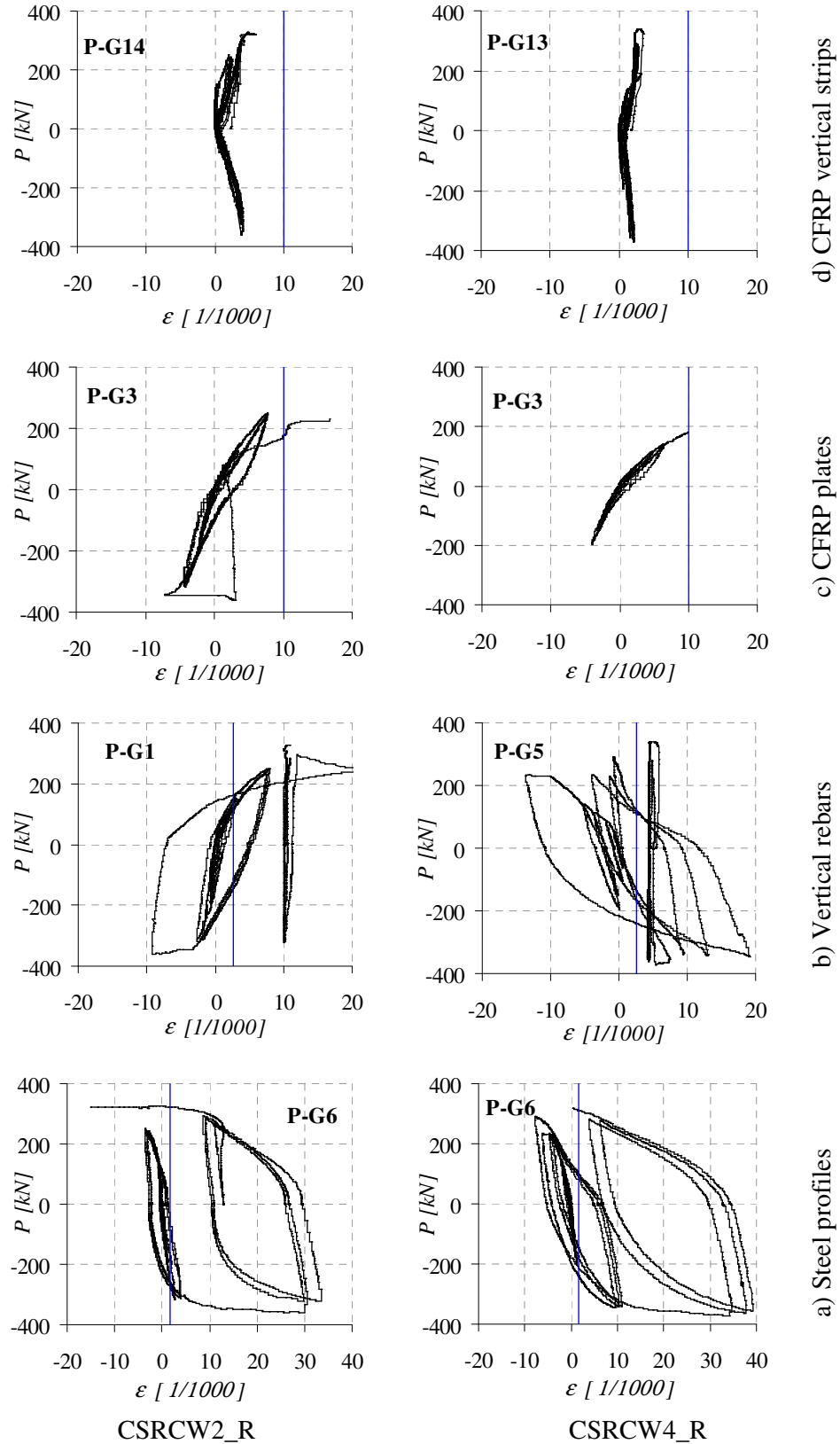


Figure 3.33 Lateral load (P) versus steel strain (ϵ)

It can be noted that in both cases the CFRP strips were activated at the beginning of the test and worked very good until the failure of the specimens occurred. All the other strain recorded values, on different monitoring points, were lower than those presented above, due to premature fracture or debonding of CFRP strips. Although the measurements did not indicate high strain values, the confinement effectiveness was evident. In Table 3.11 there is presented a summary of the strain analysis of the tested specimens.

Table 3.11 Strain analysis summary

Specimen	Maximum strain (‰)		Vertical CFRP plates	Vertical CFRP strips	Confinement CFRP strip
	Steel profile	Steel rebar			
CSRCW2_R	33.4	83.5	16.7	5.93	1.94
CSRCW4_R	39.2	18.9	9.88	3.58	1.56

3.6.3.5 Dissipated energy

The energy dissipation is defined, on the cyclic load-displacement response diagram, as the area bounded by the hysteresis loops. The energy dissipation is presented in Fig. 3.30 in three ways, i.e.: first, it was calculated at various levels of lateral displacement, than all these values were cumulated, and finally the total values of the dissipated energy are presented.

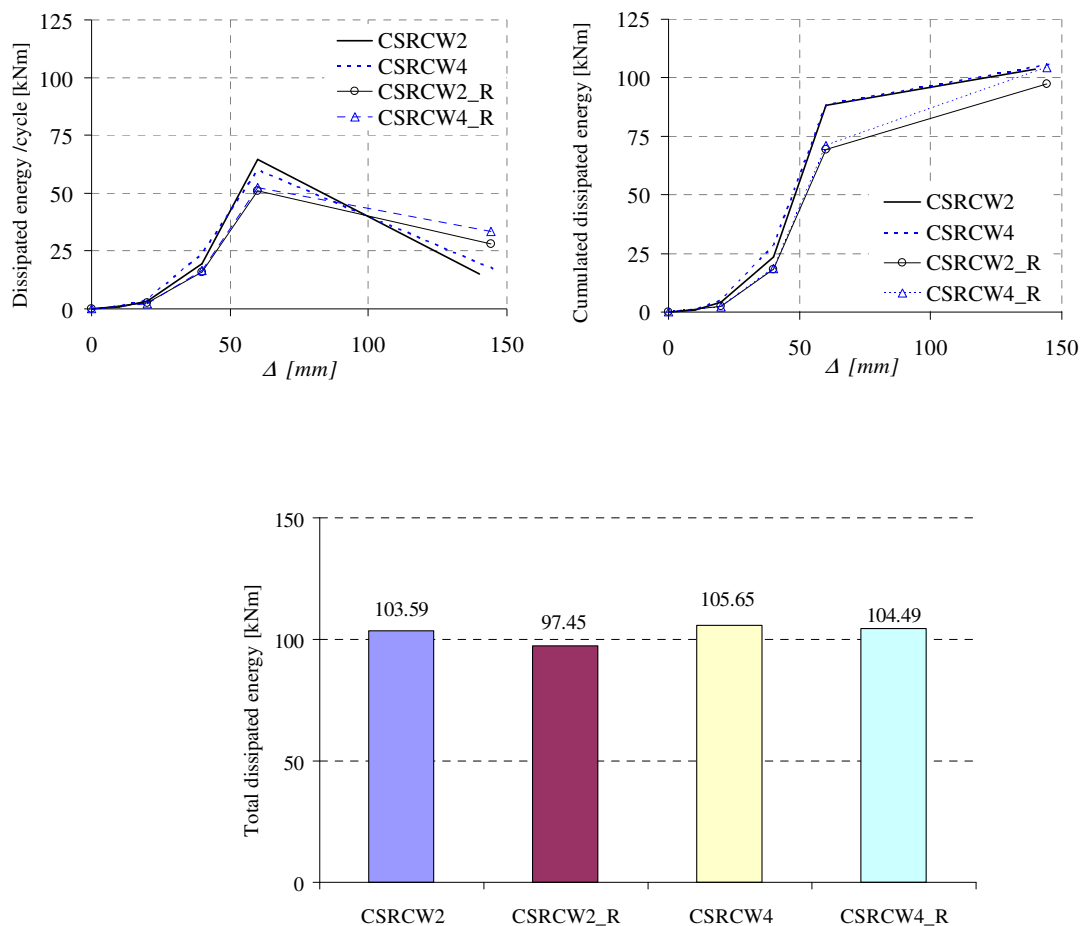


Figure 3.34 Dissipated energy

Then it is presented in all charts and compared to the values calculated for the reference elements, at similar displacement levels. It was evaluated only at the displacement levels, where the three cycles were performed at each displacement levels, in order to provide a good comparison between the reference and the retrofitted elements. It has to be noted that, in the case of typical of structures designed to modern codes, such as the ductile failure modes, a strength drop of 15% in a reinforced concrete member, hardly ever means the actual failure of the member, let alone of the structure as a whole. Considering that the performed cycles and the displacement levels were similar for the reference and strengthened elements, the values of the dissipated energy, at each displacement level, are higher for the reference elements compared to those of the strengthened elements. This leads to a similar trend in the comparison of the cumulative dissipated energy and that of the total dissipated energy.

3.6.3.6 Ductility considerations

The cyclic tests were made until the maximum lateral displacement reached 60 mm, i.e. three times the elastic limit. It seems that the specimens still have force-bearing and deformation capacity after this loading step, but due to the limited laboratory facilities, after this stage, the specimens were only tested monotonic up to failure in the positive direction. This fact influenced the value of the ultimate force and the displacement reached, the effect of fatigue due to cyclic load being removed. Anyway, if a reduction factor of 30% is applied, the values of the displacement ductility are similar to the values proposed in Eurocode 8 for medium ductility class. Due to the stable behaviour exhibited by the elements during the cycles it is possible that the reduction of the ductility not to be so high and higher values, than those presented in codes, to be obtained.

Another important behavior factor for an element of structure subjected to seismic loads, is the over-strength factor $q_{sr} = \alpha_u / \alpha_1$. Taking into account the same loading protocol used for testing the reference and retrofitted elements, the values of over-strength factor for the retrofitted elements are slightly higher than those recorded for the reference elements. Table 3.12 presents the ratio between the ductility and the over-strength factor, and respectively for the strengthened and the reference elements.

Table 3.12 Ductility characteristics

Specimen ductility	Displacement factor μ / μ^{ref}	Overstrength q_{sr} / q_{sr}^{ref}
CSRCW2_R	1.087	1.014
CSRCW4_R	1.115	1.035

3.6.4 Conclusions

The following conclusions, related to the seismic behavior of damaged CSRCW with steel encased profiles retrofitted with FRP materials, are reached as results of the experimental tests:

- The using of FRP strips and plates can serve to restore the strength and ductility of CSRCWs seismically damaged. The strengthening solutions are efficient in terms of the load bearing capacity, the ultimate load of the reference element being restored.
- The use of the horizontal FRP strips, to confine the ends of shear walls flexural strengthened with vertical strips and plates, assisted in preventing buckling and debonding. The confinement of the compressed concrete zones from the edges was efficient, denoted by the delaying of the concrete crushing and spalling.

- The anchorages provided for CFRP strips and plates were efficient, no weakening of anchorage being observed during the tests. The anchorage of the vertical FRP strips with the presented system confirmed the good behavior obtained in other experimental tests, performed on reinforced concrete shear walls. Increasing the anchorage length, along the steel angles, will help prevent the peeling and fracturing in the anchorage zone.
- The initial stiffness of the retrofitted elements was up to 80% of the initial stiffness of the reference elements, and decreased faster than that of the reference elements during the subsequent performed cyclic tests. The cracks filling and the repairing of the crushed concrete were essential for stiffness recovering.
- The dissipated energy of the strengthened CSRCW is slightly smaller than that of the reference elements. The inability of the tested CSRCW_R to exhibit higher energy dissipation under cyclic loading can be explained by the linear elastic response of the FRP materials which cannot contribute, as well as mild steel bars or profiles, to the increase of the energy dissipation capacity.
- The experimental over-strength and ductility factors obtained for the strengthened elements are slightly higher than those obtained for the reference elements.

The main technological merits of using FRP-EBR are the following: ease of installation and minimal intervention to a damaged element by lateral loads. Considering the test results it can be concluded that the application of externally bonded carbon fiber strips and plates is an effective procedure, able to restore the strength, stiffness and ductility for CSRCW with steel encased profiles.

4. Monitoring the constructional structural works and structural health of buildings

4.1 Quality Control of the Constructional Works at the Commercial Center Iulius Mall – Timisoara

4.1.1 Introduction

The commercial centre is made up of several sections, each of them with an independent structure. The first development stage of the area and the building of the commercial centre consist of the construction of 15 blocks and the technical block.

During the constructional works I monitored the constructional structural work done between 2004 and 2005. The architecture of the building was designed by a group of experts coordinated by the architect Radu Mihăilescu [4.2], as the general designer for SC IULIUS GROUP SRL and by the engineer Gherasim Mișcă [4.3], the designer of the structure.

The building will have a surface development of 73, 000 square meters distributed on 3 levels and a terrace, hosting over 200 shops; besides the shops, there will be found: multiplex cinemas, a supermarket, restaurants, food courts, bars, kids land and sports centres.

The main structure system adopted is a spatial reinforced -concrete frame structure at which, locally, spatial steel structures are added. For the infrastructure they have used concrete waterproof foundations and for the construction of the boards they have used hollow-core precast slabs, and prestressed slabs type π , respectively, in areas with great loads.

The spatial structure, mostly regular, has an opening of around 9m and an identical span. An exception is made by the areas around the central small square where the columns are 4.5m apart.

4.1.2 Constructive systems and technological solutions used

Along the building process many aspects, in what the execution technology was concerned, were slightly changed or improved.

One of the first problems that occurred was at the pouring of the foundations. Thus, while digging at block B we hit a concrete foundation, which appears to have been used for anchoring the steel posts (aerials), previously placed in this area. The concrete block had a cylindrical shape, with a 2.5 m diameter, the upper top being of approx. 70 cm above the foundation quota. (Figure 4.1). The depth of the concrete posts could not be established. According to the project, approximately 1/3 of the foundation surface of one of the concrete columns had to be placed on the newly discovered concrete block.

This column was considered to be under great stress due to the existence of a swimming pool, at the second level, that discharges through the beams into this column. The designer did not accept this fact because they considered that as a consequence extra stress is put on the foundation due to the eccentric resting.

Besides the problems pointed out, it was also revealed that around the concrete block discovered at excavations, there was a layer of filling material and silt. The land was considered improper for a foundation. The level at which the foundation quota was designed was in fact the limit of the underground water; in the construction area being a lot of local water lenses, the area being of a clay type.

In order to make the foundation, two things had to be taken into account: on one hand enhancing the quality of the foundation area and on the other side finding a solution that does not incur extra costs for the foundation. Because of the clay (cohesive) ground, there was no consideration of enhancing the quality of the foundation with extra ballast concrete.

The first suggestion was to introduce, locally, steel pipes of a length of 3.0 m and with a diameter of 70mm, in which cast concrete was to be poured. (Figure 1) After the introduction of the steel pipes and after having done the determinations to define the bearing load, we discovered that the effect was little and a new geotechnical expertise was needed to establish the solution for the consolidation of the foundation ground.

The geotechnical expertise and the consolidation solution were made by professor engineer Marin Păunescu PhD [4.1]. It was a two-phase process consisting in making some ballast columns stabilized with concrete, drilled in the influence area of the future foundations. Each column had a diameter of 500 mm and a depth of 3.0 m. For all the area under question, 54 columns were to be made, filled with concrete to enhance the consolidation capability, and the vibration one, respectively.

In the first stage, 30 columns were to be made, then, according to the determinations, decisions were to be taken regarding the necessity of the columns which remained to be made in the second phase.

In Figure 4.2 and 4.3 there are presented aspects from the preparation of the area for the building of the columns.



Figure 4.1 – Consolidation of the foundation ground by introducing steel pipes and concrete – Solution 1

Figure 4.2 – Preparation of the platform for the construction of the columns

In Figures 4.3 ÷ 4.6, there are presented a few aspects from the execution of the drillings to make the columns and to pour the concrete.



Figure 4.3 – Drilling the ground to make the columns



Figure 4.4 - Device used for the drilling of the columns



Figure 4.5 – Drilling area ready for pouring Figure 4.6 – The pouring and vibrating of the first column one column

In photos 4.7 and 4.8 there are presented some aspects of the enhanced land with concrete columns, and the tests made for determining the bearing capacity of the enhanced land.



Figure 4.7 – Columns poured at the end of phase I Figure 4.8 – Test with the board after the construction of the columns

The foundation of the column placed on the consolidated land is shown in Figure 4.9.



Figure 4.9 - The reinforced concrete foundation of the column situated on the consolidated land

The construction of this multifaceted commercial centre has imposed, from an architectural point of view, meeting certain volumes and proportions. One of the highest points of the building will be placed above a little square and above the main entrance, respectively. It will be hosted by the so called “steel box”, taking into account the fact that it is made of steel and metal sheet closings.

The surface of the steel box will be around 2100 square meters with an opening of 36m and 2 side consoles of 4.5m. The structural strength is made up of a spatial system of frame girders, designed by eng. Iuliana Foldvary [4.3].

Taking into account the 36 m opening, the 4.5 m consoles of the frameworks, the geometric dimensions of centre surpass 5m in height.

The technological problems which occurred during the construction, referred first of all to the construction of the frameworks and their transportation having in view their overall size. The large dimensions imposed the execution of each framework on sections, and then each section was to be joined by welding. To avoid the execution of the joining at the most stressed areas the variant chosen was the construction of a framework of 45 m in 3 sections.

The frameworks stand, with the help of certain metallic stays, on concrete columns of 20m height. Each framework weighs approximately 52 t. The concrete columns have a circular section with a diameter of 90 cm.

In photos 4.10 and 4.11 we present aspects from the execution of the joining of the longitudinal reinforcements of the circular columns and the detail regarding the support element for the future steel frames.



Figure 4.10 – Joining the longitudinal reinforcements at the circular columns bearing the steel box.



Figure 4.11 – Steel support for the steel frameworks

In Figures 4.12, 4.13 there are presented aspects from the raising and mounting of the longitudinal frameworks.



Figure 4.12 – Mounting the longitudinal frameworks



Figure 4.13 – Positioning the framework and its fixing on the support element



Figure 4.14 – Temporary setting of the support frameworks



Figure 4.15 – Determinations with penetrating liquids to test the quality of the welding

The large overall size and the location, where the 45 m long frameworks were mounted, needed solutions as to the place of the cranes, the lifting capacity and the crane translation. For lifting, two cranes, type COLES were used. In photos 16 and 17, aspects from the lifting moment of a framework are shown, as well as the crane translation (~14m horizontally from the initial lifting position).



Figure 4.16 - Aspects from the framework lifting



Figure 4.17 – Translation of the steel truss

The structural strength of the assembled steel box is presented in Figure 4.18. For the construction of the structural strength of the steel box 523t of steel were used.



Figure 4.18 - General view of the structural strength of the steel box

To make the structural strength of the future commercial centre they used: approximately 3,000 t of steel and over 80,000 m³ of concrete.

The completion of the structural strength represented a key moment for this investment, which coincided with the decisive phase planned for the reception of the structural strength in the program for the quality control of the works designed and under construction.

4.1.3 Conclusions

At the realization of large investments, the solutions initially designed need to be supplemented and monitored along the execution stage because of unforeseen situations which can occur or because of special situations imposed by the manufacturing technology of certain construction elements.

In Romania, the survey of the execution quality of the construction works is enforced by Law 10/1995- *The Law for the Quality of the Constructions*. The control of the works under constructions is materialized by filling in “Chapter B” documentation of The Construction Book, which provides the most important information regarding the structural strength of a construction.

A general view of the Comercial Center Iulius Mall at the end of the construction works is presented in Figure 4.19.



Figure 4.19 – General view of main entrance Iulius Mall Centre Timișoara

4.2 Structural health monitoring of reinforced concrete chimneys

4.2.1 Introduction

Structural rehabilitation of a pair of reinforced concrete chimneys belonging to an electrical power plant is presented next. The structural rehabilitation was necessary due to the numerous vertical cracks that appeared in the lifetime existence of the chimneys. The major cause of the appearance of these cracks into the structural reinforced concrete layer was the high thermal gradient between inner and outer surface in the context of insufficient horizontal reinforcement. Therefore, a radical intervention was necessary in order to replace the thermal insulation and to repair the horizontal reinforcement. Also a prestressing force was induced into the concrete layer, using segmental steel belts, in order to generate compression stresses and to prevent the reopening of the cracks. High performance special cement mortar was used to fill the cracks. In the second stage, an on site monitoring program was developed to control the possible opening of some cracks using outside observation (the interior air temperature varies between 200 and 50 Celsius degrees). Laser thermograph and special optical devices were used for health monitoring.

4.2.2 General description of the structure

The two chimneys have a tapered structure; made of reinforced concrete using climbing technology. The total height of the chimneys is approximately 220 meters. The particularity of the technological and structural solution consists in the fact that the burned gases resulted during the technological processes are introduced into the chimneys only at the approximately +100 meters elevation and not at their base as in the traditional solutions. The width of the reinforced concrete wall varies between 90 centimetres (+92 meters elevation) and 24 centimetres (at the top of the chimney, at +220 meters elevation). The reinforced concrete structure is protected by a thermal insulation (made of foam glass of 50 centimetres in width) and by an antacid protection (made of specially shaped antacid silica-aluminous refractory bricks, immured with inorganic antacid putty).

4.2.3 Structural issues of the CHIMNEYS after 30 years of service

In the process of the building of the chimneys, several design, execution, service and maintenance mistakes were made, leading to a series of important degradations of the reinforced concrete structure. The most important design errors that are worth mentioning are: the lack of thermal insulation in several sections, the design of important and abrupt variations in stiffness, misjudgement of the simultaneous action of the wind and temperature variations, which led to an insufficient horizontal circular reinforcement. Also an important design issue was the lack of a correlation between the thermal insulation and the important variations in stiffness. The most important execution mistakes took place during the climbing process used for creating the reinforced concrete structure. Due to these errors, combined in time with the effect of an insufficient concrete cover of reinforcement, the final characteristics of the materials and their behavior were severely damaged. Faulty exploitation and maintenance over important periods of time, by evacuating burned gases with higher temperatures than the designed ones, and also the long term operation without scheduled revisions or repairs, contributed decisively to the important damages in the concrete structure.

All the above mentioned factors contributed in time to the pronounced state of degradation of the structure, of the insulations and installations of the two chimneys. In the reinforced concrete structure, a series of small and large cracks (some of them piercing through the entire width of the wall) with widths up to 6 centimetres can be observed. Over the opening of some cracks, the horizontal circular reinforcement is sectioned. However, the structure of the

chimneys does not show any specific cracks due to flexure and the vertical reinforcement is in perfect shape, with no visible signs of corrosion (of course with the exception of the areas adjacent to the wide cracks, where the lack of the protecting layer triggered the start of the corrosion process). In the same time, important areas of the exterior concrete surface are highly degraded due to the chemical assault that they were subjected to. In Figure 4.20 the severe damages of the reinforced concrete structures can be observed; a detail of a large crack and of the poor condition of horizontal circular reinforcement being presented.



Figure 4.20 Severe damages of the reinforced concrete structure

4.2.4 Investigation methods

In order to determine the real characteristics of the materials, a series of chemical analyses and mechanic tests were performed. The depth of carbonatation, the value of the PH and the compressive strength of the concrete were determined on the sampled cores. The chemical analyses revealed the fact that the concrete was carbonatated on a depth of maximum 50 millimetres from the exterior surface (the value of 50 millimetres being recorded at the +134 meters elevation). After performing the mechanical tests, it was shown that the compressive strength of the concrete corresponds to a C25/30 class of concrete, proving that in the areas where the chemical attacks did not occur, concrete kept performing in a proper manner. In order to correctly monitor the later behavior of the chimneys, all the visible cracks were cartographed and their width was measured and recorded. The temperature was also recorded throughout the entire height of the chimney, on the exterior concrete surface and into the concrete wall, at various depths inside large cracks.

4.2.5 Solutions for rehabilitation

The structure of the chimneys being highly damaged, several rehabilitation procedures were proposed. Any of these procedures would have supposed interventions on the structure, on the installations and on the insulations. The first proposal involved the use of carbon fiber reinforced polymers (CFRP), for both confinement and flexural strengthening, or only for confinement (since the flexural capacity of the structure was adequate). The second solution, the chosen one, implicated the use of a large number of horizontal steel belts that were to be prestressed. Their purpose is to compensate the lack of horizontal circular reinforcement that was

undersized during the design process and which was corroded, throttled and even sectioned in time. The belts were placed at every 70 centimetres on the bottom side of the chimneys, the distance between them being larger at the superior side. Each belt was made out of several steel flat bars connected through special steel parts with the possibility of inducing posttensioning stresses in the flat bars. Before the belts were placed on the exterior side of the concrete structure, the continuity of the horizontal circular reinforcement was re-established by welding together the sectioned steel bars. All the corroded reinforcement was cleaned, sandblasted and all the cracks and cavities were filled with special mortars. In Figure 4.21, the solution for re-establishing the continuity of the horizontal reinforcement, a detail of the special prestressing steel piece and a view of the strengthened chimneys are presented.



Figure 4.21 Stages in the rehabilitation process

4.2.6 Health monitoring of chimneys

After the rehabilitation was completed, it was decided to permanently monitor the structures of the two chimneys in order to observe, in real time, the degradations that would appear. Since the main cause of the structural damages was the variation of temperature, it was settled to keep the temperature of the chimneys under strict supervision. Both chimneys are in use 100% of the time, no access being possible in their interior because of the very high temperature (50...200°C). Only the temperatures of the exterior surface of the structure were measured. Any abnormal variation of these temperatures, or any area with temperatures much different than those of the adjacent areas, would correspond to a local deterioration of the thermal insulation, requiring immediate interventions.

The temperature of the exterior surface of the concrete structure was cartographed using an infrared thermograph camera. By using this camera, absolute temperatures and exact variations of temperature were recorded, practically in every point of the exterior concrete surface. Through this thermograph images, no areas with damaged thermal insulation were discovered so far. The temperature of the exterior surface of the chimneys is much more dependent on the exterior ambient temperature, climacteric conditions and on the position of the investigated area, relative to the cardinal directions, than on the temperature of the burned gases inside the chimneys. The areas most exposed to the action of very high temperatures are those in the vicinity of the point where the burned gases are inserted into the chimneys and where the adequate insulation lacks.

In Figure 4.22, a series of images acquired with the IR thermograph are presented. The images show a uniform distribution of the temperature on the entire height of the chimneys. At the same time, the absolute values of the temperature do not exceed 27 °C, demonstrating the fact that the thermal insulation is efficient and that no areas are subjected to the very high temperatures of the burned gases inside the chimney. The pictures also proved the previously

stated affirmation, i.e.: the temperature of the exterior surface is much more dependent on exterior factors than on the temperature of the burned gases.

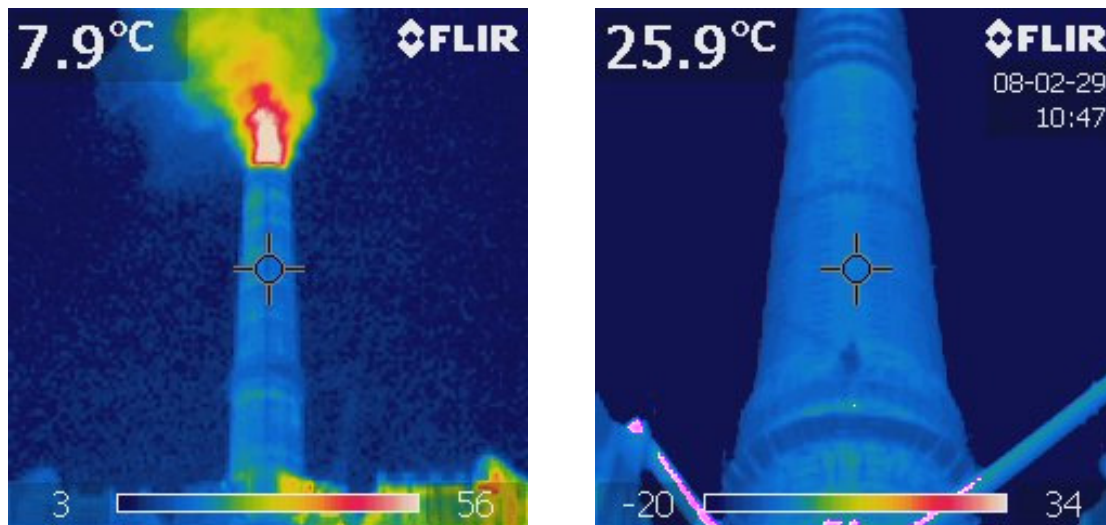


Figure 4.22 Thermograph snapshots

The mechanical condition of the exterior surface of the concrete structure was under regular surveillance using high performance optical devices and cameras. Using this equipment, the areas with multiple cracks were examined and it was possible to detect the potential reopening of older cracks which were filled in rehabilitation process.

In Figure 4.23 several cracks are detailed. A thorough examination of the concrete surface revealed the fact that these cracks are superficial ones. They have probably appeared due to the contraction of the mortar that was used to fill them. This situation could have been avoided by the use of concrete or mortar with dispersed steel fibers reinforcement. However, the surface of the chimneys that show signs of crack opening is insignificant compared to the rest of the surface which is in very good condition.



Figure 4.23 A series of superficial cracks and an area with surface in good condition

The chimneys are undergoing a process of upgrading from the monitoring point of view. New devices will be used in order to keep monitoring the structure in a proper manner. A series of transducers will be mounted at different elevations, in the vicinity of the opened cracks. This way, the important cracks will be constantly checked for variations in widths. Also, strain gauges will be placed on a large number of flat bars and on the vertical and horizontal reinforcements. When these operations are completed, it can be stated that all the aspects of the behavior of the chimneys will be thoroughly monitored.

4.2.7 Evaluation of the service period left for the chimneys

The service period of a structural reinforced concrete element is determined by the degree in which the materials keep performing in the designed manner. In the case of the two chimneys, the materials in question are: the concrete and the steel reinforcement. One of the most important effects, when establishing the durability of a reinforced concrete element, is its corrosion. In this case, the service period of the structure is composed by the period of initiation of the corrosion at the reinforcement level and the period of propagation of the corrosion up to the maximum allowable level. Using the investigations conducted in year 2002, it was established that the level of carbonization in the concrete varies between 1.3 and 4.9 centimetres. When extracting the sampled cores, it was determined that the vertical reinforcement that is protected by the concrete is in perfect shape, with no signs of corrosion. At the level of vertical and horizontal reinforcement in the vicinity of cracks it was ascertained that the corrosion process was triggered. As a result of the rehabilitation process, all the reinforcement was cleaned and sandblasted and all of the cracks were filled. These operations have increased the service period of the chimneys in an important manner. Using the formulas available in literature, the maximum period for the corrosion of the reinforcement can be determined using the formula (4.1).

$$t_{cr} = \frac{m_r \max}{v_c} = \frac{\frac{\phi_0}{2} - \frac{\phi_c}{2}}{v_c} = \frac{\frac{22}{2} - \frac{16}{2}}{0.1} = 30 \text{ years} \quad (4.1)$$

Where,

- m_r stands for the depth of corrosion;
- v_c stands for the speed of corrosion;
- Φ_0 stands for the value of the initial diameter of the reinforcement;
- Φ_c stands for the value of the corroded diameter of the reinforcement.

The speed of corrosion used to determine the maximum period of corrosion is quite high due to the extreme ambient conditions. Considering the speed of corrosion used in formula (4.1), the period in which the reinforcement is corroded, in a percentage of 30%, is 30 years, this being considered the minimal service period of the chimneys. It is important to affirm the fact that all of these statements were based on a qualitative evaluation of samples and do not refer to calculations of the structural capacity of the chimneys.

4.2.8 Structural analysis

ATENA 2D software package was used to perform the FE Analyses in order to assess the effectiveness of the proposed interventions onto the chimneys' structure. The analyses considered the effect of thermal gradient on the structure before and after the post tensioning of the horizontal belts. The performed 2D models define a range of cross sections at various elevations. Since the structure of the chimneys is tapered, and since the burned gasses are at their highest temperature at the insertion point (approximately +100 meters elevation from basement),

the section considered to be critical is defined at this level. Therefore, the model presented in this paper refers only to the situation above described.

4.2.8.1 Numerical models

The cross section that was analyzed had the shape of an annulus having external and internal radius of 6500 mm and 5600 mm, respectively (the width of the RC wall being 900 mm). In order to reduce the processing time, only a quarter of the annulus was defined. The axial symmetry of the chimney was taken into account. The thickness of the element was considered 150 mm, and the plane stress state was assumed.

Three different alternatives of the physical state of the element were modelled: V1 which corresponds to the element in its initial state, before any strengthening procedure was applied, V2 that corresponds to the strengthened element, with the post tensioning being applied previously to any temperature gradient between exterior and interior surface, and V3 which corresponds to the strengthened element, with the post tensioning being applied subsequently to all of the temperature gradients. Since the integrity of all the structural elements was restored before applying the final step of the rehabilitation process (the prestressing of the horizontal belts) it can be considered that the V2 version of the modelled element is the one that best describes the real on-site situation.

4.2.8.2 Materials

All the defined materials were standard ATENA 2D materials, with user defined characteristics. The concrete was defined as “SBeta” material which represents a damage-based material model recommended in ATENA for modelling of 2D concrete elements. Since it was determined that the concrete in the structure of the chimneys corresponds to a C25/30 concrete class, the properties were defined as follows: compressive cubic strength of 30 MPa, compressive strength of 25.5 MPa, tensile strength of 2.317 MPa and an elastic modulus of 30320 MPa. Exponential type of tension softening and crush band type of compression were defined for SBeta material.

The V1 model considered only the two embedded horizontal reinforcements (inner and outer) while the V2 and V3 considered also the post tensioned belts in the form of prestressed reinforcement. All of the reinforcement was modelled using discrete type (by means of truss elements). Two different types of “Reinforcement” material were used. A multilinear type of stress-strain law was used for normal reinforcement and a simplified bilinear with hardening type of stress-strain law was used for pre stressed belts. Both types of materials had the elastic modulus of 210000 MPa. The normal reinforcement was defined with an elastic limit of 210 MPa and an ultimate strain of 30%. Corresponding to the ultimate strain, the strength of 340 MPa was defined. For the prestressing belts an elastic limit of 400 MPa, an ultimate strain of 10% and a corresponding strength of 480 MPa were defined. The area of steel was of 78.5 mm² for both the inner and outer normal reinforcement, each corresponding to a circular reinforcement bar of 10 mm diameter. Given that the step between two horizontal belts is 600 mm, and the thickness of the model is 150 mm, the area of the steel flat bars was considered of 600 mm², corresponding to a quarter of one flat bar area. Perfect bond was assumed between reinforcement and concrete. The stress-strain laws for the two types of reinforcement are presented in Figure 4.24.

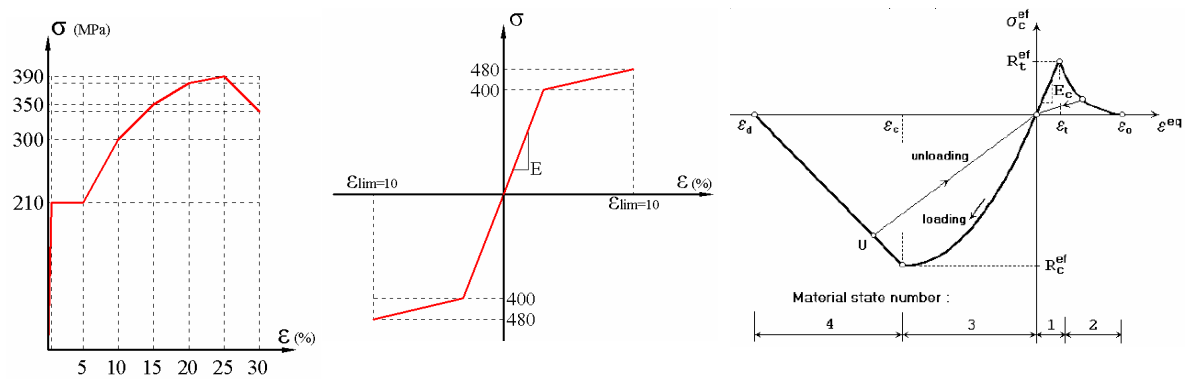


Figure 4.24 Stress-strain law for normal reinforcement, prestressed steel belts and concrete

4.2.8.3 Supports, loads and finite element mesh

Supports were considered on the entire vertical upper left edge, blocking horizontal displacements and on the entire horizontal lower right edge, blocking vertical displacements. As stated previously, the temperature gradient and the post tensioning effect were both taken into account. In order to simulate the thermal gradient between interior and exterior surface, the element was divided all along its length into 9 subdivisions perfectly connected with each other (each subdivision having a width of 100 mm). The loads were applied incrementally considering worst case scenarios, with exterior temperatures as low as -40°C and interior ones as high as $+150^{\circ}\text{C}$ and with linear distributions of temperature between interior and exterior. The post tensioning was also applied incrementally, in such a way that the final control stress in the flat bars would reach 380 MPa.

The V1 model considered first of all the situation of a decrease in the exterior temperature to a lowest of -40°C , in the condition of an adequate internal thermal insulation. Then after, the increase of interior temperature (caused by damage of thermal insulation) up to $+150^{\circ}\text{C}$ was considered. The V2 version considered in the first place the post tensioning of the horizontal steel belts and then after, the same situations in thermal gradient as for V1. The V3 version, considered the entire thermal gradients as for V1 and subsequent to all, the post tensioning of the horizontal steel belts.

A quadrilateral mesh type with size of 50 mm by means of quadrilateral elements with geometrically nonlinearity compatibility was used.

The components of the model in the V2 and V3 versions can be observed in Figure 4.25.

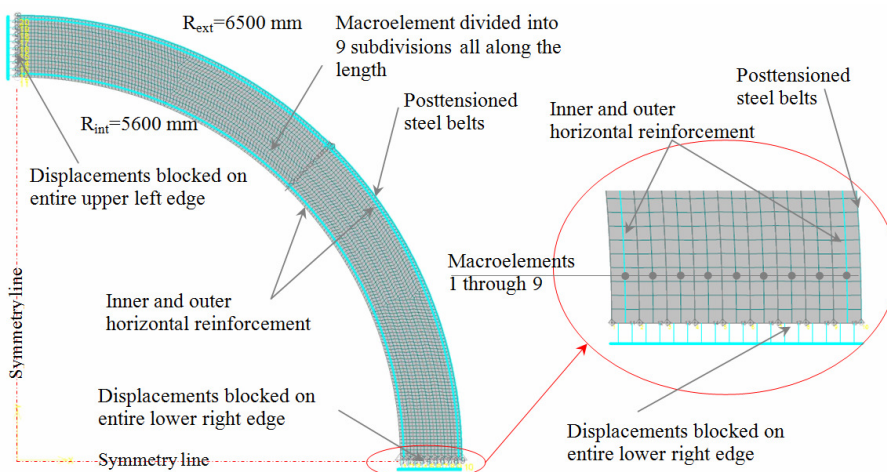


Figure 4.25 Sketch of the biaxial symmetrical model with restrained displacements

4.2.8.4 Results and discussions

The results obtained from numerical modelling show that the rehabilitation interventions have a positive effect on the overall behaviour of the chimneys' structures. Some of the most important parameters for the three models, after all of the load steps are completed, are presented in table 4.1. The final crack patterns of the three models are presented in Figure 4.26.

Table 4.1 Results of the V1, V2 and V3 models, after all of the load steps are completed

Result	V1	V2	V3	V2 vs V1
Maximum crack width [mm]	8.662	0.887	0.694	Reduction \approx 90%
Maximum principal stress in inner horizontal reinforcement [MPa]	103.000	54.860	55.520	Reduction \approx 47%
Maximum principal stress in outer horizontal reinforcement [MPa]	217.100	189.800	133.700	Reduction \approx 13%
Maximum principal stress in post tensioned steel belts [MPa]	---	403.500	402.000	---
Maximum principal stresses in concrete [MPa]	2.125	2.023	2.064	Reduction \approx 4%
Minimum principal stresses in concrete [MPa]	8.693	14.240	14.010	Increase \approx 64%

The fact alone that there is a significant increase in the amount of reinforcement in the cross section, gives the structure a much higher capacity to withstand temperature gradient. Even without the post tensioning, considering that obviously that the belts are effective the overall capacity is notably increased.

Important differences can be observed by comparing the behaviours of the three models. If, in the case of the V1 model, only a small number of cracks appear up to the final loading step, in the other two models, a large number of cracks are distributed along the entire length of the element. Obviously, the cracks in the V1 model are larger and longer than in the other two models. This leads to a very small compressed concrete area, practically all of the cross section being tensioned. This major dissimilarity is caused by the under dimensioned horizontal reinforcement, which reaches its yield strength quite soon after applying some fractions of the total thermal gradient. In all of the models, the vertical cracks appear uniformly distributed over the chimneys' envelope.

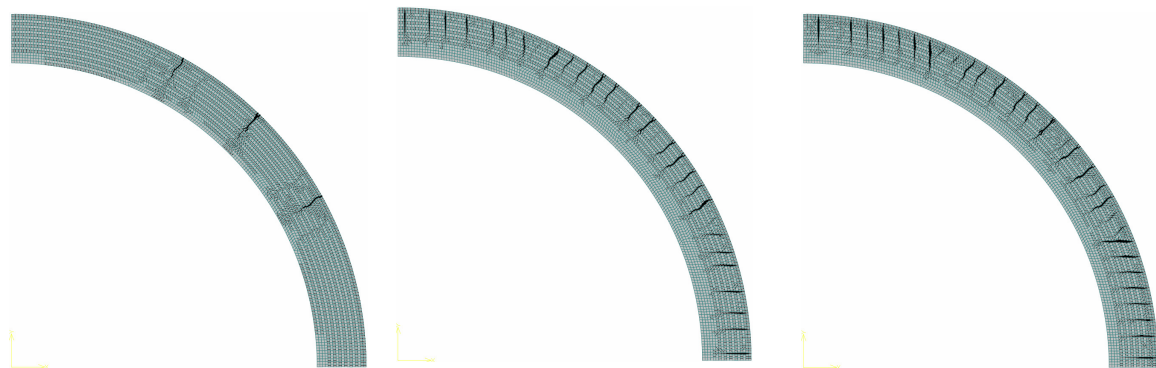


Figure 4.26 Crack pattern for V1, V2 and V3 models after all of the load steps are completed

4.2.9 Conclusions

The behaviour of the chimneys in service along with the measurements performed as part of the SHM program, have proved the effectiveness of the applied solutions. Even though the results show that the interventions have a positive outcome, either one of the modelled situation, the crack width reaches in the end values higher than those prescribed by codes. In the event that the internal thermal insulation would be damaged once more, the structures would not be safe. Finally, it can be stated that the performed interventions have increased significantly the overall capacity of the structures and have also extended the service life of the chimneys with important period of time.

The monitoring program that was developed and that will still go on in the coming years, helped to solve several issues and questions. At the same time, this program will eliminate the possibility of not discovering structural damages in real time. The monitoring program will continue and will be updated throughout the existence of the two chimneys.

(b-ii) Scientific, professional and academic future development plans

Taking into account the scientific achievements already presented, the future developments plan contains two phases: short and medium research plan and long term interventions.

- The *short and medium plan* consists of using the existing infrastructure with small adjustments, involving the existing human resources.
- The *long term plan* includes the developing of the existing infrastructure; attract more master students and Ph D. candidates in the research activities.

As far as the developing of the existing infrastructure, I envisage an integrated civil engineering laboratory. The existing infrastructure can be used for testing structural elements for buildings, at a real scale or not. I also envisage an integrated civil engineering laboratory in the field of extreme actions as earthquake, fire, blasting, wind, climatic actions etc. for structures at real scale. I am considering extending the existing laboratories with new ones which have to include a section dedicated to technological processes in civil engineering. The new laboratory has to comply with the following aspects:

- cutting and forming reinforcements;
- realizing special moulds;
- new technological aspects of concrete preparing, with section of high and ultra-high strength concrete;
- technologies for casting of normal, self-compacting and high strength concrete;
- cutting and forming structural steel;
- new technologies used for wood structures;
- new technologies for finishing;
- processes in equipments for residential and industrial buildings.

The developing of the existing infrastructure has to be implemented using an investment plan which includes the possibilities to realize micro products. For example: the acquisition of a micro station to prepare concrete can lead to obtaining contracts from the private medium, for the manufacturing of precast elements, such as: slabs, beams, poles, road borders, pavement elements, etc. The manufacturing of these elements in the micro production laboratories of the UPT can be financially efficient not only for the university patrimony, but it can also become an extra financial source for the existing research centers.

All the above mentioned programs have the underlying idea to attract new funding for the research teams, to enhance the working capacity of the research teams, mostly made up of well-known experts and young researchers in need for proper training; facts already proven by the big number of projects won at national competitions.

As presented in (b-i), the research already done is developed into two main thematic directions.

- A. Theoretical and experimental studies regarding the behavior of steel composite elements for buildings placed in seismic areas;
- B. Monitoring the structural health of special constructions or highly important buildings and monitoring certain constructions in order to validate certain calculus principles.

In the *short and medium plan* I intend to continue the research on the above mentioned fields as follows:

A. In the field of *the behaviour of steel concrete composite shear walls with high strength concrete* I aim to:

- Identify innovative solutions for composite steel-concrete shear walls with partially encased profiles, for solid composite walls and with various configurations of openings;
- Find new technologies to make shear walls using fibre reinforced concrete;
- Use Fiber Reinforced Polymers to strengthen composite shear walls as possible strengthening solutions for structural elements damaged under seismic events

A.1 General presentation of the research theme

This research theme pertains to the field of civil engineering and lays emphasis on the structures subjected to lateral loads and their lateral load resisting systems, in the shape of reinforced concrete shear walls, and a series of derived innovative, alternative systems. The need of lateral resistance for structural systems appears due to the horizontal loads which act on all common civil engineering work. The lateral loads can be generated by wind effects, earthquake phenomenon, explosions and impacts. The effects produced on structures due to these loads depend on the intensity of the lateral load and on the structural system's capacity to withstand these actions. Whilst the intensity of the wind loads, explosions and impact effects can be predicted with a high accuracy, due to the technology development, the earthquake still remains an unpredictable event, both in terms of the intensity of the lateral loads as in respect to the complete behavior of the structural system.

Urban habitation of nearly all modern cities implies the construction of a large number of high-rise buildings; the most important development projects in residential and office spaces relate to such structures. In most of these structures, the lateral load resisting system comprises reinforced concrete and/or composite steel-concrete shear walls. The traditional reinforced concrete shear walls have been used as the primary lateral load resisting system in multistory buildings and generally performed well during the past earthquakes. Even though reinforced concrete shear walls have many structural and economical advantages, some disadvantages appear when using this structural system in buildings subjected to seismic action. One of the main disadvantages is the development of tension cracks in tension zones and the compressive crushing in localized compression areas during large cycles. Based on these facts, the present program proposes studying a series of alternatives, in the form of composite steel-concrete structural walls and some specific details and solutions for enhanced performance.

Considering the previously mentioned arguments, it can be clearly stated that the theme of the project presents a high degree of applicability, positive results being able to impact significantly on technical and technological issues of traditional systems. Consequently, the economic advantages that could lead from the research results are of high implications. Should some of the proposed solutions prove to lead to adequate behavior of the experimental elements, the technological implications are to be extremely relevant, as the execution process could become less time consuming and more economic efficient.

The design of the shear walls for buildings placed in seismic regions is made by using the design codes of the composite steel and concrete structures, and the design guides of buildings for earthquake resistance, as well. Severe technological complications occur, especially in the lower stories of the frame buildings with large bays, where shear walls must be provided to limit the lateral displacement of the structure. Due to the limits of the axial force ratio and to the

requirements on the transverse reinforcement, at the confined boundary elements, imposed by the seismic codes, rather often a high percentage of steel results. The limited dimensions of the elements and the high percentage of the steel needed at the extremities of the walls, make impossible to use rebars. Thus, the designers must conceive special details using structural steel profiles.

Composite constructions can be found as suitable solutions for many different structural typologies or systems, as long as the concrete and the steel are combined in a proper manner. The complete understanding of all aspects related to the seismic behavior of composite structures requires years of research efforts and is the key to the general development of the systems. The research emphasized that by encasing steel trusses and steel plates in the reinforced concrete walls, the deformation capacity of such elements is superior to that of traditionally reinforced concrete walls. Nevertheless, the use of the composite approach led to a greater ductility, the load-carrying capacity being limited by the buckling of the concrete-encased steel. The research has evolved, and through extensive programs in the past years (2009, 2010) some of the questions found their answers, but even so, there is still a significant breach in the overall knowledge.

A.2 Objectives

Generally, the main objective and directive line of the theme consists in identifying innovative solutions and systems for composite steel-concrete shear walls with partially encased profiles.

This global objective is reflected throughout the entire components of the project, as it refers to:

- explore and rate technological solutions for the construction of the composite steel-concrete shear walls with openings;
- evaluate technical solutions for assuring the connectivity between steel and concrete in such a manner that it would lead to an increased overall ductility of the structural member;
- efficiency assessment of an innovative solution in which the traditional reinforced concrete that connects the steel profiles is replaced with steel fiber reinforced concrete, excluding the use of steel rebar; this solution can lead to an efficient technology to build up composite walls.
- generate a comparative study in order to evaluate the overall performance of the proposed structural systems related to the behavior of traditional reinforced concrete shear walls.

To the author's best knowledge, the novelty and originality of the project is quite relevant, as certain aspects, alone or combined, truly lead to remarkable innovative features, such as:

- this program would be the first important research program in the world that evaluates, explores and rates technical solutions appropriate for composite steel-concrete shear walls with openings. Moreover, the program considers two perfect possible situations, approaching both the issue of centered openings (vertically aligned) and that of staggered openings;
- a series of structural elements will be designed using an innovative approach for the steel profiles - concrete connection, through which an increase in the overall ductility of the structural element is desired. The technical solution has already been considered in an incipient conceptual design phase and the members of the research team being quite confident in the capacity of the system
- the use of steel fiber reinforced concrete in order to replace the traditionally concrete reinforced with discrete rebar is a solution that has yet not been considered for such elements.

The concept of the theme has arisen from structural reasons, but also from technological ones, if the congestion of reinforcements, which often appears in the boundary regions of reinforced concrete walls subjected to lateral loads, is considered. Taking into account the shape and the position of the partially encased structural steel element, a good confinement of the concrete could be obtained in the boundary region. If shear walls are judged as the primarily

lateral load resisting systems in a high rise building, the full or partially encasement of the structural steel profiles in concrete, could improve the connection between the wall and another structural system designed to undertake and transfer the gravitational loads, such as transfer beams, outrigger beams. Also, the possibility to connect composite steel-concrete shear walls by steel or composite coupling beams may be improved by applying this approach. Nevertheless, the connection between composite walls and moment resisting steel frames or braced frames could also be enhanced. Moreover, in the final phase of the project, one of the sets of elements will be strengthened using Fiber Reinforced Polymers (FRP).

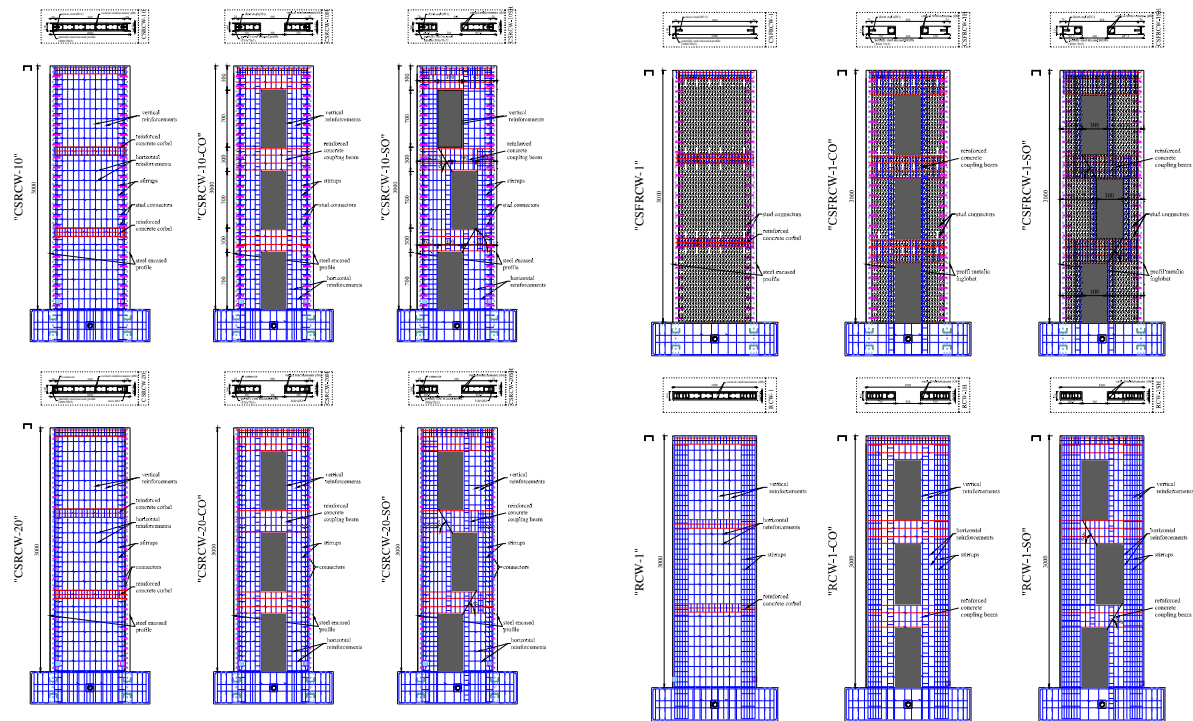
A. 3. Impact

The catalyzing and multiplying effects of the program relate to further development in this field, triggered by the results obtained in this field. By conducting the extensive research program, findings and answers on the efficiency of the proposed solutions and systems should be obtained. Furthermore, the comparison with the data obtained in the previous programs, which had studied traditional solutions for the reinforced concrete shear walls, is relevant; as it can enable other research to further study the field and to generate additional knowledge. This would lead to new enhanced competitiveness. Subsequently, if the studied solutions and systems will prove their efficiency, they can be transferred to a whole new range of applications. The proposed methods to generate structural performance present new approaches, which, if validated through research, can be later implemented on real field applications. The impact of the approached theme is quite high, as it resides, with large implications, in every-day reality.

A. 4. Methodology

All of the research activities will be accomplished using specific means such as: constitute of some complex research teams, setting up a plan of activities, clearly specifying the objectives of the research, ensuring material and logistic means for completion of theoretical and experimental investigation, completing the assigned tasks, elaboration of research papers and reports with conclusions, debating upon conclusions and re-evaluation of priorities. An experimental program for testing 1/3 scale composite shear wall specimens would be undertaken in order to obtain information on the nonlinear behavior of the elements, including the interface connection between the reinforced concrete wall panel and the boundary members. In order to compare the seismic responses of the various steel-concrete composite shear walls and reinforced concrete ductile flexural walls, all the specimens will be subjected to the same reversed cyclic loading pattern.

The theoretical and experimental program consists of 12 composite specimens that enable complex comparisons and ratings of various solutions. The main characteristics of the proposed specimens are presented below. The specimens series abbreviation CSRCW-10 refers to composite steel reinforced concrete with partially steel encased profiles, CSRCW-20 refers to CSRCW improved with innovative connection in order to increase ductility, CSFRCW-1 refers to composite steel fiber reinforced concrete wall and RCW-1 refers to traditionally reinforced concrete wall. The suffix added CO and SO stand for composite wall with centered openings respectively for composite wall with staggered openings.



Performance assessment of the designed solutions through extensive experimental program is the central objective of the project, and the most time consuming one. Secondly, considering two finite element programs specialized in the analytical evaluation on reinforced concrete, numerical modelling of the composite systems will be performed and their accuracy assessed in comparison with the experimental test data. The proposed theme is considered to be very feasible, the studies having both theoretical and experimental components. Each proposal has a specific application, very clear and with practical use. The theme combines theoretical and experimental tests on complex, pilot and innovative shear walls.

The following main activities have to be performed for the proposed theme.

Activity
Designing and detailing of proposed experimental specimens (CSRCW) and test set up
Analyzing the behavior of composite walls using Finite Element Analysis and elaborating a report with the behavior modes of composite walls during testing
Checking of testing frame, data acquisition systems for conducting experimental and purchase of materials and apparatus needed for investigations (strain gauges, transducers etc); Perform the improvements of existing set-up system if needed
Determination of elastic limit and establishing loading procedures for CSRCW subjected to cyclic loads
Completing the theoretical study of the behavior of composite steel concrete shear walls <ul style="list-style-type: none"> - Numerical analyses in elastic range - Numerical analyses in post- elastic range
Manufacturing composite steel concrete walls – 12 pieces
Testing of four structural composite shear walls (CSRCW-10, CSRCW-20, CSFRCW-1, RCW-1)
Elaborating the research report
Experimental tests on structural composite shear walls

- eight specimens -
Testing of various anchorages solutions for CFRP
Elaborating the research program report
Analyzing the strengthening solutions for CSRCW
Rehabilitation of composite shear walls using FRP
Testing of strengthened CSRCW_R
Final Research report

A. 5. Resources

The required experimental facilities are owned and administrated by the Politehnica University through the CCI Department. The experiments could be performed in own laboratory of the department (Lab. for RC elements, construction materials, civil construction Lab.), and, if necessary, in the laboratory at the Department of Steel Structures and Mechanic, or even at the INCERC research institute in Timisoara. All of these laboratories are authorized as first degree national laboratories.

B. In the field of *monitoring the structural health of special constructions or highly important buildings and monitoring certain constructions in order to validate certain calculus principles* I planed to:

- Find efficient solutions for sustainable buildings in Romania;
- Finish the research programme of monitoring the passive house and nearly energy building;
- Provide a practice guide based on recorded data.

The studies and research activities in this field are under implementation in the project PN-II-PT-PCCA-2011-3.2-1214 contract no: 74/2012, entitled "Nearly Zero Energy Building and Passive House - sustainable solutions for residential buildings" financed by UEFISCDI. I have to mention that I am the coordinator of this research program.

B1. State of the art

Passive house (PH)

Passive house refers to a voluntary standard for energy efficiency in a building that results in ultra-low energy buildings that require very little energy for heating and cooling. The "Passive House" concept was developed in May 1988 by the author host Professor Bo Adamson during a research stay (in the field of building construction) at the University of Lund/Sweden.

The first passive houses were built in 1990/1991 in Darmstadt, Germany as an experiment.

The theoretical proof for the feasibility of such houses was furnished in the thesis, "Passive Houses in Central Europe" through computerized simulations of the energy balance of buildings [Feist 1993].

In 1995, Amory Lovins, the American energy efficiency pioneer [Lovins 1977] [Lovins, Weizsaecker 1995], visited the Passive House at Darmstadt Kranichstein. Lovins contributed substantially to the development at this stage, to change the concept of the passive house from scientific experiment to solid reality.

In September 1996 the Passive House Institute was founded in Darmstadt, in order to promote and control the standard.

During the years 1998-2001 circa 250 passive houses have been built in five European countries and with are under evaluation through systematic measurement programmes, through the CEPHEUS programme, a project within the THERMIE Programme of the European

Commission, Directorate-General Transport and Energy - Project Number: BU/0127/97. As of 2010 it is estimated that ca. 20000 + passive houses have been built [Zeller 2010].

Nearly Zero Energy Building (NZEB)

Nearly zero energy buildings and passive house buildings are complementary synergistic technology approaches. A Nearly Zero Energy Building drives the already low annual energy consumption of 120 kWh/m² to 0 kWh/m² using onsite renewable resources.

One key area of debate in the field of zero energy buildings is over the balance between energy conservation and energy production. Most zero energy buildings use a combination of both technologies.

The definition of a zero energy building is widely discussed, the general consensus being that there are in practice four main definitions: net-zero site energy, net-zero source energy, net-zero energy costs, and net-zero energy emissions [Torcellini, 2006].

Worldwide tendencies

The first net zero energy house in Canada was built in 2008 - EcoTerra house in Eastman Quebec.

The Technical University in Darmstadt won the first prize with their entry in the international zero energy design 2007 Solar Decathlon competition with a passive house with added renewable energy production.

After launching, in 2005, the first standardised prefabricated passive house, the Scandinavian Homes company started, in 2009, a project to use a seasonal storage buffer together with researcher Shane Colclough from the University of Ulster.

The first Swiss certified zero-energy building was built in 2011 in Muehleberg [von Muralt 2011].

The United States aim for zero energy development through political programmes [DOE 2009].

In Germany a zero energy development in Freiburg am Schlieberg, composed of 59 plus energy houses took shape from 1999 until 2006 [Heinze 2009].

In Romania the passive house movement is at the very beginning as there are currently 5 passive houses in the country. The passive house in Dumbravita (Timis County, Romania) designed and built by ARHITIM, is one of the first 3 passive houses in Romania and constitutes valuable experience that can easily be expanded further towards achieving a NZEB.

Studies in the field are at an early stage, allowing us to further enhance the existing knowledge base and to further improve on emerging technologies and to establish reasonable guidelines for the practice of NZEB.

Given the rising energy prices and the increasing dependence of our society towards energy consumption, steps need to be taken to decentralise energy production, create a more reliable infrastructure and reduce our dependence on off-site energy.

The most relevant research can be summarized in the below provided bibliographical list:

[Feist 1993] Passive Houses in Central Europe, W. Feist; Thesis, University of Kassel, 1993

[Lovins 1977] Amory Lovins, "Soft Energy Paths"; Harmonsworth 1977

[Lovins, Weizsaecker 1995] Amory Lovins, E.U. von Weizsaecker, L Hunter Lovins: "Factor Four; Double prosperity - halve resource consumption "; Munich 1995, German

[Zeller 2010] Zeller, Jr., Tom. Beyond Fossil Fuels: Can We Build in a Brighter Shade of Green, New York Times, September 26, 2010, p.BU1.

[Torcellini 2006] P. Torcellini, S. Pless, and M. Deru, Zero Energy Buildings: A Critical Look at the Definition, NREL/CP-550-39833; June 2006

[Berneche 2008] Bradley Berneche, Achieving Net Zero, National Marketing Committee Canadian Home Builders Association Ottawa, June 6, 2008

[von Muralt 2011] von Muralt, Klaus (5 June 2011). "Mit «Nullenergie» in eine klimabewusste Zukunft".Der Bund.

[DOE 2009] DOE—U.S. Department of Energy (2009). "Zero Energy Goals" www.eere.energy.gov/buildings/goals.html, (6/2009).

[Heinze 2009] Mira Heinze and Prof. Karsten Voss, GOAL: ZERO ENERGY BUILDING Exemplary Experience Based on the Solar Estate Solarsiedlung Freiburg am Schlierberg, Germany http://www.iea-shc.org/publications/downloads/task40a-zero_energy_building.pdf (11/2011).

B.2 Methodology and associated work plan:

The work plan is structured in nine main phases, closely related to the general directive lines of the project and to the annual activities.

All of the research activities will be accomplished using specific means such as:

- constitute of some complex research teams;
- setting up a plan of activities;
- clearly specifying the objectives of the research;
- ensuring material and logistic means for completing the experimental investigation;
- completing the monitoring of two new energy efficient buildings;
- elaboration of research papers and reports with conclusions;
- debating upon conclusions and re-evaluation of priorities.

The detailed work plan is composed of 9 main phases, each of them divided in several tasks. The initial phases provided for the first year are adequate with the aim of the study, starting with an extended state-of-the-art of major projects for efficient buildings worldwide. In order to have a general view of behaviour of the Passive House, the monitored data will be compiled and the energetic evaluation phase will be completed. Taking into account the experience generated by the previous phases, the design and monitoring of the NZEB will be implemented. The sustainability of the system used for NZEB is to be analysed using Life Cycle Assessment procedures and dedicated software packages. Finally, a recommendation and general guide for designers of NZEBs placed in temperate climate will be presented.

Phase no.	Phase title
1	Design and detailing of NZEB system
2	Build-up the finishing and installation systems for NZEB
3	Evaluation of energetic performances for the PH using recorded monitoring data
4	Design of the monitoring system and set-up of equipment and accessories for NZEB
5	Monitoring of parameters for NZEB
6	PH vs. NZEB comparative study on energy efficiency
7	Optimization of global cost for NZEB
8	Life-cycle assessment of NZEB
9	Recommendations and general rules for new energy efficient residential houses in temperate climate

C. The autonomy and visibility of the scientific activity

The factual arguments of the high degree of autonomy of the research activity developed are presented in the following section.

1. I proved previously the abilities as a manager and a coordinator of a large number of research contracts, most of them I undertook as project leader (14 Research Grants). All of the contracts coordinated were finalized in due time and all of the assumed phases and activities have been entirely completed. No grants led to delays or penalties imposed by the grant's authority.

2. During the research activity, important funds have been raised for the structural development of the testing laboratory, both from national and international research organisms and by contracts with industry. Some of the latest contracts that I developed are:

- Innovative Structural Systems Using Steel-Concrete Composite Materials and Fiber Reinforced Polymer Composites; CNCSIS – UEFISCSU (PN II); 65696 euro; 2009-2011.
- Program for extensive special monitoring of the structures of chimneys 2 and 3; Rovinari Energetic Complex; 57300 euro; 2009-2010.

3. As a project leader of the Research Grant mentioned above at No. 1, I have proved as a tenacious team leader, managing to bind together a well balanced and successful research team that capitalized the results of the theoretical and experimental investigations through publishing of 25 research papers: 3 ISI Journal Papers; 3 ISI Proceeding Conference Papers; 7 papers indexed in International Data Base and 13 papers published in the proceedings of international conferences organized under the aegis of highly important professional institutions (ECCS, *fib*, IABSE).

My involvement in a series of important National, European and other international research grants as director or key member has provided me with relevant skills and competences on management of contracts.

The most important contracts and grants are presented in the followings:

a) International grants (*as member of research team*)

PASSHOUSE (Performance ASSESSment of energy efficient HOUSEs Through Monitoring), HURO/1001/221/2.2.3, 2012, Beneficiary EU, ERDF

COST Action C25 "Sustainability of Constructions - Integrated Approach to Life-time Structural Engineering"; UE; 31450 euro; 2006-2008.

Earthquake PROtection of HIstorical buildings by reversible mixed TECHnologies; EUROPEAN COMMISSION; 182853 euro; 2005-2008.

COBASE Seismic Retrofit of Masonry Structures (Studii teoretice, practice și încercări în domeniul compozitelor), 2002, Beneficiary UNC Charlotte USA

b) National grants or contracts (*as director*)

Nearly Zero Energy Building and Passive House – sustainable solutions for residential buildings, Program PN II – PCCA, No. contract 1214 / 74 /2012, 2012-2015, 533830 lei (~124.000 EUR), UEFISCDI

Innovative Structural Systems Using Steel-Concrete Composite Materials and Fiber Reinforced Polimer Composites” , Program PN II – IDEI 1004, No. contract 621/2009 , 2008-2011, 282495 lei (~75.000 EUR), CNCSIS-UEFISCSU

Optimisation of new composite solutions used for structural elements for buildings, Nr. contract 33550 AT2-190 / 2003-2004, 16600 lei (~6000 EUR) CNCSIS

Special health monitoring of chimneys from Rovinari power plant, No. contract 69/2009, 2009, 107100 lei (~30.000 EUR), SC Complexul Energetic Rovinari SA

(b-iii) References**Chapter 2: Experimental and Theoretical Studies Concerning the Load Bearing Capacity of Steel and Composite Joints for Buildings Placed In Seismic Areas**

- [2.1] Eurocode 3 – Design of steel structure –EN 1993.1.1
- [2.2] Eurocode 4 – Design of composite steel and concrete structures-EN 1994.1.1
- [2.3] Johnson R– Beams, Slabs , Columns and Frames for Buildings, OXFORD, 1994
- [2.4] Păcurar V., Aribert J.M. – Calculul structurilor mixte din oțel-beton, EUROCODE 4- Ex. de calcul 1997
- [2.5] Stoian V.– Structural solutions for new buildings in seismic area, New Technologies and Structures in Civil Engineering, Case studies on Remarkable Constructions, Edited by D.Dubina, I.Vayas, V.Ungureanu, Timisoara, 1998
- [2.6] Biograf – Program pentru calculul biografic neliniar al elementelor compuse oțel-beton în stare plană de tensiuni, UPT, Departamentul CCIA, Timișoara, 1988
- [2.7] Zandonini R., Bernuzzi C., Bursi O. S. – Steel and steel-concrete composite joints subjected to seismic actions, STESSA 1997, Kyoto – Japan
- [2.8] Dan D., Stoian V., Nagy T. - Numerical analysis and experimental studies concerning the behaviour of steel-concrete composite joints under symmetrical and asymmetrical loads, Proceedings of International conference on steel and composite structures, Manchester 2007, p389 – 395
- [2.9] Dan D., Stoian V., Nagy T. C. Daescu- Composite joint for buildings placed in seismic areas theoretical and experimental studies, 9-th International conference on Steel, Space & Composite Structures, Yantai –Beijing, China 2007, p647-655
- [2.10] Dan D., Stoian V., Nagy Gyorgy T. - Experimental and theoretical studies concerning the load bearing capacity of steel and composite joints for buildings placed in seismic areas, Contemporary Civil Engineering Practice, Novi Sad, Serbia, 2008
- [2.11] Dan D. – Contribution to the design of the composite steel-concrete elements, Ph. D. Thesis, Politehnica University of Timișoara, 2002
- [2.12] Dan D., Stoian V., Nagy-Gyorgy T. - Theoretical and experimental studies concerning the load bearing capacity of steel and composite joints, Proceedings of International Conference Steel - New and traditional material for building p387 – 396, Brasov, Romania 2006
- [2.13] Dan D., Stoian V., Nagy-Gyorgy T. - Numerical analysis and experimental studies concerning the behaviour of steel-concrete composite joints under symmetrical and asymmetrical loads, Proceedings of International conference on steel and composite structures, p 389 – 395, Manchester 2007
- [2.14] Dan D., Stoian V., Nagy-Gyorgy T. Daescu C.- Composite joint for buildings placed in seismic areas theoretical and experimental studies, 9-th International conference on Steel, Space & Composite Structures, Yantai –Beijing, China 2007, p647-655
- [2.15] Dan D., Stoian V., Nagy-Gyorgy T., Daescu C., Pavlou D.– Numerical Analysis and Experimental Studies on Welded Joint for Buildings, 3-rd International conference Applied and Theoretical Mechanics, Tenerife, Spain 2007, p106-112
- [2.16] Dan D., Stoian V., Nagy-Gyorgy T., - Theoretical and experimental studies concerning the load bearing capacity of composite joints, Eurosteel 08, Graz, Austria, 2008
- [2.17] Dan D., Stoian V., Nagy-Gyorgy T., Demeter I, - Experimental Studies on Steel and Steel Concrete Composite Joints Under Symmetrical and Asymmetrical Loads, 6-th International Conf. On Behaviour of Steel Structure. In Seismic Areas-Stessa, Philadelphia, Pennsylvania, USA, 16-20 August 2009
- [2.18] Ramires F., Andrade S., Vellasco P. - Experimental analysis of composite semi-rigid beam to column joints, Eurosteel 2008, Graz, Austria, 2008

- [2.19] Bessa W., Gonçalves R. M., Calado L., Castiglioni - C.A. Advanced numerical modelling of composite steel concrete joints, Eurosteel 2008, Graz, Austria
- [2.20] Choi S, Yun Y., Him J.,– Experimental study on seismic performance of concrete filled tubular square column-to-beam connections with combined cross diaphragm, *Journal Steel and Composite Structures*, Vol. 6, No. 4, 2006, p. 303-317
- [2.21] ECCS –Recommended testing procedure for assessing the behaviour of structural steel elements under cyclic loads, European Convention for Constructional Steelwork, 1999

Chapter 3: Theoretical and Experimental Study on Composite Steel-Concrete Shear Walls with Vertical Steel Encased Profiles

- [3.1] General report of research Grant PNII - IDEI ID_1004, Contract 621/2009, entitled „Innovative Structural Systems Using Steel-Concrete Composite Materials and Fiber Reinforced Polymer Composites, 2011
- [3.2] Plumier, A. (2000), “European research and code developments on seismic design of composite steel concrete structures”, 12th World Conference on Earthquake Engineering, Auckland, New Zealand
- [3.3] Tupper, B. (1999), “Seismic response of reinforced concrete walls with steel boundary elements”, Thesis for the degree of Master of Engineering, Department of Civil Engineering and Applied Mechanics, McGill University, Montréal, Canada.
- [3.4] Astaneh, A.A. (2002), “Seismic Behavior and Design of Composite Steel Plate Shear Walls”, Steel Tips, University of California at Berkeley
- [3.5] Tong, X., Hajjar, J.F., Schultz, A.E. and Shield, C.K. (2005), “Cyclic behavior of steel frame structures with composite reinforced concrete infill walls and partially-restrained connections”, *Journal of Constructional Steel Research*, 61 (2005), 531–552, doi:10.1016/j.jcsr.2004.10.002
- [3.6] Lu, X. and Dong, Y. (2006), “Experimental Study on seismic behavior of steel reinforced concrete walls”, IABSE Symposium Report, IABSE Symposium, Budapest 2006, 18-25
- [3.7] Liao, F.Y., Han, L.H. and Tao, Z. (2009), “Seismic behavior of circular CFST columns and RC shear wall mixed structures: Experiments”, *Journal of Constructional Steel Research*, 65 (2009), 1582-1596, doi:10.1016/j.jcsr.2009.04.023
- [3.8] Liao, F.Y., Han, L.H. and Tao, Z. (2010), “Experimental behavior of RC shear walls framed with steel reinforced concrete (SRC) columns under cyclic loading”, *Proceedings of the 4th International Conference Steel & Composite Structures*, 233-238, doi:10.3850/978-981-08-6218-3 CC-We022
- [3.9] Ji, X., Qian, J. and Jiang, Z. (2010), “Seismic behavior of steel tube-reinforced concrete composite walls”, *Proceedings of the 4th International Conference Steel & Composite Structures*, 185-190, doi:10.3850/978-981-08-6218-3 CC-We012
- [3.10] Chen L. and Lan, Z. “Seismic behavior of steel-encased reinforced concrete composite shear walls with openings”. Southeast University, Nanjing
- [3.11] Saari, W.K., Hajjar, J.F., Schultz, A.E. and Shield, C.K. (2004), “Behavior of shear studs in steel frames with reinforced concrete infill walls”, *Journal of Constructional Steel Research*, 60(10), 1453–1480
- [3.12] Hossain, A.K.M. and Wright, H.D. (2004), “Experimental and theoretical behavior of composite waling under in-plane shear”, *Journal of Constructional Steel Research*, 61(6), 59–83
- [3.13] Astaneh, A.A. (2000), “Steel plate shear walls”, *Proceedings, US–Japan partnership for advanced steel structures*
- [3.14] Guo, L., Ma, X., Zhang, S. and Guan, N. (2008), “Experimental research on seismic behavior of two-sided steel–concrete composite shear walls”, *Proceedings of Eurosteel 2008, Manchester*, 1467–1473

- [3.15] Greifenhagen, C. and Lestuzzi, P. (2005), “Static cyclic tests on lightly reinforced concrete shear walls”, *Journal Engineering Structures*, 2005, 27, 1703–1712
- [3.16] Su, R. and Wong, S. (2007), “Seismic behavior of slender reinforced concrete shear walls under high axial load ratio”, *Journal Engineering Structures*, 2007, 29, 1957–1965.
- [3.17] Fabian, A (2012) – Study on the performances of composite steel concrete structural shear walls under lateral loads, Ph.D. Thesis, Editura Politehnica
- [3.18] EN 1998 - Eurocode 8: Design of structures for earthquake resistance, European Committee for Standardization (CEN), Brussels, Belgium
- [3.19] EN 1992 – Eurocode 2: Design of concrete structures, European Committee for Standardization (CEN), Brussels, Belgium.
- [3.20] EN 1994-1-1 - Eurocode 4: Design of composite steel and concrete structures, part 1-1, general rules and rules for buildings, European Committee for Standardization (CEN), Brussels, Belgium.
- [3.21] Guo, L. & Ma., X. & Zhang, S.& Guan, N. Experimental research on seismic behavior of two-sided steel-concrete composite shear walls. *Proceedings of Eurosteel 2008, Graz, Austria: 1467-1473.*
- [3.22] Dan D., Stoian V., Nagy T. Numerical analysis and experimental studies concerning the behaviour of steel-concrete composite joints under symmetrical and asymmetrical loads, *Proceedings of International conference on steel and composite structures, Manchester 2007, 389-395.*
- [3.23] ATENA - Advanced Tool for Engineering Nonlinear Analysis, Technical specifications 2010, Cervenka Consulting Ltd., Prague, Czech Republic
- [3.24] ECCS –Recommended testing procedure for assessing the behaviour of structural steel elements under cyclic loads, European Convention for Constructional Steelwork, 1999
- [3.25] Liao F.Y., Han L.H., Tao Z. Seismic behavior of circular CFST columns and RC shear wall mixed structures: Experiments, *Journal of Constructional Steel Research* 2009; 65, 1582 - 1596.
- [3.26] Guo, L. & Ma., X. & Zhang, S.& Guan, N. Experimental research on seismic behavior of two-sided steel-concrete composite shear walls. *Proceedings of Eurosteel 2008, Graz, Austria: 1467-1473.*
- [3.27] Dan D., Fabian A., Stoian V. - Theoretical and experimental study on composite steel - concrete shear walls with vertical steel encased profiles, *Journal of Constructional Steel Research*, 2011; 67, 800 – 813 (ISI Journal)
- [3.28] Dan D., Fabian A. & Stoian V. - Nonlinear behavior of composite shear walls with vertical steel encased profiles, *Engineering Structures*, 2011; 33, 2794 – 2804 (ISI Journal)
- [3.29] Li B. & Lim C.L. Tests on seismically damaged reinforced concrete structural walls repaired using fiber - reinforced polymers, *Journal of Composites for Construction*, 2010; 14, 597 - 608
- [3.30] Antoniadis K.K., Salonikios T. N. & Kappos A.J. Evaluation of hysteretic response and strength of repaired R/C walls strengthened with FRPs, *Engineering structures*, 2007; 29, 2158 – 2171
- [3.31] Antoniadis K.K., Salonikios T. N. & Kappos A.J. Tests on seismically damaged reinforced concrete walls repaired and strengthened using fiber reinforced polymers, *Journal of Composites for Construction*, 2005; 9, 236 - 246
- [3.32] Demeter I., Nagy-György T., Stoian V., Dăescu C. & Dan D. FRP Composites for Seismic Retrofitting of RC Wall Panels with Cut-Out Openings, *First International Conference on Structures and Architecture (ICSA2010), Guimaraes, Portugal, 2010, 1902-1908*
- [3.33] Kitano A., Joh O. & Goto Y. Experimental study on the strengthening and repair of R/C wall-frame structures with an opening by CF-Sheets or CF-Grids, *Proc., 2nd International Conference on FRP Composites in Civil Engineering (CICE 2004), Adelaide, Australia*

- [3.34] Lombard J., Lau D. T., Humar J. L., Foo S. & Cheung M. S. Seismic strengthening and repair of reinforced concrete shear walls”, The 12th World Conf. on Earthquake Engineering, (CD-ROM), New Zealand, 2000, Paper No. 2032
- [3.35] Hiotakis S., Lau D.T. & Londono N. Research on seismic retrofit and rehabilitation of reinforced concrete shear walls using FRP materials, NSR-NRC, 2004
- [3.36] Ghobarah A. & Khalil A. A. Seismic rehabilitation of reinforced concrete walls using fiber composites, The Thirteenth World Conference on Earthquake Engineering Vancouver, Canada 2004, paper no. 3316.
- [3.37] Li B. & Pan T. C. Recent tests on seismically damaged reinforced concrete beam to column joints repaired using fiber reinforced polymers, Ninth Pacific Conference on Earthquake Engineering, Auckland, New Zealand, 2011, paper no. 119
- [3.38] Wei H., Wu Z., Guo X. & Yi F. Experimental study on partially deteriorated strength concrete columns confined with CFRP, *Engineering Structures*, 2009, 31, 2495-2505
- [3.39] Hatami F., Ghamari A., Rahai A. Investigating the properties of steel shear walls reinforced with carbon fiber, *Journal of Constructional Steel Research*, 70 , 2012, 36 – 42
- [3.40] Lu X., Zhou Y, Dong YG. Seismic behavior of composite shear walls with multi-embedded steel sections, Part I: Experiment. *The Structural Design of Tall and Special Buildings* 19 , 2010, 637 – 655
- [3.41] Zhou Y., LU X, Huang Z., Bo Y. Seismic behavior of composite shear walls with Multi-embedded steel sections, Part II: Analysis, *The Structural Design of Tall and Special Buildings* 19 , 2010, 618 – 636
- [3.42] Carrasco E.V.M., Rodrigues E.V., Ribeiro G.O., Queiroz G., De Paula F.A. Ultimate compressive strength of Enveloped Laminar Concrete panels, *Construction and Building Materials*, 27 , 2012, 375 – 381
- [3.43] Nagy-György T., Moşoarcă M., Stoian V., Gergely J. & Dan D. Retrofit of reinforced concrete shear walls with CFRP composites, *fib Symposium Keep Concrete Attractive*, Budapest, 2005, 897-902

Chapter 4: Monitoring the constructional structural works and structural health of buildings

- [4.1] Mihăilescu R. - Proiect arhitectură Centrul Comercial Iulius Mall Timișoara, 2004
- [4.2] Mișcă Gherasim, Foldvary Iuliana - Proiect structură de rezistență Centrul Comercial Iulius Mall Timișoara, 2004
- [4.3] Păunescu M – Studiu și soluție de consolidare pentru realizare fundație corp B, Centrul Comercial Iulius Mall Timișoara, Septembrie 2004
- [4.4] Bob, C et. all, Y. 2005. IABSE Symposium on “Structures and extreme events”. Lisbon.
- [4.5] NP 108-04, Y.2004. Demand code regarding the design, execution and behavior monitoring, repair and rehabilitation of the industrial reinforced chimneys (in Romanian)
- [4.6] Dan D., Stoian V., Nagy Gyorgy T., Florut. C, Pruna L. - Structural analysis, rehabilitation and further development of health monitoring program concerning two reinforced concrete chimneys, IABSE'2010 - Large Structures and Infrastructures for Environmentally Constrained and Urbanised Areas , Venice Italy
- [4.7] Stoian V., Dan D., Nagy Gyorgy T., Florut C., Pruna L. - Structural rehabilitation and health monitoring of reinforced concrete chimneys, International Conference on Health Monitoring on Intelligent Infrastructure SHMII-4, Zurich, 2009
- [4.8] ATENA - Advance Tool for Engineering Nonlinear Analysis, Cervenka Consulting, Prague, 2009.